UNIVERSITATEA POLITEHNICA DIN BUCUREȘTI

UNIVERSITATEA 1 DECEMBRIE 1918 DIN ALBA IULIA

ISIM & ISWIM 2023

27-30 June 2023, Bucharest, Romania

www.isimconference.eu

NATIONAL UNIVERSITY OF SCIENCE AND TECHNOLOGY POLITEHNICA BUCHAREST

Center for Research and Training in Innovative Techniques of Applied Mathematics in Engineering "*Traian Lalescu*" (CiTi)

&

"1 DECEMBRIE 1918" UNIVERSITY OF ALBA IULIA

BOOK OF ABSTRACTS
ISIM & ISWIM

International Symposium & International Student Workshop on Interdisciplinary Mathematics in the CiTi areas

Volume II

ISSN-L 2821 – 8779

2023

BUCHAREST, ROMANIA

ISIM & ISWIM 2023

The University POLITEHNICA of Bucharest, Center for Research and Training in Innovative Techniques of Applied Mathematics in Engineering "*Traian Lalescu*" (CiTi) in collaboration with "1 DECEMBRIE 1918" University of Alba Iulia organized the 2nd Edition of the **International Symposium & International Student Workshop on Interdisciplinary Mathematics in the CiTi areas (ISIM & ISWIM)** that was held at University Politehnica of Bucharest, Romania, between 28th and 30th of June 2023.

The scope of the Symposium included but not limited to, original research works and ideas related to CiTi interdisciplinary areas and Applications: ***Fractional Calculus, Wavelet Analysis, Evolutionary Algorithms, Data Analysis and Information Security, Game Theory - including Quantum, Partial and Ordinary Differential Equations, Mathematical Statistics, Graph Theory, Non-classical sets (algebraic and topological aspects) and applications.***

Keynote Speakers:

Mostafa Adimy, Senior Researcher at INRIA and Institut Camille Jordan, University Lyon

Dumitru Băleanu, Cankaya University, Ankara, Turkey

Martin Bohner, Missouri University of Science and Technology (Missouri S&T)

Juan C. Cortes, Universitat Politécnica de València, Spain

Poom Kumam, King Mongkut's University of Technology Thonburi, Bangkok, Thailand

Mohsen Razzaghi, Mississippi State University, USA

Suthep Sunatai, Chiang Mai University, Chiang Mai, Thailand

Paul Bogdan - University of Southern California, Los Angeles, USA

Francesco Villecco - University of Salerno, Italy

Thorsten Hohage - Georg-August Universität Göttingen

Symposium Contact
E-mail: office@isimconference.eu
Website: https://isimconference.eu

Antonela Toma

University POLITEHNICA of Bucharest, Romania

Ioan Lucian Popa

"1 DECEMBRIE 1918" University of Alba Iulia, Romania

TABLE OF CONTENTS

A CAPUTO-FABRIZIO FRACTIONAL-ORDER CHOLERA MODEL AND ITS SENSITIVITY ANALYSIS

Idris AHMED[1], Ali AKGUL[2] Fahd JARAD[3], Kamsing NONLAOPON[4]

[1]Sule Lamido University, P.M.B 048, Kafin Hausa, Jigawa State, Nigeria.
[2]Siirt University, 56100 Siirt, Turkey.
[3]Cankaya University, 06790 Etimesgut, Ankara, Turkey.
[4]Khon Kaen University, Khon Kaen 40002, Thailand.

Corresponding author email: idris.ahmed@slu.edu.ng

Abstract

Due to the availability of advanced computational techniques, there has been an increasing focus on fractional-order derivatives in recent years. This development has enabled researchers to investigate the complex dynamical behaviour of certain biological models using fractional-order derivatives rather than integer-order derivatives. In this paper, we propose a Caputo-Fabrizio fractional-order cholera epidemic model and utilize fixed points theorems to examine the existence and uniqueness of solutions. Furthermore, numerical schemes are employed to demonstrate the complex behaviours of the model, highlighting the advantages of fractional-order derivatives. We also conduct a sensitivity analysis to determine the most sensitive parameters. Ultimately, our findings suggest that the model offers more insights into disease transmission and can aid policymakers in devising effective strategies to manage disease outbreaks.

Key words*: Cholera, mathematical model, fixed point theorems, sensitivity analysis, numerical simulations*

1. INTRODUCTION

Cholera was recognized as one of the most dangerous and infectious communicable diseases which spread globally, and it's become threat to the survival of human population other than war and poverty. Infectious diseases are very diverse, and their outbreaks predisposes millions of people to become vulnerable to their infection and this causes huge economic burden for the health care system. Cholera is an illness that is transmitted through water and is characterized by a sudden onset of symptoms, which include the presence of large amounts of watery diarrhea, the causative agent of the disease is known as vibrio cholera which is a specie of Gram-negative, facilitative anaerobic and comma shaped bacteria, belonging to the family Vibrionacede with type 01 or 0139.

2. CONTENT

We study the Cholera model as proposed in [1]. The classical Cholera model is formulated by the following system:

$$\frac{dS(t)}{dt} = \Omega - (\lambda I - \mu)S + \eta V + \gamma R,$$
$$\frac{dI(t)}{dt} = \lambda SI - (\mu + \omega + \sigma + \beta)I,$$
$$\frac{dR(t)}{dt} = \beta I - (\mu + \gamma)R,$$
$$\frac{dV(t)}{dt} = \sigma I - \eta V.$$

Thus, the Caputo-Fabrizio fractional-order model is given by:

$$^{CF}D^{\alpha}S = \Omega - \lambda SI - \mu S + \eta V + \gamma R$$

$$^{CF}D^{\alpha}I = \lambda SI - \mu I - \omega I - \sigma I - \beta I$$

$$^{CF}D^{\alpha}R = \beta I - \mu R - \gamma R$$

$$^{CF}D^{\alpha}V = \sigma I - \eta V,$$

subject to

$$S(0) = S_0 \geq 0, I(0) = I_0 \geq 0, R(0) = R_0 \geq 0, and V(0) = V_0 \geq 0.$$

Tables 1 and 2, respectively display the biological meaning of each state variable and parameters used in the model.

Table 1. States Variables

Compartment	Description
S	Susceptible population
I	Symptomatic infected population
R	Recovered population
V	Environment

Table 2. Meaning of each parameters.

Parameters	Biological Meaning
Ω	Population recruitment rate
λ	Contact rate
β	Recovery rate
ω	Death rate due to infection
γ	Loose of immunity
μ	Natural death rate
σ	Rate of infection among I and V
η	Rate of infection among V and S

3. CONCLUSIONS

In this paper, we have successfully developed a fractional-order Cholera model to investigate the transmission dynamics of the disease using the Caputo-Fabrizio derivative and establish the existence and uniqueness of solutions via fixed point theorems. Furthermore, the sensitivity analysis of the basic reproduction number has highlighted the significant contributions of the parameters associated with the model. Specifically, the results indicate that the recruitment and contact rate are the most sensitive parameters, which significantly increase the basic reproduction number. We conclude that these findings provide valuable insights into the factors that contribute to the transmission dynamics of cholera and can inform public health policies and strategies for controlling the transmission of the disease.

REFERENCES.

1. Eustace, K. A., Osman, S., & Wainaina, M. (2018). Mathematical modelling and analysis of the dynamics of cholera. Global Journal of Pure and Applied Mathematics, 14(9), 1259-1275.

DATA ANALYSIS FOR PRECISE SEMANTIC BREAST IMAGES SEGMENTATION

Iulia-Nela ANGHELACHE NASTASE [1,2], Simona MOLDOVANU [1,3], Luminita MORARU [1,4]

[1]The Modelling & Simulation Laboratory, Dunarea de Jos University of Galati, 47 Domneasca Street, 800008 Galati, Romania
[2]Emil Racovita Theoretical Highschool, 12-14, Regiment 11 Siret Street, 800332 Galați, Romania
[3]Department of Computer Science and Information Technology, Faculty of Automation, Computers, Electrical Engineering and Electronics, Dunarea de Jos University of Galati, 47 Domneasca Street, 800008 Galati, Romania
[4]Department of Chemistry, Physics & Environment, Faculty of Sciences and Environment, Dunarea de Jos University of Galati, 47 Domneasca Street, 800008 Galati, Romania

Corresponding author email: luminita.moraru@ugal.ro

Abstract

Accurate segmentation of the breast lesions, operator-independent, asks for a computer-aided segmentation solution using deep learning techniques. Convolutional neural networks are useful tools for mass segmentation in breast ultrasound images. In this study, we aim to analyze the breast lesions segmentation efficiency of two encoder-decoder deep learning architectures. The encoder takes images as input and generates a high-dimensional feature vector. The role of decoder is to map the low resolution of the encoder's feature vector and generates a semantic segmentation mask. Specifically, we first semi-automatically segment the regions of interest by using the Local Graph Cut technique in the Image Segmenter application. The Local Graph Cut algorithm draw a region-of-interest around the breast mass of interest and the Image Segmenter app segments its automatically. This approach allows us to discuss the robustness of the Local Graph Cut segmentation method against the ground truth or standard images. Then, two pre-trained DeepLabV3+ and U-Net encoder-decoder models are used for automatic semantic segmentation of breast tumors. The output segmentation results have been evaluated by using the Dice similarity coefficient. The proposed approach has been applied using a 780 BUS's images (437 benign images and 210 malignant images) along with their 780 ground truth images taken from publicly available BUSI (Breast Ultrasound Image Dataset) image dataset. The results indicate a Dice similarity coefficient of 93.60% (malignant) and 93.24% (benign) for the DeepLabV3+ architecture when the ground truth images were compared with the CNNs predicted mask and of 62.50% (malignant) and 62.51% (benign) for the U-Net, respectively. The results of Local Graph Cut segmentation algorithm were compared with the CNNs predicted mask and they indicate a Dice similarity coefficient of 93.76% (malignant) and 92.03% (benign) for the DeepLabV3+ architecture and 61.15% (malignant) and 61.18% (benign) for U-Net, respectively. U-Net method misjudges the mass breast regions, resulting in mis-segmentation

Key words*: semantic segmentation; data analysis; breast cancer; convolutional neural network.*

1. INTRODUCTION

To accurate diagnose the breast cancer an accurate segmentation of breast lesions is necessary. Convolutional neural networks have become an important method for medical image analysis and are used in the task of segmenting regions of interest in breast ultrasound images. In this study we propose an analysis of the breast lesions segmentation efficiency provided by two encoder-decoder deep learning architectures.

2. CONTENT

The proposed approach used 780 BUS's images (437 benign images and 210 malignant images) along with their 780 ground truth images taken from publicly available BUSI (Breast Ultrasound Image Dataset) image dataset.

Two Encoder-Decoder architectures, namely DeepLabV3+ and U-Net, are implemented to analyze the segmentation efficiency of BUS images. The Encoder takes an input image and generates a high-

dimensional feature vector that then maps the features provided by the network layers. The Decoder decodes the feature vector and generates a semantic segmentation mask.
The Dice similarity coefficient performs a qualitative evaluation to assess the performance of the segmentation methods.

$$Dice = \frac{2\times(X\cap Y)}{X+Y} \quad (1)$$

The flowchart of the segmentation step is showed in Figure. 1.

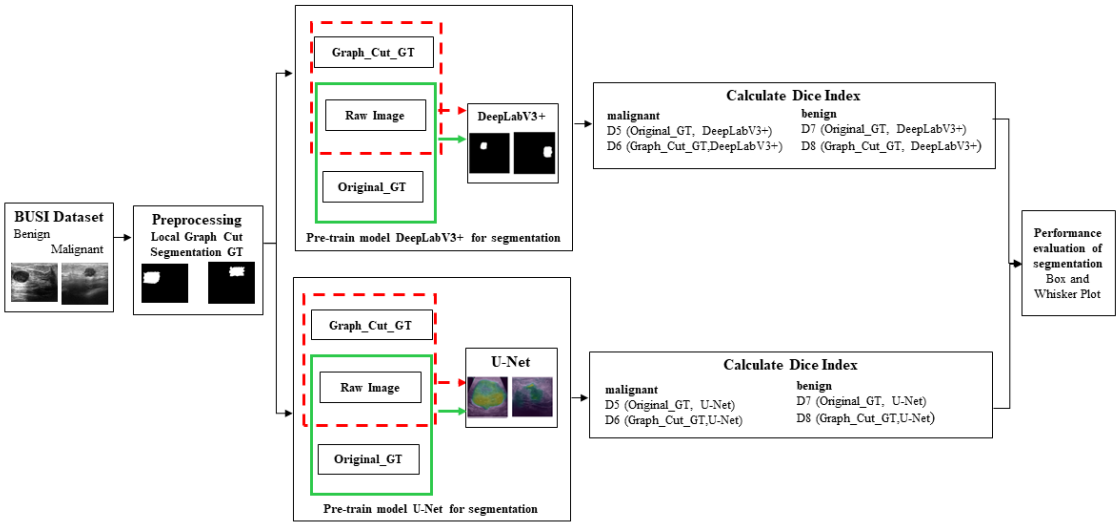

Figure 1. The segmentation flowchart of breast mass by CNNs

The following steps are operated: (i) segmentation of BUS images using the Local Graph Cut method from MathLab; (ii) segmentation of breast tumors from BUS images using the DeepLabV3+ and U-Net encoder-decoder architectures; (iii) the segmentation performance evaluation based on the Dice coefficient values; (iv) a comparative analysis of the segmentation results provided by the two CNNs.

3. CONCLUSIONS

In this paper, we analyzed the segmentation efficiency of two encoder-decoder architectures. We experimentally demonstrated the efficiency of the DeepLabV3+ architecture against the U-Net architecture. Thus, the results indicate a Dice similarity coefficient of 93.60% (malignant) and 93.24% (benign) for the DeepLabV3+ architecture when the ground truth images were compared with the CNNs predicted mask and of 62.50% (malignant) and 62.51% (benign) for the U-Net, respectively. The results of Local Graph Cut segmentation algorithm were compared with the CNNs predicted mask and they indicate a Dice similarity coefficient of 93.76% (malignant) and 92.03% (benign) for the DeepLabV3+ architecture and 61.15% (malignant) and 61.18% (benign) for U-Net, respectively. U-Net method misjudges the mass breast regions, resulting in mis-segmentation.

ACKNOWLEDGMENT

This study was financed by Dunărea de Jos University of Galați, of the project " Excelență și implicare în dezvoltarea inteligentă bazată pe cercetare și inovare la Universitatea Dunărea de Jos din Galați (UDJG) – DINAMIC "- Code 12PFE/30.12.2021.

THE EXISTENCE FOR NEUTRAL ITERATIVE SINGLE-SPECIES POPULATION GROWTH MODEL WITH HARVESTING EFFORT

Lynda MEZGHICHE[1], Rabah KHEMIS[2], Ahleme BOUAKKAZ[3]

[1,2,3] LAMAHIS Laboratory, University of 20 August 1955, Skikda, Algeria

Corresponding author email: linomezg3@gmail.com

Abstract

This present work is devoted to investigate the existence, uniqueness and stability of positive periodic solutions of a neutral iterative differential equation arising in population dynamics. The technique used in our study is based on the Krasnoselskii's fixed point theorem, Banach contraction principle and the Green's functions method. This study's findings add to some previous ones.

Key words*: Existence; uniqueness; fixed point theorem; population model; periodic solution.*

ADAPTIVE PENALTY FUNCTION METHODS EMPLOYED IN DECOMPOSITION BASED MOEAs

Akhtar Munir KHAN[1], Muhammad Asif JAN[1]

[1]Institute of Numerical Science (INS), Kohat University of Science & Technology (KUST), Kohat-26000, Pakistan

Abstract

Evolutionary algorithms (EAs) are frequently used to find decision vectors that optimize objective function(s) and such problems are called optimization problems (OPs). When the objectives are more than one, such problems are called Multi-objective optimization problems (MOPs) or Vector Optimization Problems. EAs solving MOPs are called Multi-objective evolutionary algorithms (MOEAs). If additional constraints are imposed on MOPs, such problems are called constrained MOPs (CMOPs) and MOEAs dealing with CMOPs are called constrained MOEAs (CMOEAs). In constrained optimization problems, penalty function method is one of the widely implemented constrained handling techniques (CHTs). In this method, the scaled constraint violations (known as penalty term) are added up with the objective function values of the solutions to define penalty function. .The scaling factors, also known as the penalty parameters, balances the values of the objective function and violations of the constraints. However, it is not easy to properly adjust these parameters. Some of the various settings of this include static, dynamic and adaptive setting.

In this research, penalty function method with various near feasibility thresholds (NFTs) levels are used in decomposition based approach MOEA/D-DE. Solutions in NFT region are given more priority as compared to other infeasible region. This investigation uses five NFT configurations, leading to five CHTs. The performance of these CHTs are tested on two benchmark test suits, namely CF and CTP series. To compare the obtained results with best performers of CEC2009 and other state-of-the-art algorithms, inverted generational distance (IGD) and hyper volume (HV) is used. The comparisons of results obtained through simulation places the designed algorithmic framework at first place on CF series and at second place on CTP series.

Key words*: multiobjective optimization, constraint handling techniques, penalty function methods, and decomposition based multiobjective optimization algorithms*

Analysis of implicit Hadamard–type random fractional differential equations with retarded and advanced arguments

Shahid Saifullah
Department of Mathematics, University of Peshawar, Peshawar, Pakistan
E–mail: shahidsaif78@gmail.com
Sumbel Shahid
Department of Mathematics, University of Peshawar, Peshawar, Pakistan
E–mail: sumbel.776@gmail.com
Akbar Zada
Department of Mathematics, University of Peshawar, Peshawar, Pakistan
E–mail: akbarzada@uop.edu.pk, zadababo@yahoo.com
Ioan-Lucian Popa
Department of Exact Science and Engineering, ?1 Decembrie 1918? University of Alba Iulia, Alba Iulia, Romania
E–mail: lucian.popa@uab.ro

Abstract

This paper explores the qualitative outcomes of solving boundary value problems for implicit Hadamard–type random fractional differential equations with both retarded and retarded arguments. We also investigate the existence and uniqueness of solutions for coupled system of implicit Hadamard–type random fractional differential equations with both retarded and advanced arguments. The Green function and contractive theorem are employed to demonstrate the uniqueness and existence of solutions. The paper concludes with examples that further give the applications and validation of the obtained results.

Keywords: Green's functions; Hadamard–type fractional order derivative; existence theory; retarded and advanced argument; fixed point theorem

Mathematics Subject Classification (2010): 34B27; 26A33; 39B82; 45M10

ON THE ANALYSIS OF THE INFLUENCE OF DISCRETIZATION STEP ON THE POSITIVITY OF CONFORMABLE FRACTIONAL 2D ROESSER MODELS AND THE DARBOUX EQUATION

Kamel BENYETTOU[1] And Djillali BOUAGADA[2] And Mohammed Amine GHEZZAR[3]

[1,2] Abdelhamid Ibn Badis University Mostaganem, Department of Mathematics and Computer Science, ACSY Team-Laboratory of Pure and Applied Mathematics, Faculty SEI-BP 227/118 Mostaganem 27000, Algeria.
[3] National Higher School of Mathematics, ACSY Team-Laboratory of Pure and Applied Mathematics, P.O.Box 75, Mahelma 16093, Sidi Abdellah (Alger), Algéria.

Corresponding author email: kamel.benyattou.etu@univ-mosta.dz[1]
djillali.bouagada@univ-mosta.dz[2] and amine.ghezzar@nhsm.edu.dz[3]

Abstract

This study focuses on the impact of the discretization step on the positivity of Roesser models based on the conformable fractional continuous systems and the Darboux equation. Our research investigates the effect of the sampling step on the positivity of these class of models and proposes a novel approach to analyze this effect. We examine the conditions under which the associated two-dimensional discrete-time linear system remains positive after discretization, based on the positivity requirements of the conformable fractional continuous model. Furthermore, we present examples and simulations to demonstrate the precision and applicability of the proposed discretization technique. Finally, some simulation results are presented to demonstrate the effectiveness of the new approach using Darboux conformable fractional equation, which is used to simulate gas absorption, water stream heating, and air drying.

.

Key words*: Fractional linear systems; Conformable derivative; Roesser models; Darboux equation; Positive systems; Discretization Step.*

1. INTRODUCTION

Two-dimensional systems have received significant attention in the past 30 years. These models require solving an input/output matrix using both global and local state space vectors. The usefulness of two-dimensional systems lies in their ability to help researchers solve practical problems in control theory.

Many recent publications have described the most well-known 2D systems using continuous and discrete-time state space models. These systems are often referred to Fornasini-Marchesini (1978), and Roesser (1976), Kaczorek (1985, 2002 and 2011), and Rogowski (2015, 2016 and 2020). The Roesser models are considered as the most important class of two-dimensional systems due to their numerous applications in advanced research areas and control theory. These applications include investigating physical and mechanical problems, digital and signal processing, system filtering, analyzing stability and positivity conditions of practical models, modern circuit design, and addressing chemical reaction problems.

Fractional calculus is currently a topic of great interest among researchers in basic mathematical sciences and engineering in control theory. This, because fractional calculus enables the derivation and integration of fractional orders. In literature, there are many definitions of fractional derivatives and integrals such as Caputo and Riemann-Liouville.

The most well-known fractional derivatives do not satisfy the fundamental properties of classical derivatives. To address some of these problems, Khalil (2014) has introduced a new class of

fractional derivatives known as conformable fractional derivatives. This concept offers two improvements over classical derivatives in fractional calculus such as Caputo or Riemann-Liouville. The concept of conformable fractional derivative has two significant advantages over classical fractional derivatives such as Caputo or Riemann-Liouville. Firstly, conformable fractional derivatives satisfy the most of the properties of the mathematical essential derivative, including Rolle's theorem, linearity, the fractional derivative of a constant function, product rule, quotient rule, chain rule, and power rule. Secondly, the conformable derivatives are useful for modelling many physical problems. It should be noted that differential equations with conformable fractional derivatives are computationally easier to solve compared to those using Caputo or Riemann-Liouville fractional derivatives. Some recent works on this new fractional derivative are presented by several authors in literature.

In this work, we examine a novel type of system known as conformable fractional 2D Roesser models. Then, we study the discretization of the double conformable fractional derivative and the effect of the discretization step value on the positivity of continuous fractional conformal Roesser models.

2. CONTENT

Let's us consider the 2D conformable fractional continuous time system described by the Roesser models

$$\begin{bmatrix} T_{t_1}^{\alpha} x^h(t_1,t_2) \\ T_{t_2}^{\beta} x^v(t_1,t_2) \end{bmatrix} = \begin{bmatrix} A_{11} & A_{12} \\ A_{21} & A_{22} \end{bmatrix} \begin{bmatrix} x^h(t_1,t_2) \\ x^v(t_1,t_2) \end{bmatrix} + \begin{bmatrix} B^h \\ B^v \end{bmatrix} u(t_1,t_2)$$

Where $x^h(t_1,t_2) \in R^{n_1}$, $x^v(t_1,t_2) \in R^{n_2}$ are respectively the horizontal and the vertical state vectors, $0 < \alpha \leq 1$ and $0 < \beta \leq 1$, $E \in R^{n \times n}$ is the singular matrix of the system with $0 \leq rank(E) \leq 1$, $u(t_1,t_2) \in R^m$ is the input vector, $B^h \in R^{n_1 \times m}$, $B^v \in R^{n_2 \times m}$, $A_{11} \in R^{n_1 \times n_1}$, $A_{12} \in R^{n_1 \times n_2}$, $A_{21} \in R^{n_2 \times n_1}$, $A_2 \in R^{n_2 \times n_2}$ and $n_1 + n_2 = n$. The boundary conditions are $x^v(t_1,0)$ And $x^h(0,t_2)$.

We use the conformable fractional derivative to describe Darboux equation, which is used to simulate gas absorption, water stream heating, and air drying,

$$T_{t_1,t_2}^{\alpha,\beta} s(x,t) = a_1 T_{t_2}^{\beta} s(x,t) + a_2 T_{t_1}^{\alpha} s(x,t) + a_0 s(x,t) + bf(x,t)$$

3. CONCLUSIONS

In this work, the necessary and sufficient conditions of a two-dimensional conformable fractional linear system described by the Roesser models has been established. The problems of the influence for the sampling step value on the positivity of the considered models and Darboux equation have been studied and proposed. These problems are very important when the modelling of a real problem goes through discretization because the modelled systems lose their positivity during discretization, and one would wonder why. Some interesting numerical examples are provided to demonstrate the applicability of the proposed methods.

ON THE ADMISSIBILITY OF FRACTIONAL SINGULAR ROESSER MODELS

Djillali BOUAGADA[1], Kamel BENYETTOU[2]

[1,2] Abdelhamid Ibn Badis University Mostaganem, Department of Mathematics and Computer Science, ACSY Team-Laboratory of Pure and Applied Mathematics, Faculty SEI-BP 227/118 Mostaganem 27000, Algeria.

Corresponding author email: djillali.bouagada@univ-mosta.dz[1] , kamel.benyattou.etu@univ-mosta.dz[2]

Abstract

This paper introduces a novel class of two-dimensional fractional singular systems described by Roesser continuous-time models. A new necessary and sufficient condition for asymptotic stability and admissibility using linear matrix inequalities are established. A numerical simulation for the obtained results through various examples to demonstrate the practicality and precision of our approach are presented. This work provides insights into the development of efficient and robust control strategies for fractional singular systems.

Key words*: Fractional systems, Singular systems, Fractional Roesser models, Stability, Admissibility of two-dimensional systems, Linear matrix inequality.*

1. INTRODUCTION

In recent decades, there has been a significant amount of interest in two-dimensional systems that has garnered attention from numerous researchers. The appeal of this class of systems lies in its potential for a diverse range of applications, such as modern circuit design, digital image and signal processing, mechanics, physics, and medical applications.

Roesser models are introduced by Giovanni-Roesser (1970s-1980s), and are the most commonly used models for two-dimensional linear systems. One of the distinctive characteristics of this model is its partitioning of the state vector into horizontal and vertical components. This class of systems has been the focus of recent research studies. It is worth noting that two-dimensional systems exhibit state propagation in two independent directions.

Stability analysis has been a subject of study in several research works, including Jury (1973), Sijlak(1975), Kaczorek(2009), Bouagada et al. (2011), Elosmani et al.(2021) concerning the two-dimensional systems. The stability analysis of both two-dimensional and multidimensional systems has been a topic of research for several decades. It is essential for the analysis of system robustness and finds application in engineering fields, such as circuit theory, digital filtering, and image processing.

In recent years, Kaczorek and Rogowski have introduced the singular fractional continuous Roesser models and their solutions using fundamental matrix in 2015, where they also demonstrated some of its applications. Furthermore, Marir et al. (2017) have recently investigated the admissibility problem for the one dimensional singular linear continuous-time fractional-order systems with $1 < \alpha \leq 2$.

This contribution investigates the admissibility of two-dimensional fractional singular continuous time-systems described by Roesser models using Caputo derivatives.

2. CONTENT

Let's us consider the 2D singular continuous time system described by the Roesser models

$$\begin{bmatrix} E_{11} & E_{12} \\ E_{21} & E_{22} \end{bmatrix} \begin{bmatrix} D_{t_1}^{\alpha} x^h(t_1,t_2) \\ D_{t_2}^{\beta} x^v(t_1,t_2) \end{bmatrix} = \begin{bmatrix} A_{11} & A_{12} \\ A_{21} & A_{22} \end{bmatrix} \begin{bmatrix} x^h(t_1,t_2) \\ x^v(t_1,t_2) \end{bmatrix} + \begin{bmatrix} B^h \\ B^v \end{bmatrix} u(t_1,t_2)$$

Where $x^h(t_1,t_2) \in R^{n_1}$, $x^v(t_1,t_2) \in R^{n_2}$ are respectively the horizontal and the vertical state vectors, $0 < \alpha \leq 1$ and $0 < \beta \leq 1$, $E \in R^{n \times n}$ is the singular matrix of the system with $0 \leq rank(E) \leq 1$, $u(t_1,t_2) \in R^m$ is the input vector, $B^h \in R^{n_1 \times m}$, $B^v \in R^{n_2 \times m}$, $A_{11} \in R^{n_1 \times n_1}$, $A_{12} \in R^{n_1 \times n_2}$, $A_{21} \in R^{n_2 \times n_1}$, $A_2 \in R^{n_2 \times n_2}$ and $n_1 + n_2 = n$. The boundary conditions are $x^v(t_1,0)$ and $x^h(0,t_2)$.

A new necessary and sufficient conditions for asymptotic stability and admissibility are then proposed and solved using the LMI approach.

3. CONCLUSIONS

In this paper, we have developed necessary and sufficient conditions for the stability and admissibility of 2D general singular fractional Roesser models. We have proposed a new approach that involves the Kronecker product, characteristic polynomial, and linear matrix inequality (LMI). To demonstrate the effectiveness and applicability of our approach, we have simulated and illustrated the results numerically using an electrical circuit application. Our method shows promising results and could have significant practical implications in the analysis and design of complex engineering systems.

ON THE POSITIVITY ANALYSIS OF THE THREE-DIMENSIONAL FRACTIONAL CONFORMABLE FORNASINI-MARCHESINI MODELS

Nisrine MILIANI[1], Djillali BOUAGADA[2], Kamel BENYETTOU[3]
[1,2,3] Abdelhamid Ibn Badis University Mostaganem, Department of Mathematics and Computer Science, ACSY Team-Laboratory of Pure and Applied Mathematics, Faculty SEI-BP 227/118 Mostaganem 27000, Algeria.

Corresponding author email: nisrine.miliani.etu@univ-mosta.dz[1] , djillali.bouagada@univ-mosta.dz[2] , kamel.benyattou.etu@univ-mosta.dz [3]

Abstract

In this work, we present, discuss and analyze the positivity problem of three-dimensional conformable fractional Fornasini-Marchesini models. The study aims to develop conditions for ensuring the non-negativity of system states and inputs in these models, which is important for ensuring the physical feasibility and stability of the system. We use mathematical methods and techniques based on Laplace transform to find the solution of the continuous Fornasini-Marchesini models with conformable derivatives and transition matrices to analyze the positivity of the models. We provide results and findings that can guide future research in this area. All the obtained results are simulated with numerical examples to demonstrate the applicability and accuracy of our approach.

Keywords: *Fractional linear system, Fornasini-Marchesini, Laplace transform, Conformable derivative, positivity, 3D Models*

1. INTRODUCTION

Three dimensional (3D) models appear and play a key role in several areas, more particularly in electrical engineering, mechanical and physics, control theory and also in digital and image processing, fluid dynamics. Note that 3D models propagate the information in three independent directions and they have received considerable research attention. In the field of control theory, the analysis and control of positive fractional three-dimensional systems often involves the use of mathematical models, such as state-space models, transfer function models, and others to describe the system dynamics.

In particular, the positivity analysis of fractional positive three-dimensional systems involves determining the conditions under which the system states and inputs remain non-negative, which is crucial for ensuring the physical feasibility and stability of the system.

In recent years there has been a growing interest to develop this class of models where the considered derivative is the conformable fractional derivative. In the first section the solution of this class of models by the use of the 3D Laplace transform has been derived. The following section is based on the positivity analysis of the 3D Fornasini- Marchesini Fractional continuous time linear model. The objective is to develop conditions that ensure the non-negativity of system states and inputs, which is crucial for maintaining the physical feasibility and stability of the system. Finally, some numerical examples are presented to illustrate the applicability of our results.

2. CONTENT

Let us consider the continuous 3D Fornasini-Marchenisi fractional (α, β, γ) order model described by the state-space equations.

$$\mathrm{T}^{\alpha,\beta,\gamma}\mathrm{x}(t_1,t_2,t_3) = A_0\mathrm{x}(t_1,t_2,t_3) + A_1T^{\alpha}_{t_1}\mathrm{x}(t_1,t_2,t_3) + A_2T^{\beta}_{t_2}\mathrm{x}(t_1,t_2,t_3) + A_3T^{\gamma}_{t_3}\mathrm{x}(t_1,t_2,t_3) + \mathrm{Bu}(t_1,t_2,t_3)$$

Where $x(t_1,t_2,t_3)\epsilon R^n$ is the state vector, $u(t_1,t_2,t_3)\epsilon R^m$is the input vector and $A_i\epsilon R^{n\times n}$, $i = 0,1,2,3$, $B\epsilon R^{n\times m}$, the boundary conditions $x(0,t_2,t_3)$ and $x(t_1,0,t_3)$ and $x(t_1,t_2,0)$ are given.

Through a rigorous mathematical analysis, we have established important results regarding the positivity properties of the considered models. We have shown that under certain conditions, the solutions preserve their positivity over time, ensuring the physical feasibility of the system dynamics. Additionally, we have derived explicit expressions for the positivity-preserving regions in the parameter space, providing valuable insights for system design and control.

3. CONCLUSIONS

The analysis of the positivity of three-dimensional fractional conformable Fornasini-Marchesini models has been developed. Based on the 3D conformable Laplace transform, a solution has been derived. We proposed a powerful tool for analyzing the non-negativity of system states and inputs for the considered models. Numerical examples were used to simulate and showcase the practicality and accuracy of our approach, illustrating the validity of the obtained results.

FERMATEAN FUZZY DIVERGENCES AND THEIR APPLICATIONS TO DECISION-MAKING AND PATTERN RECOGNITION

Wiyada KUMAM

Applied Mathematics for Science and Engineering Research Unit (AMSERU), Program in Applied Statistics, Department of Mathematics and Computer Science, Faculty of Science and Technology, Rajamangala University of Technology Thanyaburi (RMUTT), Pathum Thani 12110, Thailand

Corresponding author email: wiyada.kum@rmutt.ac.th

Abstract

Fermatean fuzzy sets (FFS) generalized the Intuitionistic fuzzy set and Pythagorean fuzzy set in terms of more space available to choose orthopairs. The manuscript provides Chi-square and Canberra divergence measures for FFSs. Divergence measurements' additional characteristics are looked into to ensure good performance. The entropy and dissimilarity measures from the suggested divergence measures are derived. A technique is developed to transform the real or fuzzy data into Fermatean fuzzy data. An empirically successful VIKOR method is extended for FFSs. The Australasian New Car Assessment Program (ANCAP) provides the star rankings from a safety point of view for each vehicle. The VIKOR method is employed to draw safety rankings of small cars tested from 2019 to 2021 by ANCAP. The numerical examples are given to clarify each method under discussion.

Key words*: fermatean fuzzy sets, decision making, divergence measures, VIKOR method, fuzzification technique*

Acknowledgment: *This research has received funding support from the NSRF via the Program Management Unit for Human Resources & Institutional Development, Research and Innovation [grant number B39G660025].*

A NOTE ON THE ACTIONS OF THE HECKE GROUP H(2)

Mircea CIMPOEAȘ[1,2]

[1]University Politehnica of Bucharest, 313 Splaiul Independentei, District 6, Bucharest, Romania
[2]Institute of Mathematics of the Romanian Academy, 21, Calea Grivitei, Bucharest, Romania

Corresponding author email: mircea.cimpoeas@imar.ro

Abstract

We study the action of the groups $H(\lambda)$ generated by the linear fractional transformations $x: z \mapsto -\frac{1}{z}$ and $w: z \mapsto z + \lambda$, where λ is a positive integer, on the subsets

$$Q^*(\sqrt{n}) = \left\{ \frac{a+\sqrt{n}}{c} : a, b = \frac{a^2-n}{c}, c \in Z \right\} \cup \{0,1,\infty\}$$

where $|n|$ is a square-free positive integer. We prove that this action has a finite number of orbits if and only if $\lambda = 1$ or $\lambda = 2$. Moreover, we give an upper bound for the number of orbits for $\lambda = 2$.

***Key words**: modular group, Hecke groups, quadratic field, group action, orbit*

1. INTRODUCTION

Erich Hecke introduced in [2] the groups $H(\lambda)$ generated by two linear fractional transformations

$$x: z \mapsto -\frac{1}{z} \text{ and } w: z \mapsto z + \lambda,$$

where λ is positive. He further showed that $H(\lambda)$ is discrete if and only if $\lambda = \lambda_k = 2\cos\left(\frac{\pi}{k}\right)$, where $k \geq 3$ is an integer, or $\lambda \geq 2$.

If $\lambda = \lambda_3 = 1$, then $H(1) = PSL(2, Z)$ is the modular group, which consists in all the transformations $z \mapsto \frac{az+b}{cz+d}$ with $a, b, c, d \in Z$ and $ac - bd = 1$.

The actions of the modular group on many discrete and non-discrete structures play significant roles in different branches of mathematics. Among these structures upon which the modular group acts are subsets of quadratic number fields. In [4], Q. Mushtaq studied the action of $PSL(2, Z)$ on the subset

$$Q^*(\sqrt{n}) = \left\{ \frac{a+\sqrt{n}}{c} : a, b = \frac{a^2-n}{c}, c \in Z \right\} \cup \{0,1,\infty\},$$

where $n \geq 2$ is a square-free integer. Subsequent works by several authors considered properties emerging from this action; see for instance [5] and [3].

The aim of our paper is to study the action of the groups $H(\lambda)$, where $\lambda \geq 1$ is an integer, on the subsets $Q^*(\sqrt{n})$, where $|n|$ is a square-free positive integer, tackling both the cases $n > 0$ and $n < 0$.

We prove that the action of $H(\lambda)$ on $Q^*(\sqrt{n})$ has a finite number of orbits if and only if $\lambda \in \{1,2\}$; see Theorem 1. For $\lambda = 2$ we give an upper bound for the number of orbits; see Theorem 2.

This presentation is based on a recent paper; see [1].

2. CONTENT

The main results of our paper are the following:

Theorem 1. Let $\lambda \geq 1$ be an integer. The action of $H(\lambda)$ on $Q^*(\sqrt{n})$ has a finite number of orbits if and only if $\lambda \in \{1,2\}$.

Theorem 2. The number $o(n)$ of orbits of the action of $H(\lambda)$ on $Q^*(\sqrt{n})$ is:

(1) $o(n) \leq \sum_{j=0}^{\left\lfloor \sqrt{\frac{n}{2}}-1 \right\rfloor} d(n-j^2)$, if n<0,

(2) $o(n) \leq \sum_{j=0}^{n} d(n-j^2)$, if n>0,

where $d(n)$ is the the number of integer divisors of n.

3. CONCLUSIONS

We proved that the action of the Hecke group $H(\lambda)$ on $Q^*(\sqrt{n})$ has a finite number of orbits if and only if $\lambda \in \{1,2\}$ and for $\lambda = 2$ we give an upper bound for the number of orbits arising from the respective action. Further research should be done in order to compute the exact number of orbits.

Bibliography

[1] M. Cimpoeas, *A note on the action of the Hecke group H(2) on subsets of the form* $Q^*(\sqrt{n})$, J. Algebra Appl. 22 (2023), no. 6, Paper No. 2350218, 5 pp.

[2] E. Hecke, *Uber die bestimmung dirichletscher reihen durch ihre funcktionalgleichung*, Math. Ann. **112** (1936), 664-699.

[3] M. Aslam Malik, M. Riaz, *Orbits of* $Q(\sqrt{k^2m})$ *under the action of the modular group* $PSL(2,Z)$, U.P.B. Sci. Bull. Series A **74** (2012), 109-116.

[4] Q. Mushtaq, *Modular group acting on real quadratic fields*, Bull. Austral. Math. Soc. **37** (1988), 303-309.

[5] Q. Mushtaq, *On word structure of the modular group over finite and real quadratic fields*, Disc. Math. **178** (1998), 155-164.

A MATHEMATICAL MODEL FOR ALLERGIC REACTIONS INDUCED BY THE THERAPY OF HIV

Rawan ABDULLAH[1], Florin AVRAM[2] Andrei HALANAY[3], Rodica RADULESCU[4]

[1]University Politehnica of Bucharest, 313 Splaiul Independentei, District 6, Bucharest, Romania
[2]Laboratoire de Mathematiques Appliquees, Universite de Pau, 64000, Pau,
[3]Department of Mathematical Methods and Models, University Politehnica of Bucharest

Corresponding author email: rawan.b.abdullah@gmail.com

Abstract

We develop a competition model that describes the cells of the immune system involved in allergies and the evolution of HIV infected cells during specific drug therapy.
Cell evolution is modelled using delay differential equations. Some properties of the solutions, as essential non-negativity and global existence are proved. The functioning of the immune system, as well as the HIV treatment avoiding allergic reactions induced by the medication, are then assessed through partial stability analysis and numerical simulations.

***Key words**: HIV pathogenesis model, immune system, CD4+T cells, cytotoxic T lymphocytes (CTLs)*

1. INTRODUCTION

The HIV epidemic remains a significant global health challenge, despite advancements in science and interventions. HIV is transmitted through activities like sexual contact, breastfeeding, and sharing needles with infected individuals. The virus targets and weakens the immune system, leading to acquired immunodeficiency syndrome (AIDS), a late-stage condition that often results in death.

Key players in the immune response against HIV include:

- CD8+ cytotoxic T lymphocytes (CTLs) play a crucial role in killing infected cells.
- Antigen-presenting cells (APCs), such as dendritic cells and macrophages, consume infected cells and present antigens on their surface.
- CD4+ T cells, also known as helper T cells (Th), have various roles, including activating innate immune cells, B lymphocytes, CTLs, and suppressing immune reactions. They are the primary targets of the HIV virus.

When foreign cells are detected, they are transported to the lymph nodes, where APCs interact with them and present antigens. Healthy naive CD4+ T cells recognize these antigens and undergo maturation and differentiation into specific subsets (e.g., Th1, Th2, Treg).

Cytokines play a crucial role in stimulating the production of virus-specific CTLs, which target and eliminate infected CD4+ T cells. However, CTLs can be destroyed or become anergic (non-responsive) due to interactions with infected cells.

Treatment of HIV infection involves the use of antiretroviral drugs (ARVs). There are several classes of ARVs, including NRTIs, NNRTIs, PIs, integrase inhibitors, fusion inhibitors, and CCR5 inhibitors. Highly active antiretroviral treatment (HAART) combines multiple drugs from different classes to

increase effectiveness and reduce the likelihood of drug resistance. HAART has transformed HIV into a manageable chronic disease in many countries, reducing HIV-related mortality and morbidity. However, these medications can have significant side effects, including drug reactions and hypersensitivity.

2. THE MATHEMATICAL MODEL

The mathematical framework used to model the behaviour and interactions of immune cells and other components during allergic responses and viral infections, specifically in the context of therapeutic interventions is a system of 11 delay differential equations,.

The first six equations describe the temporal behaviour of immune cells following the administration of allergens related to HAART and are conjectured to model the evolution of immune cells during therapy. The variables in these equations represent the concentrations of Th1, Th2, Treg cells (T1, T2, and Tr, respectively), naive T helper cells (N), immature and mature APCs.

The subsequent five equations in the model represent the evolution of key actors involved in viral infection under treatment. These include uninfected mature CD4+ T cells (H), infected CD4+ T cells (H'), free viruses (V), effector cells CTLs (cytotoxic T lymphocytes) (C) and the drug dosage (D).

3. RESULTS

We created a mathematical model that predicts the evolution of CD4+naïve cells, Th cells, APCs, cytokines and the HIV infection under treatment. The model's uniqueness stems from a more extensive examination of the biological mechanism.

Another significant enhancement over the current literature is the inclusion of temporal delays. These aid in capturing the correct timing of biological processes.

Existence, boundedness, and partial stability of solutions are investigated mathematically. As we are modelling cell populations, the positivity of solutions is an important study to conduct.

The numerical simulations we ran validate the theoretical conclusions, demonstrating that a little quantity of allergen does not harm in HIV treatment.

In our simulations, we also show how the Th2/Th1 ratio decreases during treatment near the equilibrium points E1, E2, E3 & E4, indicating that the concentration of Th1 outnumbers the concentration of Th2.

FIXED POINT TECHNIQUES FOR APPROXIMATION SOLUTION OF NONLINEAR PROBLEMS BEYOND NORMED SPACES

Poom KUMAM[1], Sani SALISU[2]

[1]Center of Excellence in Theoretical and Computational Science (TaCS-CoE) & KMUTT Fixed Point Research Laboratory, Room SCL 802, Fixed Point Laboratory, Science Laboratory Building, Departments of Mathematics, Faculty of Science, King Mongkut's University of Technology Thonburi (KMUTT), 126 Pracha-Uthit Road, Bang Mod, Thung Khru, Bangkok 10140, Thailand
[2]Department of Mathematics, Faculty of Natural and Applied Sciences, Sule Lamido University Kafin Hausa, Jigawa, Nigeria

Corresponding author email: poom.kum@kmutt.ac.th

Abstract

Many real-life problems are represented through mathematical models that often involve nonlinear mappings in the form of equations, inclusions, or even inequalities. In most cases, these scenarios can be transformed into optimization problems with a certain functional. If the functional possesses certain properties, such as being continuously differentiable or convex, then there are several existing approaches to solving the problem. However, many practical problems may not have such properties. Some may possess the convexity property, where the notion of subdifferential plays a significant role. In all cases, the minimization problem, the variational inequality problem, equilibrium problem and inclusion problem are substantial for accommodating many practical problems. However, this problem requires fixed-point theory to be fully understood and solved. As such, fixed point techniques remain active area of research and most of the approximation methods for the mentioned problems rely on fixed-point techniques. In this talk, we will discuss some of the basic fixed-point techniques for the problems, along with certain research directions.

Key words*: equilibrium problem; fixed point; nonexpansive mapping; minimization problem; monotone inclusion problem; projection and proximal operators; variational inequality problem*

1. INTRODUCTION

From a practical point of view, many problems arise as constrained optimization problems where concepts such as convexity, linearity, and differentiability play significant roles. In a linear setting, let's say $(H, \langle\cdot,\cdot\rangle)$, these problems are typically formulated in one of the following ways:

- Minimization problem; find $u \in H$ such that $f(u) \leq f(w)$ for all $w \in H$. (MN)
- Variational inequality problem; find $u \in C \subseteq H$ such that $\langle Au, w-u\rangle \geq 0$ for all $w \in C$. (VIP)
- Equilibrium problem; find $u \in H$ such that $F(u,w) \geq 0$, for all $w \in H$. (EP)
- Inclusion problem; find $u \in H$ such that $0 \in Bu$. (IP)

Generally, these problems are related to each other, in which we can always obtain one from another under suitable conditions. For instance, if f is smooth and convex, then (MN) is equivalent to (VIP) for $A = \nabla f$. Similarly, solutions set of (VIP) coincides with solution set (EP) when $F(x,y) = \langle Ax, y-x\rangle$.

It has been established in the literature that fixed points of certain substantial nonexpansive operators solve the aforementioned problems. In this regard, when f is a proper, convex, and lower semicontinuous function, then the solution set of (MN) coincides with the fixed points set of the proximal operator of f. For the metric projection of H onto C, denoted as P_C, the solution set of (VIP) coincides with the fixed points set of $P_C(I-\lambda A)$. In a similar fashion, there is a proximal (or resolvent) operator for which its fixed points set coincides with the set of solutions of (EP) (or (IP)). These, among other reasons, make fixed-point techniques prominent in approximating solutions to any of these problems. Thus, the famous Picard iteration, Krasnoselskii iteration, Mann iteration, and their modifications are employed to solve the problem. Recently, researchers have extended the study of such problems from a linear setting to geodesic spaces, considering the flexibility of the spaces, especially Hadamard spaces.

2. NONLINEAR PROBLEMS IN GEODESIC SPACES

A substantial feature of geodesic spaces is that nonconvex, constrained, and nonsmooth problems can be viewed, respectively, as convex, constrained, and smooth problems in the context of geodesics. This makes the setting more suitable for solving optimization problems. Furthermore, metric projections, proximal operators, and resolvent operators are well-defined in Hadamard spaces under appropriate conditions. The problems (MN) and (EP) are as defined in Section 1, while the (VIP) is defined based on the notion of quasilinearization, and (IP) requires the notion of tangent spaces, where a zero point is defined. These spaces possess various features of Hilbert spaces. Additionally, a point description of element of geodesic segments denoted by 'oplus', geodesic convexity of the distance, and the CN-inequality are crucial. Quasilinearization provides an inner product in metric settings. Detailed studies on these topics can be found in the attached references, as well as the references therein.

Regarding the (VIP) in the general setting of Hadamard spaces, with the underlying operator denoted as A, it coincides with the classical (VIP) on an inner-product space by setting $A \equiv I - T$. This type of problem is closely related to the formulation of the viscosity iteration and is of special interest. So far, it has only been considered with a few known mappings, such as the case of inverse strongly monotone mappings. However, it is evident that in the linear case, more general mappings (e.g., monotone) have numerous applications that have led to extensive research in this direction. Therefore, it is natural to inquire about the (VIP) when the mapping is at least monotone. In this context, the idea of the Korpelevich extragradient scheme becomes relevant. The scheme takes the form of $y_k = P_C((1-\alpha)x_k \oplus \alpha A x_k)$ and $x_{k+1} = P_C\big((1-\alpha)x_k \oplus \alpha T y_k\big)$ where A is the underlying operator and T satisfies certain conditions. Using this scheme, a Δ-convergence result can be achieved.

3. CONCLUSIONS

The extragradient scheme gives a step towards investigating a monotone-type of (VIP). Moreover, the general study of nonlinear problems through fixed point approaches lacks richness in unique geodesic spaces, despite the spaces being suitable for solving optimization. It is important to note that a complete Romanian manifold of non-positive curvature is a special case within this context, with numerous applications documented in the literature. The attached references provide guidance towards recent discoveries in this field.

References

[1] P. Chaipunya and **P. Kumam**, Nonself KKM maps and corresponding theorems in Hadamard manifolds, Appl. Gen. Topol. **16**(1) (2015), 37--44.

[2] **P. Kumam** and P. Chaipunya, Equilibrium problems and proximal algorithms in Hadamard spaces, J. Nonlinear Anal. Optim. **8**(2), (2017), 155--172.

[3] P. Chaipunya, F. Kohsaka, and **P. Kumam**, Monotone vector fields and generation of nonexpansive semigroups in complete CAT(0) spaces, Numer. Funct. Anal. Optim. **42**(9) (2021), 989–1018.

[4] P. Chaipunya and **P. Kumam**, On the proximal point method in Hadamard spaces, Optimization **66**(10) (2017), 1647--1665.

[5] S. Salisu, **P. Kumam**, and S. Sriwongsa, One step proximal point schemes for monotone vector field inclusion problems, AIMS Math. {\bf 7} (2022), no.~5, 7385--7402.

[6] S. Salisu, **P. Kumam**, S. Sriwongsa, and J. Abubakar, On minimization and fixed point problems in Hadamard spaces, Comput. Appl. Math. **41**(3) (2022), Paper No. 117, 22 pp.

[7] S. Salisu, **P. Kumam**, and S. Sriwongsa, Convergence theorems for monotone vector field inclusions and minimization problems in Hadamard spaces. Analysis and Geometry in Metric Spaces, **11**(1) (2023), 20220150.

[8] S. Salisu, **P. Kumam**, and S. Sriwongsa, On Fixed Points of Enriched Contractions and Enriched Nonexpansive Mappings, Carpathian Journal of Mathematics, **39**(1) (2023), 237-254

A boosted Salp Swarm optimization algorithm through the employment of Chaos Theory

Meriem NACER[1], Tayeb HAMAIZIA[2]

[1]University of Brothers Mentouri Constantine 1, Constantine, Algeria
[2]"Brothers Mentouri" University of Constantine 1, Constantine, Algeria

Corresponding author email: Souhilanacer24@gmail.com

Abstract

The salp swarm algorithm mimics the swarm behavior of salps during navigation and hunting, which has been shown to outperform the search for the optimal solution. Despite its adequate global search capability, it is nevertheless worth paying attention to issues such as falling into local optima and reduced convergence precision. Based on chaos theory, this study proposes various enhancements to the salp swarm algorithm. Chaos is one of the most prominent mathematical approaches employed to boost the performance of this type of algorithm. Using multimodal benchmark test functions, the suggested approach is assessed. The comparative results reveal that the CSSA greatly improves the SSA algorithm's performance.
Keywords*: Optimization; metaheuristics; swarm intelligence; salp swarm algorithm; chaos theory.*

1. INTRODUCTION

Meta-heuristic algorithms have recently grown remarkably popular. This is owing to their shown superiority in tackling numerous optimization challenges. Swarm intelligence (SI) algorithms are a particularly strong category among them; they are based on the swarming behavior of biological species when looking for food, fleeing predators, or surviving. The Salp Swarm system (SSA) is a new swarm intelligence system that simulates the foraging behavior of sea swarm slaps. The SSA is essentially a random search optimization method. It suffers from low precision in the later stages of iteration and it is prone to get trapped at local optima. SSA's searching behavior as a meta-heuristic algorithm is divided into two major phases: exploration and exploitation. During the exploration phase, it can effectively discover the search space mostly by randomness, although it may encounter unexpected changes. It converges toward the most promising region during the exploitation phase. However, due to its stochastic character and lack of balance between exploration and exploitation, SSA frequently traps into local optima. As a result, several studies have been presented since this time to improve the performance of SSA and overcome these flaws. We used a chaotic mapping sequence to replace the random parameter in this work, which considerably increased the convergence rate and SSA precision.

2. CONTENT

2.1 CHAOTIC SALP SWARM ALGORITHM (CSSA)

2.1.1 POPULATION INITIALIZATION BASED ON CHAOTIC MAPPING

The core of the swarm intelligence algorithm is the continuous iteration of the population, so the initialization of the population has a direct impact on the final solution and also affects the optimization ability. The more abundant and diverse the initialized population is, the more favorable it will be to find the global optimal solution for the population. Without the help of prior knowledge, most swarm intelligence algorithms are basically random population

initialization, which greatly affects their performance. The chaotic sequence has the characteristics of ergodicity and randomness, and the population initialization by a chaotic sequence can have better diversity. The chaotic sequences commonly used at present are iterative mapping, tent mapping, logistic mapping, etc. Through comparative study, Logistic mapping is used to perform population initialization in this work. The Logistic mapping mathematical formula is:

$$L^i_j = 4 \times L^i_j (1 - L^i_j) . \quad (1)$$

Where i = 1, 2, . . . , N represents the population size, j = 1, 2, . . . , D represents the ordinal number of chaotic variables. After tent mapping, the initialization formula of the population becomes:

$$X^i_j = L^i_j \times (ub_j - lb_j) + lb_j. \quad (2)$$

Where the initial value is set to 0.7.

- **2.1.2 CHAOTIC PARAMETERS**

The original SSA has mainly three main parameters which affect its performance. These parameters are r1, r2, and r3. It noticed that r2 and r1 are the two main parameters influencing the updating position of a salp. Thus, they significantly impact the balance between exploration and exploitation. In this study, a tent map is employed to adjust an r2 parameter of SSA. Equation 3 shows the updating of the r2 parameter according to the Logistic map.

$$r2 = L^{l+1}. \quad (3)$$

Where l represents the iteration.

- **RESULTS**

The performance of the newly developed variant of CSSA was tested over a set of two benchmark problems with different characteristics. we apply CSSA for each function. Results of all algorithms are recorded for a population of 30 and a maximum iteration of 500. The reported results are mean of 30 evaluations. The two functions are :

$F_1(x) = -\cos(x_1)\cos(x_2)e^{-((x_1-\pi)2-(x_2-\pi)2)}$, $F_2(x) = -^{2m}$

		SSA	CSSA
F_1	Best value	-1.000	-1
	Worst value	-1.000	-1
	(x,y)	(3.1416, 3.1416)	(3.1416, 3.1416)
	Number of iteration	500	200
	T/s	1.839424	1.778223
F_2	Best value	-1.8012	-1.8013
	Worst value	-1.8012	-1.8013
	(x,y)	(2.2022, 1.5707)	(2.2023, 1.5708)
	Number of iteration	500	150
	T/s	1.939353	1.895830

3. CONCLUSIONS

This work has investigated an enhanced and effective version of the SSA called 88 CSSA. The proposed variant is based on a chaotic map (Logistic), which is successively incorporated with the basic SSA to perform population initialization. The proposed Chaotic Salp Swarm Algorithm (CSSA) is applied on 2 test benchmark functions and compared with standard SSA. The computational results show that our proposed algorithm, CSSA, can yield better results for the two different types of test functions.

ANALYSIS OF STABILITY AND SUPERSTABILITY OF POSITIVE CONFORMABLE SINGULAR CONTINUOUS TIME LINEAR SYSTEMS

Amina FARAOUN[1], Djillali BOUAGADA[2]

[12] Department of Mathematical and Computer Science, ACSY Team LMPA
[2]"Abdelhamid Ibn Badis University (UMAB), P. O. Box 227 University of Mostaganem, 27000 Mostaganem, Algeria
amina.faraoun.etu@univ-mosta.dz, djillali.bouagada@univ-mosta.dz

Abstract

The objective of this paper is the resolution of new singular linear continuous-time systems based on a new derivative, called conformable by the applications of Weierstrass-Kronecker decomposition and using an efficient integral transform which is conformable fractional Sumudu transform. A new approach is applied and the solution of the proposed method is presented. The analysis of positivity is given and a new condition is established, Moreover, the stability and superstability of this positive system are also described and expressed. In order to show the accuracy of the result obtained some illustrative examples are presented in the last section.

Keywords*: singular systems; conformable fractional derivative; conformable fractional Sumudu transform; Weierstrass -Kronecker decomposition method; positivity; stability; superstability.*

1. INTRODUCTION

Positive systems have seen active growth for many years. The fundamental property of these systems is that the state trajectory is entirely in the non-negative orthant if the initial state is non-negative (or positive). Positive linear systems are frequently referred to be the active research field of mathematics due to its application in various fields of engineering, management science, social sciences, economics, biology, and medicine. Moreover, one of the most important components of linear systems is stability, which describes the reaction behavior of the system at infinity with respect to disturbances in the initial conditions. The notion of superstability is also an essential element in control theory. Superstable systems are a class of systems where the norm of the state vector monotonically decreases to zero, these are a specific kind of stable systems with more constrained dynamics requirements.

Fractional order systems have generated considerable interests in numerous fields of engineering, applied sciences and control theory. Nevertheless, the conformable derivative operator is a novel derivative operator that has been proposed by Khalil et al in 2014 and took part in many different areas as engineering, finances, biology, medicine, physics and applied mathematics. The greatest benefits of this derivative is that it preserves the properties of the classic derivatives, more than that, conformable derivative does not contain any integral terms, that make it much more easier to apply on the fractional differential equations.

In control theory, several authors have attempted to define the Weierstrass-Kronecker decomposition method in order to simplify the study of various concepts such as resolution, positivity, stability and superstability of singular systems. In the literature there are a number of works on the theory and applications of integral transforms such as the Laplace and Sumudu transforms that are proposed for resolving continuous-time systems. In 2019, the conformable Sumudu transform was presented by Al-Zhour et al. for the resolution of differential equation with conformable derivative.

In this work, we give the resolution of singular continuous-time linear systems using Weierstrass-Kronecker decomposition method and the conformable Sumudu transform. Necessary and sufficient

conditions for positivity and asymptotic stability are established. The notion of superstability is also proposed and determined. The numerical examples that illustrate the efficiency of our approach by using a Matlab code are also presented. Finally, we will provide some conclusions.

2. CONTENT

Consider the conformable singular continuous-time linear systems

$$\begin{aligned} ET^{\alpha}x(t) &= Ax(t) + Bu(t), \\ y(t) &= Cx(t) + Du(t), \end{aligned} \tag{1}$$

where $x \in \mathbb{R}^n$, $u \in \mathbb{R}^m$ and $y \in \mathbb{R}^p$ are, respectively, the state, the control, and the output of the system. $E, A \in \mathbb{R}^{n\times n}$, $B \in \mathbb{R}^{n\times m}$, $C \in \mathbb{R}^{p\times m}$ and $D \in \mathbb{R}^{p\times m}$. The boundary condition of the system is given by $x(0) = x_0$. The operator T^{α} represents the conformable derivative of order α with $0 < \alpha \leq 1$, and it is defined as follow

$$T^{\alpha}(x)(t) = \lim_{\varepsilon\to 0} \frac{x(t + \varepsilon t^{1-\alpha}) - x(t)}{\varepsilon}, \quad t > 0.$$

We will apply the Weierstrass-Kronecker decomposition on the system (1) and we use the conformable Sumudu transform. We will give the solution of conformable singular continuous-time linear using these approaches, then, we will study the analysis of this system (positivity, stability and superstability of this positive system).

3. CONCLUSIONS

In this paper, an alternative approach of computing the solutions of the conformable singular continuous-time linear systems is introduced. The key component of this approach is the Weierstrass-Kronecker method which is recognized for its important property in decomposition of the singular system in two subsystems. We have established a new solution of conformable singular systems by using conformable Sumudu transform. A sufficiently and necessary conditions for the positivity and asymptotic stability of positive conformable singular systems are also given. Then, the superstability of this positive system has been proposed and new conditions have been provided. Numerical examples are given for approved the results obtained.

ENHANCED DDOS ATTACK DETECTION USING NETWORK TRAFFIC ANALYSIS AND MACHINE LEARNING

George-Cătălin BARBU[1], Theodor COSTANTEA[2], Iulian-George ISAC[3], Laurențiu-Jan PREDESCU[1], Eduard-Ștefan SANDU[1], Emil SIMION[1], Ioan-Bogdan TOADER[2]

[1]University Politehnica of Bucharest, 313 Splaiul Independentei, Bucharest, Romania
[2]"Military Technical Academy "Ferdinand I", Bul. George Coşbuc nr. 39-49, Bucharest, Romania
[3]"Alexandru Ioan Cuza" University, Str. General Berthelot, no. 16, Iași, 700483, Romania

Corresponding author email: **gcatalinb@gmail.com**

Abstract

The paper is focused on a comprehensive system for DDoS attack detection and analysis. It consists of multiple modules that work together to ensure efficient data collection, preprocessing, feature extraction, model training, attack simulation, real-time detection, report generation, configuration, and storage of network traffic data.

Key words*: DDoS attack, ML, model training, simulation.*

1. INTRODUCTION

Distributed Denial of Service (DDoS) attacks are a special category of cyber attacks in which devices are compromised and used to overwhelm a target system, network, or website with a massive influx of illegitimate traffic. The goal of a DDoS attack is to disrupt the normal functioning of the target by exhausting its resources (e.g., bandwidth, processing power, or network connectivity). By coordinating attacks from multiple sources, DDoS attacks can make it difficult for the target to handle legitimate requests, resulting in service degradation or even complete unavailability.

In this paper, we propose a solution for mitigating this category of attacks. The proposed solution aims to detect and prevent Distributed Denial-of-Service (DDoS) attacks on a network. The main objectives of this solution are collecting data from the network traffic, preprocessing and extracting relevant features from this data, training and testing a machine learning (ML) model based on a dataset, simulating attacks for testing purposes, implementing the ML model for real-time detection of DDoS attacks, generating alerts and reports on detected attacks and their visualisation, configuring the system using a graphical user interface (GUI), and storing the collected data and logging them.

2. THE PROPOSED SOLUTION

The solution is composed of nine interconnected modules:

1. **Data Acquisition Module from Camera (Network Traffic)** is responsible for capturing network traffic data during simulations, uses packet sniffing techniques or network monitoring tools to collect raw network data and finally converts the captured data into a suitable format for further processing (pcap).
2. **Data Preprocessing Module (Filtering, Feature Normalisation),** performs initial pre-processing of the obtained network traffic data, includes tasks (such as data cleaning, filtering, and normalisation) and handles the extraction of features from network packets or flows.
3. **Relevant Feature Extraction Module from pcap** extracts relevant features from the pre-processed data of network traffic, focuses on features that can efficiently differentiate normal traffic

from DDoS attack patterns. examples of features may include packet rate, packet size, traffic volume, protocol distribution, etc.

4. **ML Model Training and Testing Module** on dataset prepares the dataset for training and testing the DDoS attack detection model, divides the collected data into training and testing sets and performs any necessary data augmentation or balancing techniques to improve the model's performance.
5. **Attack Simulation Module** simulates DDoS attacks to test the effectiveness of the detection model, configures and controls attack parameters (such as attack type, intensity, and duration) and sends attack traffic to the test network along with normal traffic for evaluation purposes.
6. **DDoS Detection Module implementing the ML Model (Classification, Alert Generation)** implements the trained model to perform real-time detection of DDoS attacks, classifies network traffic in real-time as normal or DDoS based on learned models, generates alerts or notifications for the detected attacks.
7. **Report Generation and Visualization Module** provides visualisations and reports on detected DDoS attacks and network traffic behaviour. presents real-time or historical analysis of attack incidents, traffic trends, and performance metrics and enables administrators to monitor and efficiently respond to detected attacks.
8. **Configuration Module (Parameter Modification) with GUI** allows users to configure and control various settings related to the DDoS attack detection system, enables customization of thresholds, detection rules, and alert mechanisms, provides a web interface for user interaction and system administration.
9. **Log and Collected Network Packet Storage Module** manages the storage and logging of obtained data, simulated attack logs, and system logs and stores captured network traffic data for later analysis or future references.

3. CONCLUSION

To sum up, our proposed solution offers a comprehensive approach to mitigate Distributed Denial of Service (DDoS) attacks. By combining data acquisition, preprocessing, feature extraction, machine learning model training, attack simulation, real-time detection, report generation, visualisation, configuration, and data storage, we have developed a robust system for effectively detecting DDoS attacks. The interconnected modules work together to provide users with valuable insights into attack incidents, traffic behaviour, and performance metrics, enabling them to respond promptly and efficiently. Our solution gives users the ability to customize and adjust the system to their own needs as a result of its user-friendly graphical interface. Overall, our solution significantly enhances network security and resilience against DDoS attacks.

4. REFERENCES

1. Mark Stamp, Corrado Aaron Visaggio, Francesco Mercaldo, Fabio Di Troia, *Artificial Intelligence for Cybersecurity*, ISBN 978-3-030-97087-1, Springer, 2022.
2. Michael Collins, *Network Security Through Data Analysis: Building Situational Awareness,* ISBN 978-1491962848, O'Reilly Media, 2017.
3. Clarence Chio, David Freeman, *Machine Learning and Security: Protecting Systems with Data and Algorithms,* ISBN 978-1491979907, O'Reilly Media, 2018.

A RANDOM MODEL FOR THE DYNAMICS OF ALLELOPATHY

Vicente J. BEVIA[1], Juan-Carlos CORTÉS[1], Ana MOSCARDO[1], Cristina Luisovna PÉREZ[1,2], Rafael-Jacinto VILLANUEVA[1]

[1] Universitat Politècnica de València, Camí de Vera, s/n, 46022 València, Spain

[2]Corresponding author email: cperdiu@upv.es

Abstract

In this contribution, we revisit a differential equation-based mathematical model for studying the dynamics of allelopathy. We consider the randomized version of the model and offer an analytical approach based on the Random Variable Transformation theorem and a computational method utilizing the Liouville equation to determine the distribution of the solution. To illustrate the applicability of the results obtained in this contribution, we calibrate some model parameters via inverse uncertainty quantification techniques using real-world data of alkaloid contents from leaching thornapple seed.

***Key words**: Allelopathy; Random Differential Equations; Model Calibration.*

1. INTRODUCTION

Allelopathy, although commonly associated with plant interactions, encompasses a wide range of interactions among diverse species, including microbes and even herbivores (Weir et al., 2004). In this biochemical phenomenon, plants release allelochemicals, which are specific biomolecules related to allelopathy. These compounds can exert both negative and positive effects on other susceptible species present in the surrounding environment. The significance of allelopathy is highlighted by the discovery of substantial quantities of these compounds in the soil that leads to the inhibition of nearby plant growth. These findings have prompted the search for active allelochemicals for use as bio-herbicides (Putnam and Duke, 1988; Soltys et al., 2013), thus deepening our understanding of this subject. Mathematics, and more particularly differential equations, have been used to propose multiple models to describe this phenomenon.

The model we studied in this work was first proposed by Min An et al. (Min An et al. 2003) and then generalized by ML Martins in 2006 (ML Martils 2006) This model is a system of first-order differential equations:

$$\begin{cases} A'_P(t) = -k_1 A_P(t) + g(t), \\ A'_E(t) = k_1\, A_P(t) - k_2\, A_E(t), \end{cases}$$

where $A_P(t)$ and $A_E(t)$ are the amount of allelochemicals present in the living plant, and in the environment at the time instant t, respectively. The coefficient $k_1 > 0$, is the rate of allelochemical release in the environment, $k_2 > 0$, is the rate of allelochemical dissipation in the environment and $g(t)$ is a squared wave function of allelochemical production impulses. The function $g(t)$ is represented in the Figure 1 below.

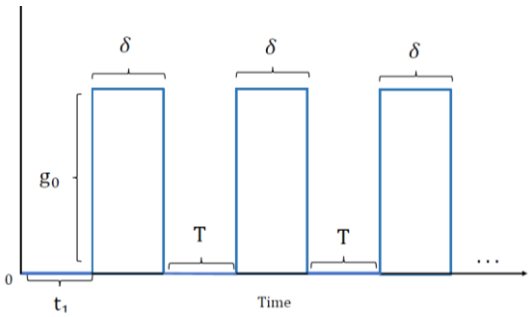

Figure 1: Graphical Representation of g(t).

In this work, we provide an exact solution to this system of equations and use the Random Variable Transformation technique to reformulate the model as a system of Random Differential Equations.

2. CONTENT

To account for the inherent uncertainties, present in the data and in the model itself, we randomized the model by assuming that model parameters, $k_1, k_{2,} g_0$ and $A_E(0)$ are continuous and positive random variables. We chose for each of them to follow a Uniform distribution (a non-informative distribution) since we had little to no information about their respective distribution shapes. We used the data from leaching thornapple seed (Lovett and Potts, 1987) to calibrate the model and obtain estimates for the distribution parameters of $k_1, k_{2,} g_0$ and $A_E(0)$. We then applied the Random Variable Transformation method to obtain the first probability density (1-PDF) function of $A_E(t)$, denoted as $f_{A_{E(t)}}(x)$ for a fixed time point t. The results, as seen in Figure 2, adjusted very well to the data, where even points that appeared as outliers and where not captured by the deterministic model, where captured by the tails of the distributions.

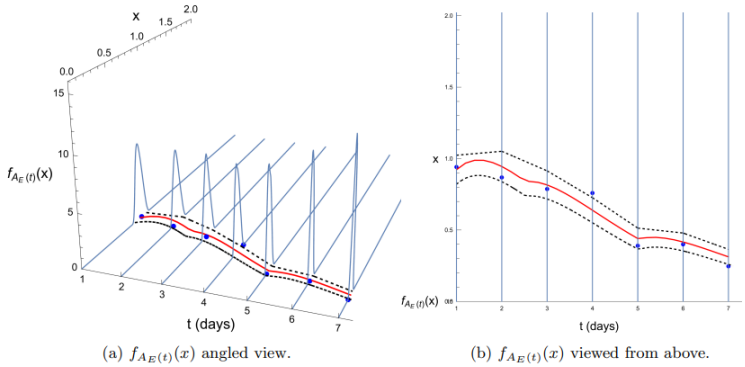

(a) $f_{A_E(t)}(x)$ angled view. (b) $f_{A_E(t)}(x)$ viewed from above.

Figure 2: 1-PDF of $A_E(t)$ (blue line), data (blue points), 95% confidence interval (dotted line), and mean (red line).

To further the analysis of the model we studied the joint probability density function of the non-trivial equilibrium points of the system. We found that the joint probability density function had an oval projection indicating the dependence of the equilibrium points. We also found that, as expected, the mean of the probability density functions of the solutions converge to the mean of the equilibrium points.

3. CONCLUSIONS

In this work we revised a deterministic model for allelopathy dynamics. We have then taken this solution from the deterministic world into the random one through the Random Variable Transformation method. This new random model has allowed us to describe some of the inherent uncertainties present in the data and the model itself. We have calibrated it with real-world data of leaching thornapple seed. The randomization of our model has successfully accounted for the uncertainties in the data and granted us an innovative perspective on the dynamics of allelopathy.

REFERENCES

Tiffany L Weir, Sang-Wook Park, and Jorge M Vivanco. “Biochemical and physiological 521 mechanisms mediated by allelochemicals”. In: Current Opinion in Plant Biology 7.4 (2004), 522 pp. 472–479.

Alan R Putnam. “Allelochemicals from plants as herbicides”. In: Weed Technology 2.4 (1988), 502 pp. 510–518.

JV Lovett and Wendy C Potts. “Primary effects of allelochemicals of Datura stramonium L.” 477 In: Plant and Soil 98 (1987), pp. 137–144.

Min An et al. “Mathematical modelling of allelopathy: II. The dynamics of allelochemicals435 from living plants in the environment”. In: Ecological Modelling 161.1-2 (2003), pp. 53–66

ML Martins. “Exact solution for the An–Liu–Johnson–Lovett model related to the dynamics483 of allelochemicals in the environment”. In: Ecological Modelling 193.3-4 (2006), pp. 809–814.

NONEXPANSIVE-TYPE MAPPINGS WITH VISCOSITY ITERATION IN HADAMARD SPACES

SANI SALISU[1,2], POOM KUMAM[1,3,*], SONGPON SRIWONGSA[1], WIYADA KUMAM[4]

[1]*Center of Excellence in Theoretical and Computational Science (TaCS-CoE) & KMUTT Fixed Point Research Laboratory,Room SCL 802, Fixed Point Laboratory, Science Laboratory Building, Departments of Mathematics, Faculty of Science, King Mongkut's University of Technology Thonburi (KMUTT), 126 Pracha-Uthit Road, Bang Mod, Thung Khru, Bangkok 10140, Thailand*

[2]*Sule Lamido University Kafin Hausa, Department of Mathematics, Faculty of Natural sciences, P.M.B 048, Jigawa, Nigeria*

[3]*Department of Medical Research, China Medical University Hospital, China Medical University, Taichung 40402, Taiwan*

[4]*Applied Mathematics for Science and Engineering Research Unit (AMSERU), Program in Applied Statistics, Department of Mathematics and Computer Science, Faculty of Science and Technology, Rajamangala University of Technology Thanyaburi (RMUTT), Pathum Thani 12110, Thailand.*

Abstract. Certain essential properties of a generalized nonexpansive mapping, showcasing an inclusion relation to known mappings within the framework of Hadamard spaces, are investigated in this work. Additionally, a viscosity-type algorithm is proposed for approximating fixed points of such mappings. The strong convergence of the sequences generated by this algorithm is demonstrated under appropriate assumptions. As an application of the findings, the existence of a solution to the variational inequality problem involving the mapping is established. Furthermore, an iterative scheme is derived, which exhibits strong convergence towards a solution of the variational inequality problem. To demonstrate the implementation of the proposed algorithm, a numerical example is provided in a non-Hilbert CAT(0) space.

Keywords. Convergence analysis; Fixed point; Hadamard space; Inverse strongly monotone; Nonexpansive mapping; Variational inequality; Viscosity iteration.

DEPTH AND SDEPTH OF POWERS OF THE PATH IDEAL OF A CYCLE GRAPH

Silviu BĂLĂNESCU[1], Mircea CIMPOEAȘ[1]

[1]University Politehnica of Bucharest, 313 Splaiul Independentei, District 6, Bucharest, Romania

Corresponding author email: silviubalanescu81@gmail.com

Abstract

Let $J_{n,m} := (x_1x_2\cdots x_m,\ x_2x_3\cdots x_{m+1},\ \dots,\ x_{n-m+1}\cdots x_n,\ x_{n-m+2}\cdots x_nx_1,\dots,x_nx_1\cdots x_{m-1})$ be the m-path ideal of the cycle graph of length \$n\$, in the ring $S = K[x_1,\dots,x_n]$. We prove several results regarding $depth(S/J_{n,m}^t)$ and $sdepth(S/J_{n,m}^t)$.

***Key words**: Stanley depth, depth, monomial ideal, cycle graph.*

1.INTRODUCTION

Let K be a field and $S = K[x_1,\dots,x_n]$ the polynomial ring over K in n variables. Let M be a multigraded S-module. A Stanley decomposition of M is a direct sum

$$\mathcal{D}: M = \bigoplus_{i=1}^{r} m_i K[Z_i]$$

as K-vector spaces, where $m_i \in M$ is homogeneous with respect to Z^n-grading, $Z_i \subset \{x_1,\dots,x_n\}$ such that $m_iK[Z_i] = \{um_i:\ u \in K[Z_i]\} \subset M$ is a free $K[Z_i]$-submodule of M.

We define $sdepth(\mathcal{D}) = \min_{i=1,\dots,r} |Z_i|$ and

$sdepth(M) = \max\{sdepth(\mathcal{D}) \mid \mathcal{D}$ is a Stanley decomposition of $M\}$.

The number sdepth(M) is called Stanley depth of M.

Herzog, Vladoiu and Zheng show in [1] that sdepth(M) can be computed in a finite number of steps if M=I/J, where $J \subset I \subset S$ are monomial ideals.

We say that a multigraded module M satisfies the Stanley inequality, if

$$sdepth(M) \geq depth(M).$$

Stanley [3] conjectured that any multigraded module satisfies the above inequality. This conjecture proves to be false in general, for M=S/I and M=J/I, where $J \subset I \subset S$ are monomial ideals, see Duval et al [2].

The explicit computation of the Stanley depth it is a difficult task, even in very particular cases, and it is interesting in itself. Also, although the Stanley conjecture was disproved in the most general set up, it is interesting to find large classes of ideals which satisfy the Stanley inequality.

The presentation is based on our preprint [1].

2. CONTENT

For $n \geq m \geq 1$, the m-path ideal of the path graph of length n is

$$I_{n,m} = (x_1x_2 \cdots x_m,\ x_2x_3 \cdots x_{m+1},\ \ldots,\ x_{n-m+1} \cdots x_n) \subset S.$$

The m-path ideal of the cycle graph of length n is

$$J_{n,m} = I_{n,m} + (x_{n-m+2}, \cdots, x_nx_1, x_{n-m+3} \cdots\ x_1x_2, \ldots, x_nx_1 \cdots\ x_{m-1}).$$

Let d=gcd(n,m) and let $t_0 \leq n-1$ maximal with the property that there exists an integer α such that

$$mt_0 = \alpha n + d$$

Our main results are the following:

Theorem 1. If d=1 then $sdepth(S/J_{n,m}^t) = depth(S/J_{n,m}^t) = 0$ for all $t \geq t_0$.
Also if d>1 then $depth(S/J_{n,m}^t) \leq d-1$ and $sdepth(S/J_{n,m}^t) \leq n - \frac{n}{d}$ for all $t \geq t_0$.
Our computer experiments yields us to conjecture that

$$sdepth(S/J_{n,m}^t) \geq depth(S/J_{n,m}^t) = d-1 \text{ for all } t \geq t_0.$$

Theorem 2. We have that

$$sdepth(S/J_{n,n-1}^t) = depth(S/J_{n,n-1}^t) = \begin{cases} n-t-1, t \leq n-1 \\ 0, t \geq n \end{cases}$$

Theorem 3. If n is odd then $sdepth(S/J_{n,n-2}^t) = depth(S/J_{n,n-2}^t) = 0$ for all $t \geq \frac{n-1}{2}$.
Also, if n is even then $\frac{n}{2} \geq\ sdepth(S/J_{n,n-2}^t) \geq\ depth(S/J_{n,n-2}^t) = 1$ for all $t \geq n-1$.

Theorem 4. If n=mt-1 then $sdepth(S/J_{n,m}^s) = depth(S/J_{n,m}^s) = 0$ for all $s \geq t$.

3. CONCLUSIONS

We proved several results regarding the depth and Stanley depth of powers of the m-path ideal of a cycle graph of length n. Also, we proposed several open questions which could be a topic for a further research.

Bibliography:

[1] S. Balanescu, M. Cimpoeas, *On the depth and Stanley depth of powers of the path ideal of a cycle graph*, https://arxiv.org/pdf/2303.15032 (2023), 18 pp.
[2] A.M Duval, B.Goeckneker, C.J.Klivans, J.L.Martine, *A non-partitionable Cohen-Macaulay simplicial complex, Advances in Mathematics*, **299** (2016), 381--395
[3] J. Herzog, M. Vladoiu, X. Zheng, *How to compute the Stanley depth of a monomial ideal*, Journal of Algebra **322(9)** (2009), 3151--3169.
[4] R. P. Stanley, *Linear Diophantine equations and local cohomology*, Invent. Math. **68** (1982), 175--193.

NEW APPLICATIONS FOR NLEES BASED ON ESTIMATION METHODS

Elena Corina CIPU[1,2,3], Cosmin Dănuț BARBU[2]

[1]University Politehnica of Bucharest, Centre for Research and Training in Innovative Techniques of Applied Mathematics in Engineering "Traian Lalescu" (CiTi), Bucharest, Romania
[2]Demographic Research Center Vladimir Trebici, INCE
[3]Department of Applied Mathematics, Faculty of Applied Sciences, University Politehnica of Bucharest

Corresponding author email: corina.cipu@upb.ro

Abstract

The existence of the solution and the dependence of conditions for solving some classes of nonlinear PDE is studied through estimation methods. Solitary wave solutions for Boussinesq-like equation and the Nonlinear Schrödinger equation (NLSE) using Extended rational Trigonometric methods and Kudryashov's R function method. The solutions obtained by expansion methods precised are graphically interpreted for different parameters and dependence of the initial conditions is discussed.

Keywords*: estimating of nonlinearities; nonlinear evolution PDE, extended rational trigonometric methods, Kudryashov's R function method*

EXTENDED ABSTRACT

For solitary solutions for NLEEs extended tangent method, extended rational trigonometric methods and Kudryashov's R function method is discussed looking for solutions of equation

$$F\left(u, u_t, u_x, u_{tt}, u_{xx}, \dots\right) = 0 \quad (1)$$

where F is polynomial in $u(x,t)$ and its partial derivatives involve nonlinear terms.

For *extended Tangent method* wave transformation

$$u(x,t) = U(v), v = x - Vt \quad (2)$$

is used and the equation to be solved becames:

$$P\left(U, U', U'', \dots\right) = 0. \quad (3)$$

Suppose that the solution of (2) has the form

$$U(v) = a_0 + \sum_{i=1}^{N} \left(a_i y^i + b_i y^{-i}\right) \quad (4)$$

$(a_i)_i, (b_i)_i$ are constants that are determined such that y satisfy the Riccati equation $(a_N, b_N \neq 0)$

$$y' = b + y^2 \quad (5)$$

I. $b < 0,\ y = -\sqrt{-b}\tanh\left(\sqrt{-b}v\right)$ or $y = -\sqrt{-b}\coth\left(\sqrt{-b}v\right)$

II. $b > 0, y = \sqrt{b}\mathrm{tg}\left(\sqrt{b}v\right)$ or $y = -\sqrt{-b}\,\mathrm{ctg}\left(\sqrt{b}v\right)$

III. $b = 0, y = -\frac{1}{v}$

the integer N is determined in (3) by balancing the hightest order derivatives and the nonlinear terms. Collecting all the terms of the same power of y and equating with zero an algebraic equation system is obtained for the constants $(a_i); (b_i), i \in \overline{1, N}$. The solution for (3) could be written using the constants just determined.

For *rational Trigonometric method* with the same notation (2) the solutions of many nonlinear equations such as Boussinesq equation

$$u_{tt} - (6u^2 u_x + u_{xxx})_x = 0 \quad (6)$$

and Hirota equations

$$\left(\frac{1}{2} - 3\alpha_3 V\right)u'' + \left(\alpha_3 V^3 - \frac{1}{2}V^2 - \mathrm{k}\right)u + (1 - 6\alpha_3 V)u^3 = 0 \quad (7a)$$

$$-\alpha_3 u''' + (3\alpha_3 V^2 - V - q)u' - 6\alpha_3 u^2 u' = 0 \quad (7b)$$

obtained from SH equation:

$$\mathrm{i}\psi_z + \psi_{tt} + |\psi|^2\psi - \mathrm{i}\alpha_3\psi_{ttt} - 6\mathrm{i}\alpha_3|\psi|^2\psi_t = 0 \quad (8)$$

and assuming a travelling wave solution of the form

$$\psi(z,\mathrm{t}) = u(x)\mathrm{e}^{\mathrm{i}(\mathrm{k}z - Vt + \theta)} \quad (9)$$

can be expressed in the form:

$$u(v) = \frac{a_0 \sin(\mu v)}{a_2 + a_1 \cos(\mu v)},\ \cos(\mu v) \neq -\frac{a_2}{a_1},$$

or in the form

$$u(v) = \frac{a_0 \cos(\mu v)}{a_2 + a_1 \sin(\mu v)},\ \sin(\mu v) \neq -\frac{a_2}{a_1},$$

where a_0, a_1 and a_2 are parameters that will be determined, and μ and V are the wave number and the wave speed, respectively.

We substitute Equation (10) or (11) into the reduced equation obtained above in Equation (7). Then by equating each coefficient of all terms with the same power in $\cos^m(\mu\xi)$ or $\sin^m(\mu\xi)$ to zero, we obtain a set of algebraic equations for a_0, a_1, a_2, c and μ. By solving the system of equations and substituting a_0, a_1, a_2, c and μ into Equation (8) or (9), we can get a variety of exact solutions for Equation (5).

For *Kudryashov's R function method* the function $R(z)$ defined as $R(z) = \frac{1}{ae^{\alpha z} + be^{-\alpha z}}$, where a, b and α are parameters of the function. The logistic function $R(z)$ is a solution of the differential equation:

$$R_z^2 = \alpha R^2(1 - \chi R^2),$$

where $\chi = 4ab$. It has a pole of the first order on the complex plane and its maximum is at $z = 0$ with maximum value given by $(a + b)^{-1}$. The Kudryashov function $R(z)$, satisfying the differential Equation (2), further has the property that its higher-order even derivatives are all expressible in terms of polynomials of R. However, its higher (odd)-order derivatives are polynomials of R and R_z. The last feature distinguishes the function R from the function Q of the Kudryashov method which is usually taken as the solution of the Riccati equation $Q_z = Q^2 - Q$ or $Q_z = Q^2 - 1$. The study for (7b) is made in two cases: $V = \frac{1}{6\alpha_3}$, $k = -\frac{1}{3}V^2 = -\frac{1}{108\alpha_3^2}$ and $6\alpha_3 V - 1 \neq 0$.

CONCLUSIONS

Estimations methods are coming in the paper through extended Tangent and extended rational Trigonometric methods or Kudryashov's R function method for finding wave solutions of the Schrödinger-Hirota and Boussinesq type equation. The Kudryashov function *R* satisfies a first-order second degree ODE and provides an efficient tool for symbolically calculating solitary wave solutions of nonlinear PDEs through their travelling wave reductions. Comparisons between solutions for different methods are made.

BIBIOGRAPHY

[1] M. T. Darvishi, M. Najafi, A. M. Wazwaz, *New extended rational trigonometric methods and applications*, Waves in Random and Complex Media, Vol 30, NO. 1, 5–26, Taylor & Francis, 2020, Doi: 10.1080/17455030.2018.1478166

[2] Jayita Dan, Sharmistha Sain, A. Ghose-Choudhury, Sudip Garai, *Solitary wave solutions of nonlinear PDEs using Kudryashov's R function method*, Journal of Modern Optics, 67:19, 1499-1507, 2021, Taylor & Francis, Doi:10.1080/09500340.2020.1869850

[3] Yusufoglu E. and Bekir A., *On the extended tanh method applications of nonlinear equations*, Int. Journal of Nonlinear Science, Vol.4(2007), No.1, pp10-16.

[4] Parkes E.J. *Comments on the use of the tanh-coth expansion method for finding solutions to nonlinear evolution equations*, 2009, Applied Mathematics and computation, doi: 10.1016/j.amc.2009.11.037

ON THE STABILITY RADIUS OF A FRACTIONAL GENERALIZED MULTIDIMENSIONAL STATE-SPACE SYSTEMS

Souad SALMI[1], Djillali BOUAGADA[2]

[1,2]Department of Mathematics and Computer Science, ACSY Team-Laboratory of Pure and Applied Mathematics Abdelhamid Ibn Badis University Mostaganem, P.O.Box 227/118, 27000 Mostaganem, Algeria.

Corresponding author email:
[1]souad.salmi.etu@univ-mosta.dz ,
[2]djillali.bouagada@univ-mosta.dz .

Abstract

In this work, a new class of generalized fractional linear multidimensional stat space systems described by Roesser model is considered. A new techniques for analysing the stability robust is discussed, the stability radius of the closed-loop system is described according to the $\mathcal{H}_2$ *and* $\mathcal{H}_\infty$ *norms. We treat both the discrete-time and continuous-time* cases in such region of the complex plane. *Sufficient conditions to ensure the stability margins of the perturbed system are offered in terms of linear matrix inequalities. Motivated examples are presented to demonstrate the effectiveness of our main results.*

Key words*: Fractional systems, Multidimensional systems, Roesser model, Stability Radius, Linear Matrix Inequalities.*

1. INTRODUCTION

In recent decades, fractional dD systems have attracted more attention from many researchers due to their application in different area such as circuit theory, digital processing, etc.

Parameterization of multidimensional systems is the only possible parameterization to design or produce implementations that work at least at the same level. For such systems, times propagate state in several distinct spatial directions with examples in the application of image processing, mixed variables of time and space or in the processing of data related to natural phenomena such as seismic or volcanic.

Stability analysis is a crucial part of the study of dynamic systems, especially when handling safety-critical systems such as power grids, nuclear reactors, self-driving cars, railway infrastructure or traffic systems, aircraft handling. Motivated by some work obtained in D. BOUAGADA P. VAN DOOREN (2006), in this paper, a new result on the stability margins of the generalized fractional dD closed-loop systems in a certain region of the complex plane is investigated. Based on the bounded real lemmas, novel sufficient conditions in the sense of $\mathcal{H}_\infty$ norm for the considered system are proposed in the form of LMIs.

2. CONTENT

In the following, we introduce a general formulation of multidimensional dD fractional continuous-time systems described by the Roesser model

$$\boldsymbol{K^{\alpha_1,\cdots,\alpha_d}E_dX_d(t_1,\cdots,t_d) = A_dX_d(t_1,\cdots,t_d) + B_du_d(t_1,\cdots,t_d)} \quad (1)$$

$$\boldsymbol{y_d(t_1,\cdots,t_d) = C_dX_d(t_1,\cdots,t_d) + D_du_d(t_1,\cdots,t_d)} \quad (2)$$

where,

$$E_d = \begin{pmatrix} E_{11} & \cdots & E_{1d} \\ \vdots & \ddots & \vdots \\ E_{d1} & \cdots & E_{dd} \end{pmatrix} \in \mathbb{R}^{n\times n}$$, which be assumed invertible.

$$A_d = \begin{pmatrix} A_{11} & \cdots & A_{1d} \\ \vdots & \ddots & \vdots \\ A_{d1} & \cdots & A_{dd} \end{pmatrix} \in \mathbb{R}^{n\times n}$$, is the dynamic matrix.

$$B_d = \begin{pmatrix} B_1 \\ \vdots \\ B_d \end{pmatrix} \in \mathbb{R}^{n\times m}$$, is the control matrix.

$$C_d = [C_1, \cdots, C_d] \in \mathbb{R}^{p\times n},$$

$$D_d \in \mathbb{R}^{p\times m},$$

$$X_d = \begin{pmatrix} x_1(t_1, \cdots, t_d) \\ \vdots \\ x_d(t_1, \cdots, t_d) \end{pmatrix}$$, represent the state of the sub-vectors,

$$K_d^{\alpha_1,\cdots,\alpha_d} = \begin{pmatrix} \lambda_1^{\alpha_1} I_{n_1} & \cdots & 0 \\ \vdots & \ddots & \vdots \\ 0 & \cdots & \lambda_d^{\alpha_d} I_{n_d} \end{pmatrix} \in \mathbb{R}^{n}$$, represent matrix of differentials operators $diag_{i=1}^{d}\, s_i I_{n_i}$

in the Laplace transform when (1,2) is the continuous-time and $diag_{i=1}^{d}\, z_i I_{n_i}$ in the Z-transform when (1,2) is the discrete-time.

$u(t_1, \cdots, t_d) \in \mathbb{R}^m$, is the input vector.

$y(t_1, \cdots, t_d) \in \mathbb{R}^p$, is the output vector.

3. CONCLUSIONS

In this paper, a new fractional generalized multidimensional system described by Rosser model is presented. Novel sufficient conditions for the stability margin of such system are formulated in terms of linear matrix inequalities. The obtained results are illustrated by a numerical example in the case of standard 2D state space model in order to show the applicability of our method.

FRACTIONAL UNMATCHED BACK PROJECTOR FOR RICHARDSON-LUCY DECONVOLUTION

Ștefan-Răzvan ANTON[1,2], Octavian POSTAVARU[1], Antonela TOMA[1,2]

[1]University Politehnica of Bucharest, 313 Splaiul Independentei, District 6, Bucharest, Romania
[2]Center for Research and Training in Innovative Techniques of Applied Mathematics in Engineering "Traian Lalescu" (CiTi)

Corresponding author email: antonstefan000@gmail.com

Abstract

The enhancement of image contrast and resolution obtained via optical microscopes has long been a challenging task. Traditionally, this task is tackled by methods such as deconvolution or the computational fusion of multiple views of the same sample. However, these approaches tend to be computationally intensive, making them less feasible for handling large datasets. In response to this challenge, we present a novel unmatched back projector built upon the fractional Fourier transform which is suited for the rapid deconvolution of microscopy images using the Richardson Lucy algorithm. Our results show great improvements in the number of iterations needed to obtain a quality deconvolved image, decreasing the number of iterations to one in the case of the deconvolution of fluorescent beads.

***Key words**: Richardson-Lucy; fractional calculus; fractional Fourier transform; deconvolution.*

1. INTRODUCTION

Fluorescence microscopy techniques enable the imaging of biological samples with submicrometric spatial resolution, yet most techniques come with intrinsic blurring and noise degradation of the underlying fluorescence data. If we can describe the imaging procedure, it is possible to partially undo such deterioration by employing deconvolution techniques, leading to enhanced clarity and signal to noise ratio. For instance, when presented with the point spread function (PSF) and data that has been corrupted by Poisson noise (which is commonly prevalent in fluorescence microscopy), the Richardson-Lucy deconvolution (RLD) algorithm sharpens the estimation of the sample density with every iteration. The utilization of iterative deconvolution has proven beneficial in these scenarios; however, achieving a resolution-limited outcome using RLD typically demands 20 or more iterations. Although the computational load associated with this process is feasible for microscopes capturing single views, deconvolving extensive datasets from multiples views can take up to several days, often surpassing the time required for data acquisition.

2. CONTENT

Iterative deblurring techniques strive to infer the underlying sample density from distorted, smudged, and noisy images. Key elements of these methods include a forward projector which outlines the transformation from the target image to the distorted, smudged, and noisy one captured by the microscope, and a back projector, which retraces the captured image back to the target one. For example, in RLD:

$$e_{k+1} = e_k \left\{ \frac{i}{e_k * f} * b \right\} \tag{1}$$

Where e_k is the kth (current) approximation of the target image o, e_{k+1} signifies the future (k+1)th approximation, i symbolizes the captured image, f denotes the forward projector, b stands for the back projector, and the asterisk represents the convolution operation. The PSF (Point Spread Function) is generally used for f given its requirement to precisely account for the distortions effects

produced by the imaging system. Although traditionally, b is matched to f as its transpose, this is not the sole viable solution. When the forward operator works as a shift-invariant convolution, commonly observed in microscopy, the iteration count of the RLD algorithm can be significantly diminished if b is selected such that the multiplication of the magnitudes of the Fourier transforms (FT) of f and b approximates a constant in spatial frequency space. We propose that modifying this procedure by using the fractional Fourier transform (f-FT) will give iterations that move more rapidly towards the desirable reconstructed images. For this purpose, we use the discrete fractional Fourier transform as defined by Jun Lang in his paper "Image encryption based on the multiple-parameter discrete fractional Fourier transform and chaos function".
In a simulation, we examined the relative performance of the traditional, unmatched, and fractional unmatched back projectors in the deconvolution of simulated fluorescent beads (Figure 1). Each of the deconvolution methods improved the signal-to-background and spatial resolution relative to the raw data, better revealing the distribution of fluorescent beads. However, using the unmatched and fractional unmatched (of order 1.05) back projectors also substantially reduced the number of iterations needed to obtain similar results to the traditional method.

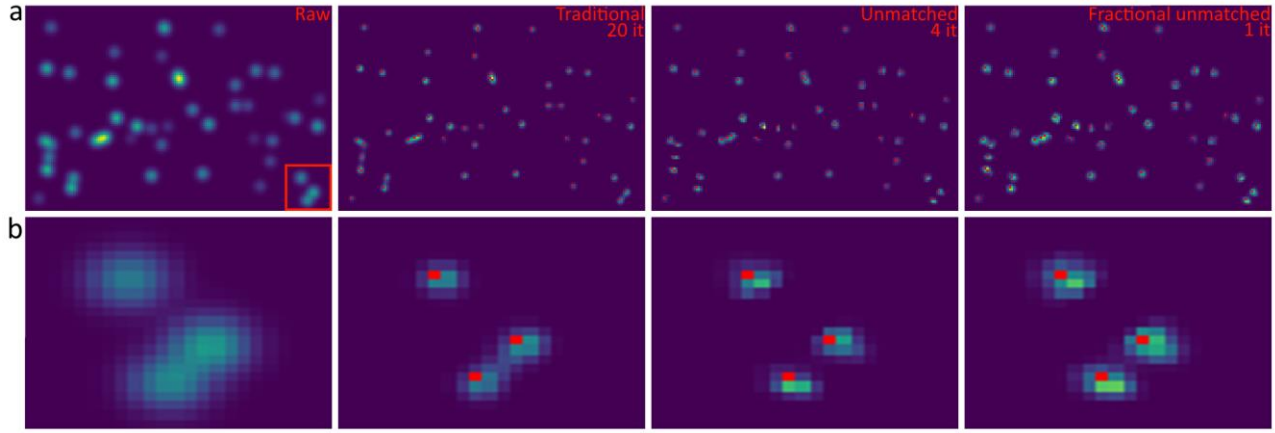

Figure 1: **a**, Simulated fluorescent beads highlight the deconvolution results, with the true location of the beads, iteration number and back projector as indicated. **b**, Higher-magnification views, corresponding to the red rectangular region in **a.**

3. CONCLUSIONS

Our deconvolution method is inspired by RLD with an unmatched back projector but achieves the same high-quality reconstructions more rapidly. Even though the fractional unmatched back projector allows for deconvolution in fewer iterations than a conventional back projector or even a normal unmatched back projector, the chance of an artefact creation remains, especially with an excessive number of iterations. We suggest a single iteration as a general guideline since this approach led to quality results in our simulations. With this considered, the algorithmic advancements, obtained by the introduction of the fractional Fourier transform, we outline here should hasten image deconvolution, particularly for the increasingly elaborate and sizable datasets obtainable with contemporary light microscopes.

BIOLOGICAL BARCODES FOR ENGINEERING AND MEDICAL APPLICATIONS

Ioana Corina BOGDAN[1], Fabian Pavel VELICEA[1]

[1]University Transilvania of Brasov, Blvd Eroilor, Brasov, Romania

Corresponding author email: corina.bogdan@unitbv.ro

Abstract

Ensuring privacy and security with minimal storage and computation requirements is critical to any technology. Towards this end, we develop a design strategy for constructing barcodes in the context of human facial expressions. The barcodes can be used to classify species (e.g. of insects, ocean fauna or plants), a technique also known as DNA barcoding. This work has applicability in various fields, from image processing to the field of engineering and medicine, and even in the field of security.

Key words*: barcodes, facial expressions, DNA barcoding, security, algorithms.*

1. INTRODUCTION

Barcodes are a visual way to display information on a surface, consisting of bars and spaces of different widths, encoding alphanumeric characters and symbols in different forms (Code 128, Code 39, EAN etc...). This technology has the ability to store as much information as possible in the smallest possible space [1], enabling fast and automatic data entry into computer systems. Facial expressions are important to us. From facial expressions we learn information about a person (age, emotions, diagnosis), [6]. Researchers have tried to understand how this process of identifying faces works through various methods (AI, neural networks, fuzzy logic), [2-4]. Each face has a place in a multi-dimensional space, and each dimension is an attribute of the face such as eye distance, nose shape, nose-mouth distance, chin, or forehead. The "average" face is the reference point, and the actual person's face is represented by how different it is from the "average" one [5]. However, the approach does not explain all aspects of face recognition. By inverting the colours of a photo or changing the direction of the light, the face becomes harder to recognize. The control points (centres of eyes or tip of nose) do not change. Moreover, the brain is sensitive to certain image properties (orientation, spatial frequency). To solve these issues and constraints we use different spatial frequencies to process information about a face (identity, emotions). Parts of the brain process this information and some emotions (fear) can be quickly processed by one area of the brain, the amygdala (the emotional centres) [5]. On the other side, the DNA barcoding is a method of species identification using a short section of DNA from a specific gene or genes, [7]. The premise of DNA barcoding, compared to a reference library of such individual DNA sequences can be used to uniquely identify an organism to species (aquatic, insect, plant), in the same way that a UPC barcode supermarket scan, [7]. DNA barcodes are markers used to identify species of organisms. The goal is to create components that detect and differentiate species in a group of organisms. The length of the DNA barcode sequence must be short enough to be used with current methods of sample collection, DNA extraction, amplification and sequencing, [7].

2. BIOLOGICAL BARCODES. DNA BARCODES

To generate biological barcodes facial expressions, Python was used as a tool allowing programming and computation tasks referring to: image processing, filtering and generation of barcodes associated with face contours. Additional to Python, several libraries are included:

OpenCV, NumPy and matplotlib. It also relies on OpenCV's Haar cascade classifier to detect human faces in input images and the Sobel filter to extract contours from them. Once the human face images have been processed, the script generates a barcode for each image based on the number of non-zero elements in the filtered image. The chain line to obtain the biological barcodes for a human facial expression is to process the images from a real time acquisition. The results presents the human face as an array of images containing the original image, the filtered image, and the corresponding barcode (see Fig.1). The barcode is generated vertically. Evaluating the results, the essential points on the face are transformed into a horizontal position (rotated 90^0), and overlapped with the sample image, it is the face barcode or biological barcode as presented in [5].

Fig. 1: Biological barcodes for facial expression.

For the DNA barcoding it is proposed an algorithm that goes through a number of steps to identify suitable primers. (Primers are short sequences of nucleotides that can bind to a specific DNA template, allowing the synthesis process to begin. Primers are essential in the process of polymerase chain reaction (PCR). For data processing NCBI BLAST+ program is used, allowing accessing the ByoPython, Bio.SeqUtils, Bio.SeqIO libraries, in addition to the other libraries: pandas, numpy, os, subprocess. Primer candidates are generated by applying a sliding window to the DNA sequence of the target species in the reference database. The algorithm checks for off-target amplification by performing a BLAST search of candidate primers against a BLAST database. The results are analysed to determine if there is any off-target amplification, and information about each candidate primer is presented (see Fig. 2 and Fig. 3).

ID	Species	Sequence
1	Species_A	ATGCTAGCTAGCTAGCTAGCTAGCTAGCTAGCTAGCTAGCTAGCTA
2	Species_A	ATGCTAGCTAGCTAGCTAGCTAGCTAGCTAGCTAGCTAGCTAGCTG
3	Species_A	ATGCTAGCTAGCTAGCTAGCTAGCTAGCTAGCTAGCTAGCTAGCTC
4	Species_A	ATGCTAGCTAGCTAGCTAGCTAGCTAGCTAGCTAGCTAGCTAGCTT
5	Species_A	ATGCTAGCTAGCTAGCTAGCTAGCTAGCTAGCTAGCTAGCTAGCTG
6	Species_A	ATGCTAGCTAGCTAGCTAGCTAGCTAGCTAGCTAGCTAGCTAGCTA
7	Species_A	ATGCTAGCTAGCTAGCTAGCTAGCTAGCTAGCTAGCTAGCTAGCTT
8	Species_A	ATGCTAGCTAGCTAGCTAGCTAGCTAGCTAGCTAGCTAGCTAGCTG
9	Species_B	ATGCTAGCTAGCTAGCTAGCTAGCTAGCTAGCTAGCTAGCTAGCTC
10	Species_B	ATGCTAGCTAGCTAGCTAGCTAGCTAGCTAGCTAGCTAGCTAGCTA
11	Species_B	ATGCTAGCTAGCTAGCTAGCTAGCTAGCTAGCTAGCTAGCTAGCTG
12	Species_B	ATGCTAGCTAGCTAGCTAGCTAGCTAGCTAGCTAGCTAGCTAGCTT
13	Species_B	ATGCTAGCTAGCTAGCTAGCTAGCTAGCTAGCTAGCTAGCTAGCTA
14	Species_B	ATGCTAGCTAGCTAGCTAGCTAGCTAGCTAGCTAGCTAGCTAGCTC

Fig. 2: Data base with several species

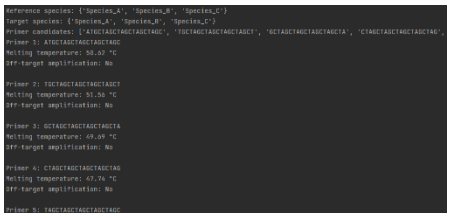

Fig. 3: Species classification

3. CONCLUSIONS

In this work we developed design strategies for constructing barcodes, first in the context of human facial expressions, secondly in the context of biology, the DNA barcodes. This work has an extensive applicability, from image processing to the field of engineering and medicine, and even in the field of security. Python script is a useful tool for processing images of human faces and generating associated barcodes, as it combines image processing and visualization techniques to help users analyse and understand the results obtained. The algorithm addressed to solve the problem of identifying suitable primers for PCR amplification of target species in the context of using biological barcodes contributes to obtain more accurate results in the study of genetic diversity and species.

BIBLIOGRAPHY

[1]. N. Pradhan et al., *Barcode Recognition Techniques: Review & Application*, Int. Journal of Innovative Research in Computer Science & Technology, ISSN: 2347- 5552, Vol.9, Iss.3, 2021.

[2]. A. Habib et al., *Learning human-like facial expressions for Android Phillip K. Dick,* IEEE CASE, Taiwan, pp. 1159-1165, 2014,

[3]. I.C. Bogdan et al.,„Games theory involvement in the social robots' facial expressions", U.P.B. Sci. Bull., Series C, Vol. 85, Iss. 1, 2023.

[4]. T.A Sumi et al., *Human Gender Detection from Facial Images Using Convolution Neural Network*. 2021.

[5]. Steven C. Dakin, Roger J. Watt; *Biological "bar codes" in human faces*, Journal of Vision, Iss. 4, 2009.

[6]. M. Yuri et al., *A Simple Method for Generating Facial Barcodes*, 2014

[7]. H. Liu., *DNA Barcoding.* Encyclopedia. 2022.

VITAL PARAMETERS MONITORING USING A PORTABLE DEVICE

Silviu Alin JECU, Andreea Georgiana DEMETER, Ioana Corina BOGDAN

[1]Transilvania University of Brasov, 29 Eroilor Blvd., Brasov, Romania

Corresponding author email: silviu.jecu@student.unitbv.ro, georgiana.demeter@student.unitbv.ro, corina.bogdan@unitbv.ro

Abstract

Portable devices have become essential for real-time monitoring human vital parameters. These kinds of devices improve the quality of life by offering a convenient and reliable solution for everyday life monitoring heart rate and oxygen blood saturation. In this work we propose a portable device for medical use in a non-invasive way. The device is able to track the amount of oxygen carried by the red blood cell, also called oxygen saturation, and monitor the heart rate. By using a microcontroller together with a pulse oximeter sensor, the results were accurate and provided in real time. With autonomy of 5 days and a weight of less than 300g, this device is perfect for monitoring life parameters under any conditions. Virtual life parameters monitoring using a portable device may be used in healthcare settings, at home or on the road, providing valuable insights into an individual's vital signals.

***Key words**: portable device, accuracy, non-invasive device,*

1. INTRODUCTION

Around 60% of Romania's population suffers from cardiovascular diseases (CVDs), [1] (see Fig. 1). The main purpose of this work is to develop a health monitoring system using pulse oximetry [2], which can help people diagnosed with diseases such as cardiac insufficiency, anemia, lung disease, in monitoring heart rate and saturation level of oxygen in the blood, in real time. The device is designed to be portable and easy to use. In a convenient way, the patient can wear this device wherever it moves. His vital signs are monitored by the responsible medical institution that can make quick decisions in order to maintain the quality of the state of affairs health. Heart rate and oxygen saturation in the blood help the user or the patient to understand his health and take the necessary measures to maintain a healthy lifestyle.

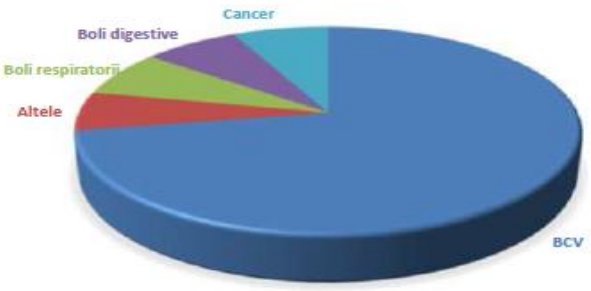

Fig.1: Disease percentages in Romania, [1].

2. PORTABLE DEVICE AND VITAL SIGNS

The purpose of the application is to recreate the pulse oximeters sold via online marketplace, of which accuracy differs by more than 4%. The accuracy is given by the quality of the components and his specifications. This device is using a pulse oximeter sensor to measure the user/patient's heart rate and blood oxygen saturation levels. Data collected from the pulse oximeter are

transmitted to the device and displayed on a user-friendly interface. The device is powered by accumulators with a battery life of approximately 5 days. The MAX30100 sensor is used to monitor heart rate and blood oxygen saturation. The heart rate is displayed on the serial monitor along his status, which can be categorized as "Normal," "Low," or "High." The heart rate is measured by counting the number of heart contractions per minute. In practice, the oxygen saturation, which refers to the amount of oxygen carried by red blood cells, is often the first parameter measured in critical conditions. It is measured using a non-invasive medical device called a pulse oximeter, which is typically attached to a finger.

The pulse oximeter is a non-invasive monitor that measures blood oxygen saturation by shining light at specific wavelengths through tissue (most commonly though fingertip). Deoxygenated and oxygenated haemoglobin absorb light at different wavelengths (660 nm and 940 nm), and the absorbed light is processed by a patented algorithm in the pulse oximeter to display a saturation value. The blood oxygen saturation level is also displayed on the serial monitor along with its status, which can be also categorized: "Normal," "Low," or "High." The normal range for blood oxygen saturation is considered to be between 96% - 100% at sea level. It's important to note that individuals living at higher altitudes may have lower saturation levels due to reduced oxygen availability.

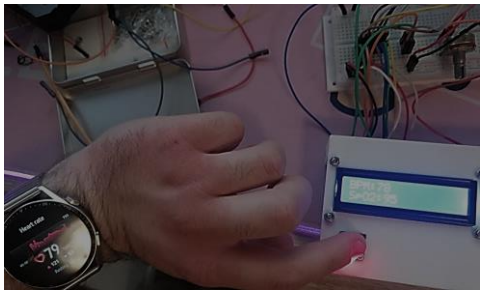

Fig.2: Portable device results on serial monitor

3. CONCLUSIONS

The aim of the project was touched, successfully implementing a portable device for medical use in a non-invasive way (see Fig. 2). By using a microcontroller together with a pulse oximeter sensor, the results were accurate and provided in real time. With autonomy of 5 days and a weight of less than 300g this device is perfect for monitoring life parameters under any conditions. This device can be used by athletes in fitness and sports, in medical field and personal. It may help detect potential health issues, provide insight for medical field a promote proactive management of personal health and well-being. Further works will include a cyber secured system for health care services environments, allowing 24/7 monitoring remotely, as well as on-site, in order to obtain a higher quality in medical assistance.

BIBLIOGRAFIE

[1] https://www.reginamaria.ro/articole-medicale/bolile-cardiovasculare-la-romani

[2] https://www.hopkinsmedicine.org/health/treatment-tests-and-therapies/pulse-oximetry

[3] https://www.ncbi.nlm.nih.gov/books/NBK470348/

[4] https://microcontrollerslab.com/max30100-pulse-oximeter-heart-rate-sensor-arduino-tutorial/

CHARACTERIZING CHAOS IN A FRACTIONAL DUFFING EQUATION

Sara HAMAIZIA[1], Salvador JIMÉNEZ[1], M. Pilar VELASCO[3]

[1]Departamento de Matemática Aplicada a las T.I.C., E.T.S.I Telecomunicación, Universidad Politécnica de Madrid, 28040-Madrid, Spain
[3]Departamento de Matemática Aplicada a las T.I.C., E.T.S.I. Sistemas de Telecomunicación, Universidad Politécnica de Madrid, 28038-Madrid, Spain

Corresponding author email: hamaizia.sara@alumnos.upm.es

Abstract

In this work, we study Duffing's equation with a fractional damping term using the Caputo fractional derivative, of order α in (0,2), and two different numerical methods, one of them, new. Both methods are used to check their agreement and the new one, which has a better truncation error, is used to analyse the behaviour of the system, with the control parameter being the amplitude of the exterior forcing. We characterise-the chaos estimating the Lyapunov Characteristic Exponents with a linearized approximation extending to the range1<α<2. We obtain a good agreement with the Lyapunov Exponent obtained using the fiduciary orbit technique.
Key words*: fractional calculus; Caputo derivative; Duffing equation; chaos; Lyapunov characteristic exponents, ….*

1) INTRODUCTION

Nonlinear differential equations with fractional order derivatives are standard modelling tools with applications in many areas of science. It has been shown that modelling some physical phenomena using fractional calculus is more accurate than using integer calculus when many time scales or memory effects are present. The Duffing equation is a paradigmatic model of competition between internal and external oscillations that lead to different behaviours, including chaos. Different fractional extensions have been considered depending on which integer order derivatives are replaced by fractional ones.

The Lyapunov Characteristic Exponents are a useful tool for examining chaotic motions: the presence of positive exponents supposes, in general, chaos, while regular orbits correspond to all exponents being negative. In our case, we have two exponents, λ_1, λ_2. The presence of a λ_{max} positive Lyapunov exponent means there is an exponential divergence of nearby orbits and a strong sensitivity to initial conditions (two trajectories of a chaotic system starting close to each other will diverge after some time). We study the chaos in our system estimating the Lyapunov characteristic exponents, using a linearized approach that we extend from the case $0 < \alpha < 1$ to $1 < \alpha < 2$, and, also, using the fiduciary orbit technique to obtain the largest exponent, as a confirmation of the validity of the method.

2) CONTENT

1) Classical and fractional Duffing equation

We recall the "classical"(i.e., nonfractional) Duffing equation:

$$\ddot{x} + \gamma\dot{x} - x + x^3 = f_0 cos\,(\omega t)$$

with initial conditions:

$$x(0) = x_0, v(0) = v_0$$

where x_0 and v_0 are real constants. The parameters γ, f_0, ω correspond to the damping coefficient, the amplitude of the periodic driving force and the angular frequency.

For the fractional case, we replace the dumping term with a fractional derivative, to obtain the following fractional equation:

$$\ddot{x} + \gamma D_t^{\alpha}(t) - x + x^3 = f_0 cos\,(\omega t)$$

where D_t^{α} is the Caputo fractional derivative of fractional order α:

$$D_t^{\alpha}(t) = \frac{1}{\Gamma(n-\alpha)} \int_{t_0}^{t} \frac{x^{(n)}(\tau)}{(t-\tau)^{\alpha+1-n}} d\tau, t > t_0, 0 \le n-1 < \alpha < n, n \in N$$

The "classical" case corresponds to the limit when α tends to one, either from the left or from the right.

2) Strauss-Vazquez + Odibat numerical method for both cases $0 < \alpha < 1, 1 < \alpha < 2$

The numerical method that we use to approximate the fractional model is based on two different approaches. We approximate the fractional derivative in the equation with the Odibat method and use the Strauss-Vazquez approach for the other terms. The discrete equation is for $0 < \alpha < 1$:

$$\frac{x_{n+1}-2x_n+x_{n-1}}{h^2} + \frac{h^{1-\alpha}}{\Gamma(3-\alpha)} \left(C_{n,0}\dot{x}_0 + \sum_{j=1}^{n-1} C_{n,j}(\alpha,1) \frac{x_{j+1}-x_{j-1}}{h^2} + \frac{x_{n+1}-x_{n-1}}{2h} \right) - \frac{x_{n+1}+x_{n-1}}{2} + \frac{x_{n+1}^3+x_{n+1}^2 x_{n-1}+x_{n+1}x_{n-1}^2+x_{n-1}^3}{4} = f_0 \frac{cos(wt_{n+1})+cos(wt_{n-1})}{2}$$

where $C_{n,j}$ are coefficients.

For $1\alpha < 2$, we substitute the Caputo derivative approximated by the Odibat approach in the fractional equation and simplify the scheme.

3) Lyapunov characteristic exponents for $1 < \alpha < 2$

As an extension to the case $0 < \alpha < 1$, we approximate the linearization of the fractional duffing equation and obtain the Jacobian matrix presented in the following formula:

$$J = \begin{bmatrix} 0 & 1 \\ \frac{-U''(x)}{C} & \frac{B}{C} \end{bmatrix}$$

Where B and C are two coefficients:

$$C = 1 + \frac{\gamma h^{2-\alpha}}{\Gamma(3-\alpha)} - \frac{2\gamma(2-\alpha)h^{2-\alpha}}{3\Gamma(4-\alpha)},$$

$$B = \frac{-2\gamma(2-\alpha)h^{1-\alpha}}{9\Gamma(4-\alpha)}, 1 < \alpha < 2.$$

4) Numerical results

In this section we present the Lyapunov exponents for both cases $0<\alpha<1$ and $1<\alpha<2$. We calculate both Lyapunov exponents λ_1, λ_2 of the system using the Jacobian matrix approach and compare them with the maximum Lyapunov exponent λ_{max} obtained with the fiduciary orbit method, where we see a good agreement.

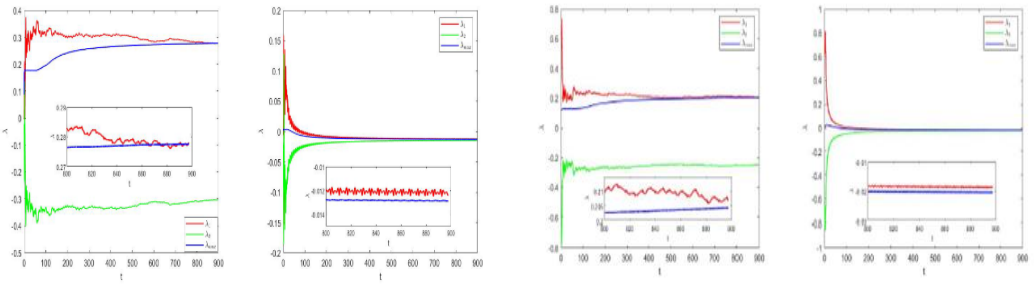

(a) LCEs for a chaotic solution for $\alpha = 0.5$. (b) LCEs for a regular solution for $\alpha = 0.5$. (a) LCEs for a chaotic solution for $\alpha = 1.1$. (b) LCEs for a regular solution for $\alpha = 1.1$.

Fig. 1. Estimation of LCEs for the fractional order between 1 and 2

3. CONCLUSIONS

We study Duffing's equation with fractional damping term and linear stiffness using the Caputo fractional derivative, numerically using two approaches SV+ Odibat method and the SV + Diethelm method. The approximation of the fractional term in the Duffing equation using the Odibat method which has the truncation error O (h^2)-is better than the approximation of the fractional term with the

Diethelm method which has the truncation error O ($h^{2-\alpha}$). We use this latter as a reference to compare the numerical results of the SV + Odibat method. It helped us to conclude that this method is a practical tool for the fractional Duffing equation. Based on these numerical results, we found a strange attractor with the SV + Odibat method quite similar to the strange attractor which we can obtain for the classical case for several values of α and different initial conditions.
Several behaviours appear in this system depending on the values of alpha and the amplitude f_0. We characterised the chaos by calculating the Lyapunov exponents with the Jacobi matrix obtained. we extend the study of the Lyapunov exponents for $1 < \alpha < 2$ and we get a good agreement between all the Lyapunov exponents obtained and the largest Lyapunov exponents.

EFFICIENT MESHLESS METHOD FOR MODELING RANDOM GROUNDWATER FLOW IN HETEROGENEOUS POROUS MEDIUM

Fouzia SHILE[1], Mohamed SADIK[1]

[1] Ibn Zohr University, Faculty of Sciences, Agadir, Morocco

Corresponding author email: fouzia.shile@edu.uiz.ac.ma

Abstract

We conducted numerical investigations to assess the accuracy and efficiency of a meshless method that is based on radial basis functions (RBFs) for modelling random flows in heterogeneous aquifers. In order to account for the heterogeneity of the aquifer, we utilized a statistical description of hydraulic conductivity through a random field with a predetermined statistical structure. Our evaluation of the method focused on its effectiveness in the presence of high levels of heterogeneity. To that end, we performed numerical experiments to solve the flow problem, which demonstrated the exceptional performance of our proposed approach in the field of subsurface hydrology.

Key words*: meshless method; random flow; heterogeneous porous medium.*

1. INTRODUCTION

In recent years, the scientific community has devoted significant attention to numerical methods aimed at approximating the solution of flow equations that model flow in heterogeneous porous media. Several studies have been published on this topic. However, these methods encounter challenges in terms of computational feasibility. The objective of this work is to leverage the innovative characteristics of a meshless method that relies on radial basis functions to address the issues discussed in the literature.

2. CONTENT

Our proposal involves the utilization of the meshless method based on radial basis function as an efficient computational technique. This approach has gained popularity owing to its advantages in solution approximation and reduced computational costs, eliminating the need for mesh generation. We use the Randomization spectral method for generating the random hydraulic conductivity. We perform numerical experiments for the solution of the flow problem to prove the efficiency of the proposed approach.

3. CONCLUSIONS

We conclude the efficiency and computational feasibility of the proposed meshless approach to cope with higher heterogeneity. The numerical tests confirm the high performance of the proposed method for modelling random flow in heterogeneous aquifers. In detail, we obtained remarkably accurate results without using high computing resources.

ON THE STABILITY RADIUS OF A FRACTIONAL GENERALIZED MULTIDIMENSIONAL STATE-SPACE SYSTEMS

Souad SALMI[1], Djillali BOUAGADA[2]

[1,2]Department of Mathematics and Computer Science, ACSY Team-Laboratory of Pure and Applied Mathematics Abdelhamid Ibn Badis University Mostaganem, P.O.Box 227/118, 27000 Mostaganem, Algeria.

Corresponding author email:
[1]souad.salmi.etu@univ-mosta.dz,
[2]djillali.bouagada@univ-mosta.dz.

Abstract

In this work, a new class of generalized fractional linear multidimensional stat space systems described by Roesser model is considered. A new technique for analysing the stability robust is discussed, the stability radius of the closed-loop system is described according to the $\mathcal{H}_2$ *and* $\mathcal{H}_\infty$ *norms. We treat both the discrete-time and continuous-time cases in such region of the complex plane. Sufficient conditions to ensure the stability margins of the perturbed system are offered in terms of linear matrix inequalities. Motivated examples are presented to demonstrate the effectiveness of our main results.*

Key words*: Fractional systems, Multidimensional systems, Roesser model, Stability Radius, Linear Matrix Inequalities.*

1. INTRODUCTION

In recent decades, fractional dD systems have attracted more attention from many researchers due to their application in different area such as circuit theory, digital processing...etc.
Multidimensional systems setting are the only possible setting for designing or producing implementations that perform at least the same level. For such systems, times propagate the state in several separate spatial directions with examples in application of image processing, mixed time and space variable or in data processing related to natural phenomena such as seismic or volcanic. Stability analysis is a crucial part of the study of dynamical systems, especially when handling safety-critical systems such as electrical networks, nuclear reactors, self-driving cars, railway infrastructure or aircraft handling systems. Stability margin is one of the basic problems in the field of systems control; it can represent how well the system can withstand disturbance before losing its stability. In this paper, a new result on the stability margins of the generalized fractional dD closed-loop systems in a certain region of the complex plane is investigated. Based on the bounded real lemmas for the continuous and discrete times, novel sufficient conditions in the sense of $\mathcal{H}_\infty$ norm for the considered system are proposed in the form of LMIs.

2. PRELIMINARIES

In the following, we introduce a general formulation of multidimensional dD fractional continuous-time systems described by the Roesser model

$$\boldsymbol{K^{\alpha_1,\cdots,\alpha_d}E_dX_d(t_1,\cdots,t_d) = A_dX_d(t_1,\cdots,t_d) + B_du_d(t_1,\cdots,t_d)} \quad \mathbf{1}$$

$$\boldsymbol{y_d(t_1,\cdots,t_d) = C_dX_d(t_1,\cdots,t_d) + D_du_d(t_1,\cdots,t_d)} \quad \mathbf{2}$$

where,

$$E_d = \begin{pmatrix} E_{11} & \cdots & E_{1d} \\ \vdots & \ddots & \vdots \\ E_{d1} & \cdots & E_{dd} \end{pmatrix} \in \mathbb{R}^{n\times n}$$, which be assumed invertible.

$$A_d = \begin{pmatrix} A_{11} & \cdots & A_{1d} \\ \vdots & \ddots & \vdots \\ A_{d1} & \cdots & A_{dd} \end{pmatrix} \in \mathbb{R}^{n\times n}$$, is the dynamic matrix.

$$B_d = \begin{pmatrix} B_1 \\ \vdots \\ B_d \end{pmatrix} \in \mathbb{R}^{n\times m}$$, is the control matrix.

$$C_d = [C_1, \cdots, C_d] \in \mathbb{R}^{p\times n},$$

$$D_d \in \mathbb{R}^{p\times m},$$

$$X_d = \begin{pmatrix} x_1(t_1, \cdots, t_d) \\ \vdots \\ x_d(t_1, \cdots, t_d) \end{pmatrix} \in \mathbb{R}^{n}$$, represent the state of the sub-vectors,

$K_d^{\alpha_1,\cdots,\alpha_d} = \begin{pmatrix} \lambda_1^{\alpha_1} I_{n_1} & \cdots & 0 \\ \vdots & \ddots & \vdots \\ 0 & \cdots & \lambda_d^{\alpha_d} I_{n_d} \end{pmatrix} \in \mathbb{R}^{n\times n}$, represent matrix of differentials operators $diag_{i=1}^{d}\, s_i I_{n_i}$

is the Laplace transform when (1,2) in the continuous-time and $diag_{i=1}^{d}\, z_i I_{n_i}$ is the Z-transform when (1,2) in the discrete-time.

$u(t_1, \cdots, t_d) \in \mathbb{R}^{m}$, is the input vector.

$y(t_1, \cdots, t_d) \in \mathbb{R}^{p}$, is the output vector.

3. CONCLUSIONS

In this paper, a new fractional generalized multidimensional system described by Rosser model is presented. Novel sufficient conditions for the stability margin of such system are formulated in terms of linear matrix inequalities. The obtained results are illustrated by a numerical example in the case of standard 2D state space model in order to show the applicability of our method.

ON THE CALCULATION OF FUNCTIONALLY GRADED PLATES

Vasile NASTASESCU[1], Silvia MARZAVAN[1*]

[1]Military Technical Academy "Ferdinand I", District 5, Bucharest, Romania

Corresponding author email: smarzavan@yahoo.com

Abstract

This paper presents our researching results regarding numerical calculus of the Functionally Graded Plates (FGP). Two approching ways were used: the concept of multilayered plate and the concept of equivalent plate. These two concepts can be used in both analytical and numerical calculations using the finite element method or the Galerkin free element method. In addition, those two concepts used in the numerical analysis can also take into account the variation of the Poisson ratio, which is usually neglected, and in the analytical calculation it is always neglected. The influence of Poisson's ratio is analyzed with quantitative arguments on a case study. The influence of the number of layers is also analysed, when the concept of a multilayer plate is used. The models, methods and methodology presented are valid for any type of flat plate, for any type of load, shape and support method. Practically, we bring to the attention of specialists an accessible and efficient way to calculate functionally graded plates.

***Key words**: Functionally graded materials, Functionally graded plate, Material property law, Multilayer plate, Equivalent plate, Finite element method*

1. INTRODUCTION

Functionally graded materials (FGMs) are new and special composite materials, microscopically inhomogeneous, in which the elastic and mechanical properties vary smoothly and continuously from one point to another, in the direction of the thickness of the material, according to a adopted material law, like a continuous function on a continuous domain. The current importance of FGMs is very high one, due to their special properties, which makes them suitable for use in many fields such as aerospace, chemical plant, electronics, energy conversion, mechanical engineering, nuclear energy, biomaterials and in many other fields.

3. FUNCTIONALLY GRADED PLATES

Usually, one of the materials is a high resistance material (ceramics) and other is a common material (aluminum, steel etc.) having low resistance. Intuitively, a FGM can be represented like in the Figure 1, where $F(z)$ is a function that describes the variation of Young's modulus, or Poisson's ratio, or density, or any other material property.

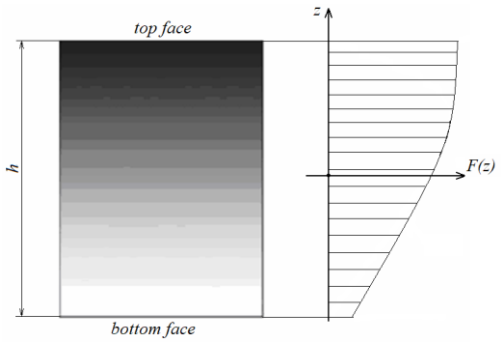

Fig. 1. Material property variation in FGMs

Of course, there are many other material pairs such as: metal-ceramic, polymer-elastomer, organic-inorganic glasses etc. There are many material property laws. The most used material law is the power law:

$$E(z) = E_b + (E_t - E_b)(0.5 + z/h)^k \tag{1}$$

The relation (1) is referring at Young's modulus, but the same relation can be used for any other material property (density, Poisson ratio etc.). In the relations (1), z is the coordinate that describes the position of a point on the thickness of the material, h is the material thickness and k is a coefficient (power coefficient), which may have different values, less than or greater than 1.
The indices b and t refer to the extreme edges of the material: b for the lower face and t for the upper face (Figure 1). Functionally graded plates are made of such materials.

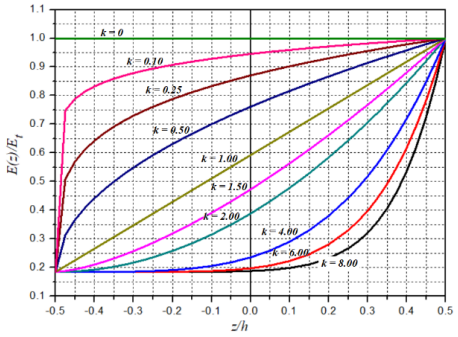

Fig. 2. Young's modulus versus z and k

The calculus of Functionally Graded Plates (FGPs), using the concept of multilayer plate consists in changing the continuous variation of the elastic properties with a variation in steps, in accordance with the number of layers, homogeneous and isotropic, considered on the plate thickness.
The concept of equivalent plate is a plate with homogeneous and isotropic properties, but these properties are fictitious, virtual, equivalent. An equivalent plate has the same value of the rigidity as the real plate. For the displacement calculus $w(x, y)$, the equivalent stiffness D_{eq} is equal to the real stiffness of the plate (D), calculated analytically (D_a), or based on the concept of multilayer plate (D^*), this being an known analitical calculus too. So,

$$D_{eq} = D = D_a = D^* \tag{2}$$

When Poisson ratio ν is constant,

$$D = \frac{1}{1-\nu^2}\int_{-h/2}^{h/2} E(z)\cdot z \cdot dz \tag{3}$$

and the material power law is used - relation (1) - by integration of relation (3) is obtained:

$$D = D_a = \frac{E_b h^3}{12(1-\nu^2)} + \frac{(E_c - E_b)h^3}{1-\nu^2}\left[\frac{1}{3+k} - \frac{1}{2+k} + \frac{1}{4(k+1)}\right] \tag{4}$$

Our research contains an extensive study, for a case study, compared to the analytical solution, regarding displacements, stresses and natural frequencies. The carried out numerical study is based on both the finite element method and the element free Galerkin method. It is also analyzed, with quantitative arguments, the influence of the variation of the Poisson ratio, in accordance with the adopted material law. Our comparative study also followed the establishment of some practical recommendations regarding the choice of the number of layers, for the use of the respective concept. The analysis is accompanied by graphical representations and post-processing of the results.

3. CONCLUSIONS

The aim of the paper was to provide accessibility to solve a complex and difficult problem such as the calculus of plates from functionally graded materials, with the current means of calculus, through appropriate methodologies. Our proposed methodology for FGPs can easily also used for the functionally graded beams.

PROBABILISTIC ANALYSIS OF A RANDOM NONLINEAR OSCILLATOR VIA THE RANDOM PERTURBATION TECHNIQUE

J.C. Cortés[1], E. López-Navarro[1], J.V. Romero[1], M.D. Roselló[1],

[1]Instituto Universitario de Matemática Multidisciplinar, Universitat Politècnica de València. Camí de Vera, s/n, 46022, València, Spain.

Corresponding author email: ellona1@doctor.upv.es

Abstract

In this work, we perform a probabilistic study of a random nonlinear oscillator whose external source is defined by a stationary Gaussian stochastic process. We apply the stochastic perturbation technique to obtain an approximation of the steady-state solution. Once we compute the solution, we obtain approximations of the main statistical properties (first moments, variance, ...). Furthermore, by using the principle of maximum entropy we can compute an approxima-tion of the probability density function of the stationary solution. Finally, we will show a numerical example applying the theoretical findings.

Keywords*: perturbation technique; random nonlinear oscillator; probability density function; principle of maximum entropy.*

1. INTRODUCTION

Random or stochastic differential equations incorporate uncertainty into the equations governing the behaviour of dynamical systems, allowing, for example in engineering, to capture and understand the inherent randomness of various physical phenomena. In this work, we are going to study the following general equation for a pendulum

$$\frac{d^2X(t)}{dt^2} + 2\beta\frac{dX(t)}{dt} + \omega_0^2\left(X(t) + \epsilon sin\big(X(t)\big)\right) = Y(t), \quad (1)$$

where we assume $\beta > 0$, ϵ is the perturvative parameter ($|\epsilon| \ll 1$), and the external source $Y(t)$ is a Gaussian stationary stochastic process with zero mean. In the following sections, we obtain an approximation of the solution by taking advantage of the perturbation technique, we compute the first three moments to obtain an approximation of the probability density function (PDF) using the principle of maximum entropy and finally, using the theoretical results we present a numerical example.

2. OBTAINING AN APPROXIMATION OF THE SOLUTION

This stochastic differential equation does not have a closed-form solution, so we can apply the perturbation technique to obtain an analytical approximation of the stochastic solution. The perturbation technique consists in expanding the solution in terms of the small parameter ϵ, obtaining an infinite cascade system of $X_n(t)$. By neglecting higher-order terms, an approximate solution is obtained that captures the behavior of the system under small perturbations. We truncate at first order, $\hat{X}(t) = X_0(t) + \epsilon X_1(t)$. Furthermore, in the nonlinear term $sin\big(X(t)\big)$, we will take advantage of the Taylor approximation. Using the linear theory of Laplace transformation, we can obtain the solutions $X_0(t)$ and $X_1(t)$ that are given by the following integrals

$$X_0(t) = \int_0^\infty h(s)Y(t-s)ds, X_1(t) = \omega_0^2\sum_{m=0}^M \int_0^\infty h(s)\frac{(-1)^{m+1}}{(2m+1)!}\big(X_0(t-s)\big)^{2m+1}ds, \quad (2)$$

where

$$h(t) = \begin{cases} (\omega_0^2 - \beta^2)^{-1/2} e^{-\beta t} sin\left((\omega_0^2 - \beta^2)^{1/2} t\right), & t \geq 0 \\ 0, & t < 0 \end{cases}. \quad (3)$$

2. COMPUTING FIRST MOMENTS

In order to apply the principle of maximum entropy we need to compute the first moments of the solution to approximate the PDF. In this case, we compute the mean, $\mu_1 = E\left[\hat{X}(t)\right]$, the second order moment, $\mu_2 = E\left[\hat{X}^2(t)\right]$ and the third order moment, $\mu_3 = E\left[\hat{X}^3(t)\right]$, which are given by the following expressions

$$\mu_1 = \mu_3 = 0 \quad (4)$$

$$\begin{gathered} \mu_2 = E[X_0^2(t)] + 2\epsilon E[X_0(t)X_1(t)] = \int_0^\infty \int_0^\infty h(s)h(s_1)\Gamma_{YY}(s - s_1)ds_1 ds \\ -2\epsilon\omega_0^2 \int_0^\infty \int_0^\infty \int_0^\infty h(s)h(s_1)h(s_2)\Gamma_{YY}(s_1 - s - s_2)ds_2 ds_1 ds \\ +\epsilon\omega_0^2 \int_0^\infty \int_0^\infty \int_0^\infty \int_0^\infty h(s)h(s_1)h(s_2)h(s_3)h(s_4)\Gamma_{YY}(s_1 - s - s_2)\Gamma_{YY}(s_3 - s_4)ds_4 ds_3 ds_2 ds_1 ds \\ \frac{-\epsilon\omega_0^2}{4} \int_0^\infty \int_0^\infty \int_0^\infty \int_0^\infty \int_0^\infty \int_0^\infty h(s)h(s_1)h(s_2)h(s_3)h(s_4)h(s_5)h(s_6) \\ \Gamma_{YY}(s_1 - s - s_2)\Gamma_{YY}(s_3 - s_4)\Gamma_{YY}(s_5 - s_6)ds_6 ds_5 ds_4 ds_3 ds_2 ds_1 ds \end{gathered} \quad (5)$$

Then, using this statistical information available, according to the Principle of Maximum Entropy [2], the PDF will have the following form

$$f_{X(t)}(x) = e^{-1-\lambda_0-\lambda_1 x-\lambda_2 x^2-\lambda_3 x^3}. \quad (6)$$

3. NUMERICAL EXAMPLES

These theoretical results can be illustrate by a numerical example. Let us consider that the stochastic process $Y(t) = \xi(t)$ is a white Gaussian noise (which complies with the conditions established). The values of the deterministic parameters are given by $\beta = 5/100$ and $\omega_0 = 1$. Once we have computed the first moments, we can apply the principle of maximum entropy to obtain the PDF. In Figure 1 we show a graphical representation of the PDF of the steady state solution for different values of ϵ.

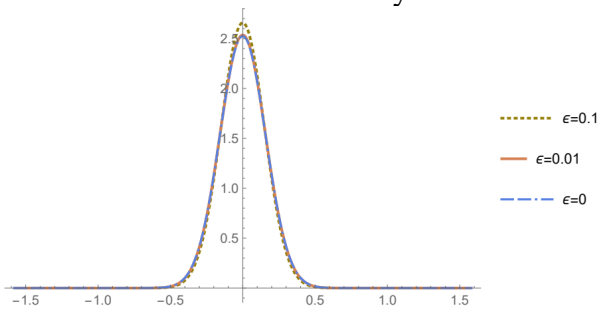

Figure 1: Approximate PDF of the steady state solution for different values of ϵ.

4. CONCLUSIONS

In this contribution we perform a probabilistic study of a nonlinear random oscillator using the perturbation technique and taking advantage of the principle of maximum entropy. A numerical example has been computed.

REFERENCES

[1] T. Soong, *Random Differential Equations in Science and Engineering*, vol. 103 (Academic Press, New York, 1973).

[2] JC. Cortés, E. López-Navarro, JV. Romero, MD. Roselló, *Probabilistic analysis of random nonlinear oscillators subjected to small perturbations via probability density functions: theory and computing*. Eur. Phys. J. Plus 136, 723 (2021).

ACKNOWLEDGEMENTS

This work has been supported by the grant PID2020-115270GB-I00 funded by MCIN/AEI/10.13039/501100011033 and the grant AICO/2021/302 (Generalitat Valenciana).

LINEAR MATRIX EQUATIONS DEDUCED FROM MATRIX EQUIVALENTS

Vasile POP[1], Alexandru NEGRESCU[2]

[1]Technical University of Cluj-Napoca, 26-28 G. Barițiu, Cluj-Napoca, Romania
[2]University Politehnica of Bucharest, 313 Splaiul Independenței, District 6, Bucharest, Romania

Corresponding author email: alexandru.negrescu@upb.ro

Abstract

We present a characterization of matrices with blocks whose rank is equal to the rank of one of its blocks. As applications, we offer results related to the rank of matrix polynomials, as well as characterization results of pairs of matrices on which the rank function is additive.

Keywords*: linear algebra, matrix equation, matrix polynomial, block matrix.*

1. INTRODUCTION

The main problem we pursue in the present paper is the characterization of block matrices whose rank is equal to the rank of one of its blocks. Several applications of the main result (Theorem 1) are related to the rank of matrix polynomials (Theorems 2, 3 and 4) or to results characterizing pairs of matrices on which the rank function is additive (Theorems 5 and 6), problems treated extensively in [1] and [2]. The obtained characterizations find applications in statistics [12], quantum physics [8], machine learning [7], computer science [9] etc.

2. CONTENT

The following constitutes the main result of this paper.

Theorem 1. *Let* $A \in \mathcal{M}_{m,n}(\mathbb{C})$, $B \in \mathcal{M}_{m,p}(\mathbb{C})$, $C \in \mathcal{M}_{q,n}(\mathbb{C})$, $D \in \mathcal{M}_{q,p}(\mathbb{C})$, *and* $M = \begin{bmatrix} A & B \\ C & D \end{bmatrix} \in \mathcal{M}_{m+q,n+p}(\mathbb{C})$. *Then the following statements are equivalent:*

1) $\operatorname{rank} M = \operatorname{rank} A$.

2) *there exist* $X \in \mathcal{M}_{n,p}(\mathbb{C})$ *and* $Y \in \mathcal{M}_{q,m}(\mathbb{C})$ *such that* $B = AX$, $C = YA$, *and* $D = YAX$.

A first consequence is the following.

Theorem 2. *Let* $f, g \in \mathbb{C}[X]$ *be two polynomials and let* $d = (f, g)$ *and* $m = [f, g]$ *be their greatest common divisor and their lowest common multiple, respectively. Then, for any matrix* $A \in \mathcal{M}_n(\mathbb{C})$, *we have*

$$\operatorname{rank} \begin{bmatrix} d(A) & f(A) \\ g(A) & m(A) \end{bmatrix} = \operatorname{rank} d(A).$$

Before giving a new result, we recall the following theorem (see [5]).

Theorem 3. *Let* $f, g \in \mathbb{C}[X]$ *be two polynomials and let* $d = (f, g)$ *and* $m = [f, g]$ *be their greatest common divisor and their lowest common multiple, respectively. Then, for any matrix* $A \in \mathcal{M}_n(\mathbb{C})$, *the following relation holds:*

$$\operatorname{rank} f(A) + \operatorname{rank} g(A) = \operatorname{rank} d(A) + \operatorname{rank} m(A).$$

Consequently, the following result occurs.

Theorem 4. *Let $f, g \in \mathbb{C}[X]$ be two polynomials and let $d = (f, g)$ and $m = [f, g]$ be their greatest common divisor and their lowest common multiple, respectively. If $A \in \mathcal{M}_n(\mathbb{C})$ is such that $m(A) = O$, then*

$$\operatorname{rank}\begin{bmatrix} d(A) & f(A) \\ g(A) & O \end{bmatrix} = \operatorname{rank} d(A) = \operatorname{rank} f(A) + \operatorname{rank} g(A).$$

Finally, we offer the following two characterizations.

Theorem 5. *Let $A, B \in \mathcal{M}_{m,n}(\mathbb{C})$. Then* $\operatorname{rank}(A + B) = \operatorname{rank} A + \operatorname{rank} B$ *if and only if there exist $X \in \mathcal{M}_n(\mathbb{C})$ and $Y \in \mathcal{M}_m(\mathbb{C})$ such that $AX = A$, $YB = B$, $YA = O$ and $BX = O$.*

Theorem 6. *Let $A, B \in \mathcal{M}_{m,n}(\mathbb{C})$. Then* $\operatorname{rank}(B - A) = \operatorname{rank} B - \operatorname{rank} A$ *if and only if there exist $X \in \mathcal{M}_n(\mathbb{C})$ and $Y \in \mathcal{M}_m(\mathbb{C})$ such that $AX = BX = A$, $YA = O$ and $YB = B - A$.*

3. CONCLUSIONS

We characterized matrices with blocks whose rank is equal to the rank of one of its blocks. As applications, we provided results related to the rank of matrix polynomials, as well as characterization results of pairs of matrices on which the rank function is additive.

4. BIBLIOGRAFY

[1] Dennis S. Bernstein, *Matrix Mathematics. Theory, Facts, and Formulas*, Second Edition, Princeton University Press, 2009.

[2] Randall E. Cline, Robert E. Funderlic, The rank of a difference of matrices and associated generalized inverses, *Linear Algebra and its Applications*, **24** (1979), pp. 185-215.

[3] George Marsaglia, *Bounds for the Rank of the Sum of Two Matrices*, Mathematical Note No. 344, Mathematics Research Laboratory, Boeing Scientific Research Laboratories, 1964.

[4] George Marsaglia, George P.H. Styan, When does $\operatorname{rank}(A + B) = \operatorname{rank} A + \operatorname{rank} B$?, *Canadian Mathematical Bulletin*, **15** (1972), pp. 451-452.

[5] Vasile Pop, Relations between ranks of matrix polynomials, *Journal of Algebra, Number Theory: Advances and Applications*, **24** (2021), pp. 35-41.

[6] Victor V. Prasolov, *Problems and Theorems in Linear Algebra*, American Mathematical Society, 1994.

[7] Qiang Qiu, Guillermo Sapiro, Learning Transformations for Clustering and Classification, *Journal of Machine Learning Research*, **16** (2015), pp. 187-225.

[8] Philippe Raynal, Norbert Lütkenhaus, Optimal unambiguous state discrimination of two density matrices: Lower bound and class of exact solutions, *Physical Review A*, **72** (2005), 022342.

[9] Susanna de Rezende, Or Meir, Jakob Nordström, Toniann Pitassi, Robert Robere, Marc Vinyals, Lifting with Simple Gadgets and Applications to Circuit and Proof Complexity, *61st IEEE Annual Symposium on Foundations of Computer Science (FOCS)*, 2020, pp. 24-30.

[10] William E. Roth, The equations $AX - YB = C$ and $AX - XB = C$ in matrices, *Proceedings of the American Mathematical Society*, **3** (1952), pp. 392-396.

[11] Joseph J. Rotman, *Advanced Modern Algebra*, Prentice Hall, 2003.

[12] Dean M. Young, John W. Seaman, Laurie M. Meaux, Independence Distribution Preserving Covariance Structures for the Multivariate Linear Model, *Journal of Multivariate Analysis*, **68** (1999), pp. 165-175.

APPLICATIONS OF LAPLACE AND SUMUDU TRANSFORMS IN MECHANICAL ENGINEERING

Larisa Georgiana UNGUREANU[1,2], Narcisa VOINEA[1,2]
Elena Corina CIPU[1,3], Cosmin Dănuț BARBU[3]

[1]University Politehnica of Bucharest, Centre for Research and Training in Innovative Techniques of Applied Mathematics in Engineering "Traian Lalescu" (CiTi), Bucharest, Romania
[2] Power Engineering Faculty, University Politehnica of Bucharest
[3]Department of Applied Mathematics, Faculty of Applied Sciences, University Politehnica of Bucharest

Corresponding author email: larisa.ungureanu@energ.stud.upb.ro

Abstract

Laplace transform is a very powerful mathematical tool applied in various areas of engineering and science. Important properties of Laplace Transform are specified at the beginning of the paper. Next section is dedicated to examples of mechanical systems, such as harmonic vibration of a beam or vapor bubble oscillating in an acoustic field, that are modelled using Laplace transform, enabling obtaining the solution of complex equations with the purpose of understanding system behaviour under certain conditions and performance. Additionally, Laplace Transform facilitates frequency domain analysis, allowing the determination of resonances, natural frequencies, and system characteristics.The deformable integral and DLT properties are also introduced with application on non-homogeneous deformable fractional equations. In final section conclusions are made.

Keywords*: Laplace Transform, Sumudu Transform, Mechanical system.*

1.INTRODUCTION

The Laplace transform is a mathematical technique widely employed in mechanical engineering for its numerous applications. By converting complex differential equations into simpler algebraic equations in the Laplace domain, the Laplace transform enables engineers to analyse and solve problems in mechanical systems. This powerful tool finds use in studying dynamic system behaviour, solving differential and integral equations, conducting frequency domain analysis, and solving boundary value problems. Its versatility and efficiency make the Laplace transform an invaluable asset in modelling, analysing, and optimizing mechanical systems, contributing to advancements in the field of mechanical engineering.

2. CONTENT

Laplace Transform (LT) in Engineering Analysis.

Starting with the definition of LT: $L_t[f(t)] = \int_0^\infty e^{-st} f(t)\, dt = F(s)$ (1)

of the original function f(t) (with known properties) involving parameter s, Laplace transform is used to simplify nonlinear equations and find easier the solutions or parameter dependences. Laplace transform can only be used to transform variables that cover a range from "zero" (0) to infinity, (∞). Any variable that does not vary within this range cannot be transformed using Laplace transform. The most common variable that is transformed by Laplace Transform is the time. As principal properties of Laplace Transform, we can specify linearity, shifting property, changing scale property, image and original integration, convolution theorem.

Applications

1. A very simple application of Laplace transform in physics is to find out the ***harmonic vibration of a beam*** which is supported at its two ends. Let us consider a beam of length *l* and uniform cross

section parallel to the yOz plane so that the normal deflection w(x,t) is measured downward if the axis of the beam is towards x axis. The basic equation defining this phenomenon is as given below:

$$EI\frac{d^4w}{dx^4} - m\omega^2 w = 0 \quad (2)$$

where E is Young's modulus of elasticity; I is the moment of inertia of the cross section with respect to the Y axis; m is the mass per unit length; and ω is the angular frequency. Rewriting the equation (2) for $\alpha^4 = \frac{m\omega^2 w}{EI}$, we obtain $\frac{d^4w}{dx^4} - \alpha^4 = 0$, and applying the LT, the equation became:

$$s^4 f(s) - s^3 F(+0) - s^2 F'(+0) - sF''(+0) - sF'''(+0) - \alpha^4 f(s) = 0 \quad (3)$$

The boundary conditions for this problem are: $F(+0) = 0; F(+l) = 0; F''(+0) = 0; F''(+l) = 0.$

The equation (3) leads to $f(s) = s^2F'(+0) + \frac{F'''(+0)}{s^4} - \alpha^4$with the solution:

$$w = A_1 \sinh \alpha x + A_2 \sin \alpha x. \quad (4)$$

Using boundary conditions, the resulting vibrations are:

$$w_n = A_n \sin(n\pi x/l), \text{ and the frequencies: } \omega_n = \frac{\pi^2 n^2}{l^1}\sqrt{EI/m}.$$

If n = 1, it represents the fundamental vibration and if n = 2 the first harmonic and so on.

2. For the oscillation of a single ***spherical vapor bubble*** driven by a single-frequency acoustic field, if the compressibility and the viscosity of the liquid are small enough to be neglected, the bubble wall motion can be expressed by the classical Rayleigh-Plesset equation:

$$R\ddot{R} + \frac{3}{2}\dot{R}^2 = \frac{p_{\text{ext}}(R,t) - p_{\text{s}}(t)}{\rho_1},\ p_{\text{ext}}(R,t) = p_{\text{v}} - \frac{2\sigma}{R},\ p_{\text{s}}(t) = p_0 + p_{\text{a}}\sin(\omega_{\text{a}} t) \quad (5)$$

with R is the instantaneous vapor bubble radius and ρ_1 is the liquid density. p_{v} is the pressure of the vapor inside the bubble. σ is the surface tension coefficient. p_0 is the ambient pressure. p_{a} is the pressure amplitude of the acoustic field. ω_{a} is the angular frequency of the acoustic field. t is the time. The solution for the linearized equation of (5)

$$\ddot{x} + \omega_0^2 x = f,\ x = \frac{R - R_0}{R_0},\ f = -\frac{p_{\text{a}}}{\rho_1 R_0^2}\sin(\omega_{\text{a}} t) \quad (6)$$

leads to $x = x_0 \cdot \cos\ \omega_0 t + \frac{\dot{x}_0}{\omega_0} \cdot \sin\ \omega_0 t + f * \frac{\sin\ \omega_0 t}{\omega_0}$ (7)

Using Laplace transform the result can be obtained as follows:

$$x = x_0 \cdot \cos\ \omega_0 t + \frac{\dot{x}_0}{\omega_0} \cdot \sin\ \omega_0 t - \frac{p_{\text{a}}}{\rho_1 R_0^2}\frac{1}{\omega_0}\int_0^t \sin\ \omega_{\text{a}}\tau \cdot \sin\ \omega_0(t-\tau)d\tau \quad (8)$$

3. *LT and Sumudu transform application*

$$F(u) = S[f(t);u] = \frac{1}{u}\int_0^\infty e^{-(t/u)} f(t)dt,\ u \in (-\tau_1, \tau_2) \quad (9)$$

over the set of the functions

$$A = \left\{f(t) | \exists M, \tau_1, \tau_2 > 0, |f(t)| < Me^{t/\tau_j} \text{ if } t \in (-1)^j \times [0,\infty)\right\} \quad (10)$$

where $f(t)$ is a function which can be expressed as a convergent infinite series, see [4]. The double convolution with respect to x and y is defined and the theorem of the Sumudu transform of the double convolution of the $f(t,x)$ and $g(t,x)$ given by $S_2[(f ** g)(t,x); v,u] = uvF(v,u)G(v,u)$.

is used for ***a non-homogenous wave equation*** without and with convolution term expressed connected to the following problems:

$$\begin{aligned} &u_{tt} - u_{xx} = xte^{x+t} && x^2t^3 ** (u_{tt} - u_{xx}) = xte^{x+t} \\ &u(0,x) = r_1(x),\ u_t(0,x) = r_1{}'(x), \quad (11) && u(0,x) = r_1(x),\ u_t(0,x) = r_1{}'(x), \quad (12) \\ &u(t,0) = h_1(t),\ u_x(t,0) = h_1{}'(t). && u(t,0) = h_1(t),\ u_x(t,0) = h_1{}'(t). \end{aligned}$$

CONCLUSIONS

The Laplace and Sumudu transform is a powerful tool extensively used in mechanical engineering. Their applications include analysing dynamic systems, studying responses, conducting frequency domain analysis, and solving boundary value problems. With its versatility and effectiveness, the Laplace transform enables engineers to gain insights, tackle complex problems, optimize performance, and drive innovation in the field. The oscillation characteristics of mechanical systems are obtained.

REFERENCES

[1] Sarina Adhikari, *Laplace Transforms and its Applications*. Department of Electrical Engineering and Computer Science, University of Tennessee.

[2] Xiaoyu Wang, Xuan Du, Dan Gao,Yuning Zhang, Ting Chen, Yuning Zhang *Theoretical investigation on resonance characteristics of a vapor bubble based on Laplace transform method*, Ultrasonics Sonochemistry 92 (2023) 106275, https://doi.org/10.1016/j.ultsonch.2022.106275

[3] A. Kılıcmana, H.E.Gadainb, *On the applications of Laplace and Sumudu transforms*, Journal of the Franklin Institute 347 (2010) 848–862

[4] G.K. Watugala, The Sumudu transform for functions of two variables, Mathematical Engineering in Industry 8 (4) (2002) 293-302.

CONTROLLER SYNTHESIS FOR POSITIVE FRACTIONAL 2D CONTINUOUS-DISCRETE LINEAR SYSTEM

Mohammed Nadjib BENAMAR[1], Mohammed Amine GHEZZAR[2], Djillali BOUAGADA[3]

[1,3]Abdelhamid Ibn Badis University, Department of Mathematics and Computer Science, P.O.Box 227/118 University of Mostaganem, Mostaganem, Algeria
[2]"National Higher School of Mathematics, P.O.Box 75, Mahelma (Sidi Abdellah), Algiers, Algeria

Corresponding author email: nadjib.benamar.etu@univ-mosta.dz

Abstract

This paper focuses on addressing the stability and control design associated with a class of positive fractional 2D continuous-discrete linear system described by the Roesser model and based on the Caputo fractional derivative in the continuous part and the difference fractional in the discrete part. The main contribution of this work is the establishment of necessary and sufficient conditions for asymptotic stability of these systems. Additionally, a necessary and sufficient condition is proposed to ensure the existence of state-feedback controllers that guarantee both non-negativity and stability of the resulting closed-loop systems. Finally, a numerical example is provided to illustrate our results.

Keywords*:fractional calculus;asymptotic stability;2D continuous-discrete linear system; positive systems;control design; Roesser model.*

1. INTRODUCTION

In recent years, the study of two-dimensional 2D systems has gained significant attention from researchers due to their theoretical and practical importance. These systems have found wide-ranging applications in fields such as circuit analysis, digital image processing, signal filtering, and thermal power engineering. The dynamics of 2D systems are commonly described using several models, including the Roesser model [1] and the Fornasini-Marchesini model [2], have been employed to describe the dynamics of 2D systems in different time as: continuous, discrete, and continuous-discrete-time. These models have greatly facilitated research in areas such as stabilization, H_∞control and filtering problems in 2D systems.

The incorporation of fractional calculus in the study of 2D linear systems brings several advantages and importance. It enables the modelling and analysis of systems with memory effects enhances system representation and simulation accuracy, opens new avenues for control design and optimization, facilitates system identification and parameter estimation, and contributes to the advancement of mathematical theory and methods.

In practical systems, many real-world phenomena involve nonnegative variables, such as absolute temperature, concentrations of substances, and population levels. These systems fall under the category of positive systems, where the output signal and state variables are constrained to the first quadrant of the state space. Studying the stability of two-dimensional linear systems is crucial for various applications in engineering, as it allows us to design and control physical systems to ensure their reliable and safe operation.

This work takes an initial step by investigating the stability of fractional 2D continuous-discrete linear system described by the Roesser model. The objective is to determine whether the stability of these systems can be solely determined by the system matrices. In this study, we employ a simple and novel proof approach that analyses the structural properties and trajectory evolution of positive Roesser models. By leveraging the positive property, we establish a proof line that demonstrates the sufficiency and necessity of the stability condition. Furthermore, we have developed a necessary

and sufficient condition that guarantees the existence of state-feedback controllers in fractional 2D continuous-discrete linear system described by the Roesser model. This condition ensures both non-negativity and stability of the resulting closed-loop system.

2. PROBLEM FORMULATION

Consider the unforced fractional 2D continuous-discrete linear system described by the Roesser model and introduced in [3]:

$$D^{\alpha}x_h(t,i) = A_{11}x_h(t,i) + A_{12}x_v(t,i) \qquad (1a)$$
$$\Delta^{\beta}x_v(t,i+1) = A_{21}x_v(t,i) + A_{22}x_v(t,i) \qquad (1b)$$

where $D^{\alpha}x_h(t,i) = \frac{d^{\alpha}x_h(t,i)}{d^{\alpha}t}$ represents the α-order Caputo fractional derivative, $\Delta^{\beta}x_v(t,i+1)$ represents the β-order of fractional difference, with $0 < \alpha, \beta < 1$. $x_h(t,i) \in R^{n_1}$, $x_v(t,i) \in R^{n_2}$ are the horizontal and vertical state vector respectively, ($n=n_1+n_2$), $A_{11} \in R^{n_1 \times n_1}$, $A_{22} \in R^{n_2 \times n_2}$.

In this work, we will present some concepts for fractional calculus. Based on the works of Kazcorek [3], we will provide definitions and lemmas regarding the positivity of systems (1). We investigate the problem of asymptotic stability of positive systems (1). Furthermore, we derive the necessary and sufficient conditions for the stability of positive considered systems in the context of linear programming problems. Building upon the obtained results, we investigate the stabilization problem of a fractional 2D continuous-discrete linear system (1).

2. CONCLUSIONS

In this work, Necessary and sufficient conditions for the stability of positive fractional 2D continuous-discrete linear system described by the Roesser model are derived. The objective of designed the state feedback of system such that the close-loop systems is positive and stable has been investigated. Necessary and sufficient conditions for solving this problem have been established. It has been demonstrated that the problem can be transformed into a linear programming problem, which can be solved using established methods.

REFERENCES

[1] R.P. Roesser, A Discrete State-Space Model for Linear Image Processing, IEEE Transactions on Automatic Control 20, No. 1, 1-10, (1975).

[2] E. Fornasini, G. Marchesini, Doubly-indexed dynamical systems: State-space models and structural properties, Mathematical systems theory 12, 59-72, (1978).

[3] T. Kaczorek, Positive fractional 2D continuous-discrete linear systems, Bulletin of the Polish Academy of Sciences. Technical sciences, 59, No 4 575-579, (2011).

REVEALING THE CYBERATTACKS: PHISHING

Eduard-Ștefan SANDU

University Politehnica of Bucharest, 313 Splaiul Independentei, District 6, Bucharest, Romania

Corresponding author e-mail: edy.eminem@yahoo.com

Abstract

The Internet has revolutionized communication, providing individuals with convenient and widespread access to various online activities. However, this accessibility has also given rise to numerous forms of Internet fraud, with phishing attacks being a prominent concern. Phishing involves the use of deceptive tactics, such as fraudulent emails and counterfeit websites, to trick users into disclosing their sensitive personal information. This paper highlights the prevalence of phishing attacks and the risks they pose to individuals' security and privacy. The aim is to raise awareness about the deceptive nature of phishing and its potential impact on Internet users. By understanding the tactics employed by attackers, individuals can take proactive measures to protect themselves from falling victim to phishing scams.

Key words*: phishing, e-mail, cyber-attack, human factor, social engineering.*

1. INTRODUCTION

The APWG (Anti-Phishing Working Group) has put forth an extended definition for phishing: “criminal mechanism employing both social engineering and technical subterfuge to steal consumers' personal identity data and financial account credentials. Social-engineering schemes use spoofed emails purporting to be from legitimate businesses and agencies, designed to lead consumers to counterfeit websites that trick recipients into divulging financial data such as user-names and passwords”.

Phishing attacks employ a deceptive tactic whereby users are enticed through phishing e-mails to access fraudulent websites, aiming to illicitly obtain their private information. The effectiveness of phishing sites relies on users actually connecting to and utilizing the site's functionalities. Hence, the detrimental consequences can be mitigated if users possess the ability to recognize phishing e-mails. However, due to insufficient training and limited awareness regarding such attacks, users often lack the necessary knowledge to effectively identify and safeguard against them.

According to Mannan and Oorschot (Mannan, M., & Oorschot, P. C. v. (2008)), certain online services, particularly banking services, require a heightened level of security due to the involvement of sensitive and private information, which parallels the security measures employed by their traditional counterparts. In the traditional banking system, customers are advised to verify the legitimacy of automated teller machines (ATM) and safeguard the secrecy of their personal identification number (PIN). Similarly, in online banking, customers are urged to verify the authenticity of the websites they visit and refrain from disclosing personal information, such as passwords. Regrettably, there are instances where users fail to adhere to these security requirements, consequently attracting criminal activities.

2. EFFECTIVE PHISHING DETECTION AND PREVENTION

The progression of a phishing attack closely resembles the process of fishing, which is where the term "phishing" originated. Just as a fisherman strategically selects bait to lure fish, a phisher employs similar tactics to entice unsuspecting individuals. The initial stage involves the creation of a deceptive website, designed to mimic a legitimate entity. Subsequently, the phisher initiates a large-scale e-mail campaign, casting a wide net to reach a vast audience. The e-mails contain carefully crafted messages, often accompanied by links directing recipients to the fraudulent website. The success of the attack hinges on victims voluntarily engaging with the bait, accessing the deceptive website, and

inadvertently divulging sensitive personal information. This information can encompass a wide range of critical data, including financial credentials, social media login details, and e-mail account information. Once obtained, this illicitly acquired data can be exploited by the phisher for various malicious purposes, such as financial fraud and identity theft.

Phishing detection and prevention tools play a crucial role in protecting on-line users from phishing attacks. However, despite advancements in technology, there is still a need for improved accuracy to minimize the significant losses caused by these attacks. This paper examines various technical methods employed for detecting and preventing phishing, categorizing them based on their techniques. The classification focuses on the lifecycle of phishing attacks, encompassing detection, prevention, and remediation strategies. The study delves into popular detection methods such as blacklisting, whitelisting, security toolbars, and virus scanners, highlighting their strengths and limitations. Additionally, it explores heuristic-based solutions and novel approaches to tackle zero-day phishing attacks. By analysing existing approaches and emerging trends, this research aims to contribute to the development of more effective and accurate anti-phishing measures for the protection of online users.

The following list provides an overview of toolbars commonly used to detect phishing attacks:

- The SpoofGuard Toolbar is a browser plug-in designed to monitor user activity and calculate a spoof index by analysing user behaviour and comparing it to predefined thresholds, determining the likelihood of spoofing attempts (Boneh et al., 2007; Gupta and Shukla, 2015; Kang and Lee, 2007),
- Netcraft Toolbar: has built-in blacklist and whitelist maintained by Google and works by preventing users from entering personal information on known phishing websites (Likarish et al., 2008),
- Cloudmark Anti-Fraud Toolbar: Website legitimacy rating depends on user ratings and is displayed as a green, red or yellow icon (Gupta and Shukla, 2015),
- PwdHash: This is a browser plug-in that handles Man-In-The-Middle attacks and uses a hashing algorithm to merge user input data that will render data stolen by phishers meaningless (Blocki and Sridhar, 2016).

3. CONCLUSIONS

In conclusion, the effectiveness of anti-phishing measures for detecting phishing websites remains a persistent challenge, with limited success achieved thus far. A comprehensive evaluation of commonly suggested tips for end users to identify individual phishing websites is crucial. Furthermore, exploring new defensive possibilities has yielded promising results in enhancing anti-phishing effectiveness. Effective anti-phishing strategies should prioritize user education and training, ensuring that individuals are well-informed about the phishing phenomenon, regardless of their technical proficiency. Notably, newer approaches have shown greater efficacy compared to traditional methods. Additionally, findings indicate that individuals with higher levels of education tend to exhibit greater scepticism and caution when assessing emails, while age plays a significant role in one's ability to accurately discern genuine emails from fraudulent ones. Lastly, emails that incorporate recognizable company logos are more likely to be perceived as authentic, underscoring the importance of visual cues in email evaluation. Moving forward, continued research and development efforts are necessary to advance anti-phishing technologies and empower users with effective tools to combat phishing attacks.

IMAGE RECONSTRUCTION WITH A CONVOLUTIONAL AUTOENCODER AS SUPPORT FOR A DATA ASSIMILATION MODEL

Cătălin-Ionuţ MOLDOVAN[1], Bogdan SEBACHER[1]

[1]Military Technical Academy "Ferdinand I" of Bucharest, 39-49 George Coşbuc, District 5, Bucharest, Romania

Corresponding author email: pantarcatalin@gmail.com

Abstract

The estimation and uncertainty quantification of channelized reservoirs in a data assimilation framework is very hard to achieve due to the geometrical and topological characteristics of the facies fields. The channelized structure of the fields is broken after the updated step of the data assimilation process, and this causes unrealistic updated reservoir models. Geological realism can be achieved in two ways, either by learning or by conditional sampling from the prior distribution. In this study, we train a convolutional autoencoder (CAE) to reconstruct the channelized structure. Each facies field is treated as an image, and the geometry is restored through the aid of the convolutional autoencoder. The training of the neural network is done with a set composed of pairs of images, of which one is perturbed, and the other has a correct geometrical and topological structure. The results show very good reconstruction capabilities of the CAE.

Keywords*: convolutional autoencoder (CAE); image reconstruction; channelized reservoirs; data assimilation.*

1. INTRODUCTION

In this study, a convolutional autoencoder (CAE) is trained for image reconstruction purposes as the support for a data assimilation method. The context consists of the estimation and uncertainty quantification of a hydrocarbon reservoir with a channelized structure with three facies types. The CAE will be a part of a parameterization of the spatial distribution of rock types (facies) and helps in restoring the geometry and topology of the facies fields. The autoencoders are deep neural networks that learn useful low-representation of data through unsupervised learning. The applications include data compression, noise removal, dimensionality reduction, anomaly detection, and feature extraction.

2. CONTENT

The architecture of an autoencoder consists of an encoder and a decoder. The encoder takes the input data and maps it to a lower-dimensional latent space representation, capturing the most important features. The decoder then reconstructs the original input data from the latent representation. During training, the network learns to minimize the difference between the input and the output, effectively learning to encode and decode the data.

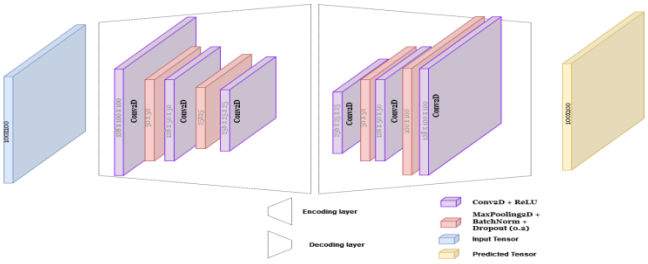

Figure 1: Architecture of the Convolutional autoencoder

In this paper, the autoencoder is used for the reconstruction of a specific channelized structure of noised images. During training, the autoencoder learns to minimize the discrepancy between the reconstructed image and the corresponding clean image. This process encourages the network to capture the underlying structure and patterns of the clean images, allowing it to effectively denoise or restore perturbed images during the reconstruction process. Both the encoding and decoding

layers are composed of three sets, with each set comprising convolutional layers, batch normalization layers, max pooling layers, and dropout layers. Convolutional layers consist of a set of learnable filters, also known as kernels or feature maps that slide over the input data. These filters perform convolution operations, where they scan the input and compute dot products between the filter weights and local patches of the input. For this scenario, the *ReLU* (Rectified Linear Unit) activation function is applied in the convolutional layer, and the functionality of the learnable filters is dependent on their depth. Max Pooling layers are used for dimensionality reduction and for preventing overfitting, each set has layers of batch normalization and dropout. After thorough experimentation and evaluation, it was found that the optimal choice for the compiled model configuration parameters is the *Adam optimizer* with a learning rate of 0.005. Furthermore, the most effective loss function for the model is the *mean squared error*. The training set of the autoencoder consists of 45000 pairs of images, and the validation set has 5000 all having 10000 pixels with the values 0(blue), 1(green), and 2(red). Each pair has a perturbed image (the input of the CAE) and a clear image (used as the output of the CAE). The clear images are simulated from a training image (first row of the right side of Fig.2) with a multi-point geostatistical method named Single Normal Equation Simulation (SNESIM). The training image plays the role of a conceptual geological model that explains the possible geometry and topology of the spatial distribution of the rocks in the reservoir domain. In our case, they are three rock types, each corresponding to a color. The green one corresponds to fine sand, the red one is coarse sand, and the blue one is shale. The construction of the perturbed fields (second row at the left-hand side of Fig.2) is done by a Gaussian perturbation applied to a parameterization of the original facies fields.

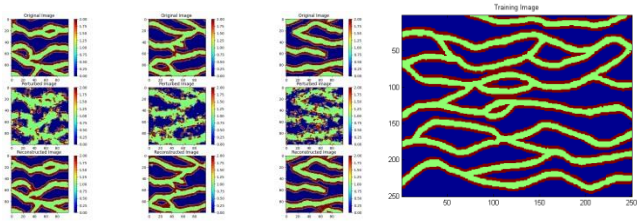

Figure 2: Right side: Training Image; Left side: First row: Facies fields simulated from training image. Second row: Perturbed fields. Third row: Reconstructed image with the convolutional autoencoder.

The clean images, as they are the output of the autoencoder, are presented in the last row on the left side of Fig.2). After conducting 10 epochs of training, we have generated informative visualizations that capture the performance of the model. These visualizations include accuracy curves and loss curves, which provide a comprehensive overview of the model's learning progress and performance trends over the training period.

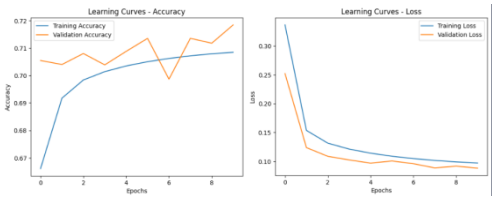

Figure 3: Right side: Loss function curves; Left side: Acuracy curves

As it is illustrated in Fig.3, the model has an accuracy of 72% and a loss of 10%. As seen from the curves, the model didn't overfit. After applying a thresholding function and analyzing the similarities between a set of desired output images and reconstructed images, the similarity percentage increases up to 98% and is not lower than 88%, with a mean accuracy for 5000 images being 96%.

3. CONCLUSIONS

In this paper, a convolutional autoencoder (CAE) is trained for the reconstruction of images. The CAE input consists of Gaussian noised images, while the output is clear images. The images are simulated from a training image and represent layers of facies distributions of a hydrocarbon reservoir. The results showed very good reconstruction capabilities of the deep neural network.

APPLICATIONS OF HYBRID STATISTICAL MODELS AND QUANTUM COMPUTING IN DATA SECURITY

Emil SIMION[1,2], Elena Corina CIPU[1,3]

[1]University Politehnica of Bucharest, Centre for Research and Training in Innovative Techniques of Applied Mathematics in Engineering "Traian Lalescu" (CiTi), Bucharest, Romania
[2] Department of Mathematical Methods and Models, Faculty of Applied Sciences, University Politehnica of Bucharest.
[3]Department of Applied Mathematics, Faculty of Applied Sciences, University Politehnica of Bucharest

Corresponding author email: corina.cipu@upb.ro

Abstract

Nowadays simulation methods with stochastic processes were used. In the cross-disciplinary methodologies cathegory, Evolutionary algorithms such as Variable-Chromosome-Length Genetic Algorithm (VCL_GA) are useful in analysing the random data when the length of the optimal length of a string is unknown. To improve the quality of previous estimations different machine learning techniques could be added and robust hybrid statistical models being derived. Scientific development in the direction of quantum technologies makes algorithms like Shor or Grover easily implemented on quantum supercomputers, which leads to the compromise of classical cryptography. The solution to this problem also comes via quantum: in recent research, Quantum Cryptography is the most mature quantum technology today. In this paper we studied the problem of ignorance in this new type of cryptography. We also performed the security analysis on ideal states.

Keywords*: EA, Machine Learning, Quantum Fourier transform, Quantum Computation, Shor's Algorithm.*

EXTENDED ABSTRACT

Mixture models combine multiple probability distributions to model complex data. In a hybrid setting, mixture models can be used to capture different components or subpopulations within the data. A hybrid model might use a mixture of Gaussian distributions to generate data with multiple clusters or modes.

Bayesian networks are graphical models that represent probabilistic relationships between variables. In a hybrid approach, Bayesian networks can be combined with other statistical models to generate synthetic data. The network structure captures the conditional dependencies between variables, while the individual conditional probability distributions can be estimated using various techniques, such as parametric distributions or non-parametric methods.

Gaussian processes are flexible probabilistic models that can capture complex patterns in data. Hybrid models may use Gaussian processes to model the underlying structure of the data, capturing trends, seasonality, or non-linear relationships. By sampling from the learned Gaussian process, synthetic data points can be generated.

Sequential Monte Carlo (SMC) methods, also known as particle filters, are used to estimate the posterior distribution of a hidden state variable given a sequence of observations. In a hybrid context, SMC methods can be combined with other statistical models to generate random data that adheres to a specific time series structure or exhibits dynamic behavior.

When dealing with data security, the design and implementation of hybrid statistical models should adhere to recognized cryptographic standards and best practices to ensure the integrity and confidentiality of the generated random data.

True Random Number Generators (TRNG) generate random numbers by utilizing physical processes that are inherently unpredictable, such as electronic noise or radioactive decay. Hybrid models combine the use of TRNGs with statistical tests to ensure the quality and security of the generated random numbers.

Cryptographically Secure Pseudo-Random Number Generators (CSPRNG) with Entropy Sources	◊ CSPRNGs are deterministic algorithms designed to produce random-like numbers that pass certain statistical tests. To maintain the security of the generated numbers, CSPRNGs require a source of entropy, which is typically obtained from physical processes or external data sources. ◊ Hybrid models combine CSPRNGs with entropy sources, such as environmental noise or user input, to enhance the randomness and security of the generated random numbers.
Hybrid Approaches for Key Generation	◊ Cryptographic key generation is a critical aspect of data security. Hybrid statistical models can be employed to generate cryptographic keys by combining the strengths of different methods. ◊ A model may use a combination of a physical entropy source, such as a hardware random number generator, with statistical techniques like hashing or post-processing algorithms. This hybrid approach ensures that the generated keys have high entropy, are statistically secure, and suitable for cryptographic purposes
Randomized Encryption Algorithms	◊ Randomized encryption algorithms are often used to provide confidentiality and prevent patterns from being revealed. HSM can be employed within these encryption algorithms to introduce randomness and enhance security. ◊ By combining statistical techniques like random number generation or noise injection with encryption algorithms, the resulting hybrid models can provide stronger protection against cryptographic attacks
Machine Learning-based Randomness Generation	◊ Hybrid models can also involve the use of machine learning algorithms for generating random data in data security applications. Machine learning models can be trained on large datasets of random numbers or cryptographic keys to learn the underlying patterns and dependencies. Once trained, these models can generate new random data points that adhere to the learned statistical properties. ◊ By combining machine learning models with cryptographic techniques, hybrid approaches can offer novel ways of generating secure random data

To ensure the generated numbers are truly random and suitable for cryptographic applications, statistical tests can be applied. These tests assess the statistical properties of the generated data, such as randomness, uniformity, and independence.

A classical or canonical GA is characterized as follows: the representation of the population is realized by means of binary strings, the selection operator of an individual in the multiset of parents is proportional to the value of the evaluation function calculated for that individual, the probability of carrying out a mutation is low, the emphasis being on the process of recombination, of biological inspiration, as a means of generating new candidates for the solution. Variable-Chromosome-Length Genetic Algorithm (VCL_GA) is useful in analysing the the random data when the length of the optimal demography is unknown, see [1].

CONCLUSIONS

Hybrid statistical models are used with success in cryptography. Comparisons between different models are made, including quantum computing [2].[3].

BIBLIOGRAPHY

[1]Huang GB, Zhu QY, Siew CK. Extreme learning machine: theory and applications. Neurocomputing 2006;70(1):489–501.

[2]Emil Simion and Elena-Corina Cipu and Vasile-Laurențiu Dosan and Andrei-Voicu Tomuț and Eugen Neacsu, A note on the QFT randomness spectral test a new approach of DST, https://eprint.iacr.org/2021/1625, Cryptology ePrint Archive: Report 2021/1625.

[3]E. Simion, *Entropy And Randomness: From Analogic To Quantum World*, IEEE Acces, april 2020, vol. 8, pp. 74553 – 74561, DOI: 10.1109/ACCESS.2020.2988658, Electronic ISSN: 2169-3536, (ISI Web of Science CPCI-S, Factor Relativ de Impact 1.51 cf JCR 2017 (ediţia iunie 2018), SRI 2.76, IEEEXplore), WOS:000530830800089.

SOME CRITERIA FOR UNIFORM DICHOTOMY OF SKEW-EVOLUTION COCYCLES IN BANACH SPACES

Ariana GĂINĂ[1], Rovana BORUGA (TOMA)[1]

1 West University of Timișoara, 4 Bd. Vasile Pârvan, Timișoara, Romania

Corresponding author email: ariana.gaina@e-uvt.ro

Abstract

The main aim of this paper is to present some criteria in an uniform setting for dichotomic behaviors of skew-evolution cocycles in Banach spaces. We improved the techniques of stability and instability concepts in order to characterize the dichotomy concept. Besides the classical concepts of uniform exponential dichotomy and uniform polynomial dichotomy, we also study the concept of uniform dichotomy with growth rates. Using the obtained connections between these three concepts we proved the logarithmic, majorization and Hai criteria for skew-evolution cocycles in Banach spaces.

Key words*: skew-evolution cocycle; uniform exponential dichotomy; uniform dichotomy with growth rates.*

1. INTRODUCTION

In the last years, an impressive development is represented by the study of asymptotic behaviors for skew-evolution cocycles in Banach spaces, which can be considered generalizations for evolution operators and skew-product semiflows.

Exponential dichotomy is one of the most important behavior in the dynamical systems studied for the first time by Perron [10] and continued by Massera and Schäffer [8], Daleckii and Krein [5] and others [9], [3]. In order to generalize the concept of exponential dichotomy it is introduced by Barreira and Valls [2] the concept of polynomial dichotomy. Their study was continued by Dragicevic, Sasu and Sasu [6], Boruga and Megan [3]. Throughout the years an important extension of exponential dichotomy and polynomial dichotomy is introduced, and it is called dichotomy with growth rates (or h-dichotomy). Pinto [11] studied for the first time the notion of a growth rate, which is a nondecreasing and bijective function $h : R+ \to [1, \infty)$.

In this paper we present the concepts of uniform exponential dichotomy, uniform polynomial dichotomy and uniform h-dichotomy for skew-evolution cocycles in Banach spaces and the connection between them. More precisely we give logarithmic, majorization and Hai criteria for these three concepts.

2. CONTENT

1. PRELIMINARIES

Let X be a metric space, V a Banach space, $B(V)$ the Banach space of all bounded linear operators acting on V and $\Delta = \{(t, s) \in R_+^2 : t \geq s\}$ and $T = \{(t, s, t_0) \in R_+^3 : t \geq s \geq t_0\}$.

This paragraph begins with the introduction of the notion of skew-evolution cocycle $C = (\Phi, \phi)$ in Banach spaces defined by means of evolution semiflow $\phi: \Delta \times X \to X$ and skew-evolution semiflow $\Phi: \Delta \times X \to B(V)$ and with the families of projectors $P,Q: R_+ \times X \to B(V)$. The notions of uniform exponential dichotomy, uniform polynomial dichotomy, uniform dichotomy with growth rates, uniform exponential growth, uniform polynomial growth and uniform h-growth are presented as in [7] by Găină.

MAIN RESULTS

Theorem 1. Let be the skew-evolution semiflow $\Phi_h : \Delta \times X \to B(V)$, $\Phi_h(t, s, x) = \Phi(h^{-1}(e^t), h^{-1}(e^s), x)$ and the projector's families P_h, Q_h: $N \times X \to B(V)$, $P_h(t, x) = P(h^{-1}(e^t), x)$, $Q_h(t, x) = Q(h^{-1}(e^t), x)$. The pair (C, P) is uniformly h-dichotomic if and only if the pair (Ch, Ph) is uniformly exponentially dichotomic.

Theorem 2. If the pair (C, P) has uniform h-growth, then the following assertions are equivalent:

(i) (C, P) is uniformly h-dichotomic;

(ii) (logarithmic criterion) there exists $L > 1$ with (uhL_1) $\|\Phi(t, s, x)P(s, x)v\| \ln h(t)/h(s) \leq L\|P(s, x)v\|$ and (uhL_2) $\|Q(s, x)v\| \ln h(t)/h(s) \leq L\|\Phi(t, s, x)Q(s, x)v\|$, for all $(t, s, x, v) \in \Delta \times X \times V$;

(iii) (majorization criterion) there exist $L > 1$ and a nondecreasing and bijective function $f: [1,\infty) \to R_+$ with: (uhM_1) $f(h(t)/h(s))\|\Phi(t, s, x)P(s, x)v\| \leq L\|P(s, x)v\|$ and (uhM_2) $f(h(t)/h(s))\|Q(s, x)v\| \leq L\|\Phi(t, s, x)Q(s, x)v\|$, for all $(t, s, x, v) \in \Delta \times X \times V$;

(iv) (Hai criterion) there exist $r > e$ and $c \in (0, 1)$ with (uhH_1) $\|\Phi(h^{-1}(rs), h^{-1}(s), x)P(h^{-1}(s), x)v\| \leq c\|P(h^{-1}(s), x)v\|$ and (uhH_2) $\|Q(h^{-1}(s), x)v\| \leq c\|\Phi(h^{-1}(rs), h^{-1}(s), x)Q(h^{-1}(s), x)v\|$, for all $(s, x, v) \in R_+ \times X \times V$.

3. CONCLUSIONS

The article gives logarithmic, majorization and Hai criteria for uniform exponential dichotomy, uniform polynomial dichotomy and uniform dichotomy with growth rates of skew-evolution cocycles in Banach spaces. The three presented criteria are used to obtain integral characterization of Datko [4] and Barbashin [1] type for the studied concepts. For the future the authors would like to investigate these three criteria for the nonuniform case of exponential, polynomial and h-dichotomy of skew-evolution cocycles in Banach spaces.

4. REFERENCES

[1] E. A. Barbashin, Introduction in the Theory of Stability; Izd. Nauka: Moscow, Russia, 1967.
[2] L. Barreira, C. Valls, Polynomial growth rates. Nonlinear Anal.71 (2009), 5208–5219.
[3] R. Boruga, M. Megan, On some characterizations for uniform dichotomy of evolution operators in Banach spaces, Mathematics 10(19) 3704 (2022), 1-21.
[4] R. Datko, Uniform asymptotic stability of evolutionary processes in Banach space. SIAM J. Math. Anal. 3 (1972), 428-445.
[5] J. L. Daleckii, M. G. Krein, Stability of Solutions of Differential Equations in Banach Spaces. Trans. Math. Monographs, 43, Amer. 402 Math. Soc., Providence, R.I., 1974.
[6] D. Dragicevic, A. L. Sasu, B. Sasu, On polynomial dichotomies of discrete nonautonomous systems on the half-line. Carpathian J. 413 Math. 2022, 38(3), 663 - 680.
[7] A. Găină, On uniform h-dichotomy of skew-evolution cocycles in Banach spaces, Annals of West University of Timisoara Mathematics and Computer Science 58, 2, (2022), 1-11.
[8] J. L. Massera, J. J. Schaffer, Linear Differential Equations and Function Spaces. Pure Appl. Math. 21 Academic Press, New 400 York-London, 1966.
[9] M. Megan, A. L. Sasu, B. Sasu, Uniform exponential dichotomy and admissibility for linear skew-product semiflows, Operator Theory: Advances and Applications 153 (2004), 185-195.
[10] O. Perron, Die Stabilitatsfrage bei Differentialgleichungen, Math. Z. 32(1930), 703-728.
[11] M. Pinto, Asymptotic integration of a system resulting from the perturbation of an h-system, J. Math. Anal. Appl. 131 (1988), 194-216.

PROBABILISTIC STUDY OF THE STOCHASTIC SOLUTION OF THE PSEUDO-*N* ORDER KINETIC MODEL APPLIED TO A REAL CASE

Carlos ANDREU-VILARROIG[1], Juan-Carlos CORTÉS[1], Ana NAVARRO-QUILES[2], Sorina-Madalina SFERLE[1]

[1]Instituto Universitario de Matemática Multidisciplinar, Universitat Politècnicia de València, Camino de Vera s/n, 46022, Valencia, Spain.
[2]Department of Statistics and Operational Research, Universitat de València, Dr. Moliner 50, 46100, Burjassot, Spain.

Corresponding author email: smsferle@doctor.upv.es

Abstract

We present a generalized adsorption kinetic model, also known as the pseudo-n order equation, considering its parameters as absolutely continuous random variables with an arbitrary joint probability density function, and analyse the stochastic solution of the model from a probabilistic point of view, computing its first probability density function using the Random Variable Transformation technique, under general assumptions about the parameters. From it, we obtain significant information about the model, such as the mean, variance, or confidence intervals. We apply these theoretical results to a real case of chemical adsorption, incorporating an uncertainty quantification method to assign suitable distributions to the model parameters and account for data uncertainty.

Key words*: adsorption; kinetic model; pseudo-n order; uncertainty quantification; random variable transformation technique; Bayesian approach; random variables; probability density function.*

1. INTRODUCTION

One of the most widely used and quite fundamental processes in the environmental field is the adsorption process, which is part of an extensive spectrum of chemical, biological, and physical processes and operations. Adsorption is a surface phenomenon in which a substance called adsorbate interacts with another substance called adsorbent and adheres to it on a surface. Nowadays, adsorption is considered a superior method for wastewater treatment and reclamation due to its simple design, easy maintenance, high efficiency, and the availability of various adsorbents at low cost. In addition, it also plays a key role in air pollution.

The efficiency of this process is determined by the study of adsorption kinetics, which provides meaningful information on the mechanisms and speed of this process and the time required to complete it. In the literature, we can find several models that address the modeling of the kinetics of these processes, but in the present work, we will introduce and study the pseudo-n-order adsorption kinetic model, whose form is given by the following equation,

$$\frac{dq(t)}{dt} = k_n\big(q_e - q(t)\big)^n, \quad n > 1, \tag{1}$$

where $q(t)$ represents the adsorption capacity at time t (mg/g), q_e the adsorption capacity at equilibrium (mg/g), n the reaction order and k_n the rate ratio $\frac{\left(\frac{mg}{g}\right)^{1-n}}{min}$, which is defined as follows,

$$k_n = \frac{r}{q_e^{n-1}},$$

where r is the adsorption rate $1/min$.

2. PROBABILISTIC SOLUTION

Since the model parameters are calculated from experimental data and depend on molecular properties that are not completely known and on external random factors such as temperature, they contain measurement errors and intrinsic uncertainty, respectively, so that, unlike many studies in

which they are considered deterministic, it is convenient to consider and treat them as random variables. In this way, they explain and better fit the complexity of the real world. Therefore, equation (1) becomes a random differential equation, the solution of which is now, unlike the deterministic counterpart, a stochastic process as follows,

$$q(t,\omega) = q_e(\omega)\left(1 - \left(\frac{1}{1+t(n(\omega)-1)r(\omega)}\right)^{\frac{1}{n(\omega)-1}}\right),\ \omega \in \Omega,$$

where $q_e(\omega)$, $r(\omega)$ and $n(\omega)$ are assumed to be absolutely continuous random variables defined on a common complete probability space (Ω, F_Ω, P), with a known joint probability density function (PDF) $f_0(q_e, r, n)$.

The aim of this work is to solve the problem probabilistically by computing the first probability density function (1-PDF) of the solution stochastic process using the Random Variable Transformation technique, which also allows the computation of other data of interest, such as the PDF of the time needed to reach a fixed value. From it, we can obtain statistical characteristics such as the mean, the variance, or the probability that the solution lies within a particular interval of interest.

To apply the theoretical results, it is first necessary to establish a joint PDF of the model parameters, which will be the product of the marginals assuming independence between them. This step is crucial in practice, as suitable parameters have to be found for the distributions, which must adequately capture the uncertainty of the data. For this purpose, we employ the Bayesian approach, which, through Bayes 'theorem, allows us to obtain posterior distributions based on all the available prior information about the model parameters, which are defined by the prior distributions, and updates them using the information obtained from experimental data.

Finally, the model presented is applied to the study of cadmium adsorption in tree ferns, obtaining the following graph, which represents the 1-PDF of the solution using the Bayesian method. We observe that the PDF is concentrated approximately around the adsorbed quantity for each moment in time and follows a Gaussian shape. It is also observed that the density mass moves over time towards the equilibrium point with a leptokurtic tendency.

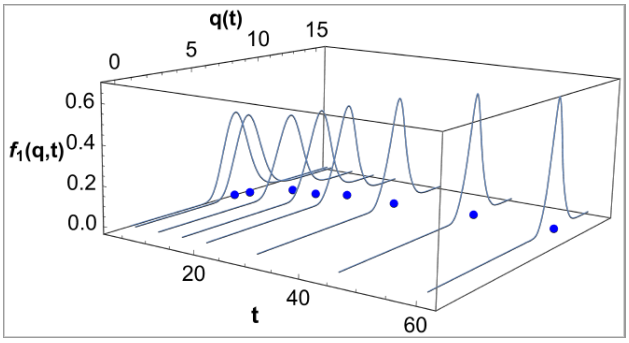

3. CONCLUSIONS

We have introduced a methodology to analyse the pseudo-n-order model by considering all its model parameters as random variables with arbitrary distributions. Additionally, we have presented an uncertainty quantification technique to assign suitable distributions to each parameter when applying this random equation to a real-world data.

4. ACKNOWLEDGMENT

This work has been partially supported by the Spanish Ministerio de Economía, Industria y Competitividad (MINECO), the Regional (FEDER UE) grant PID2020-115270GB-I00, the Generalitat Valenciana (grant AICO/2021/302), el Fondo Social Europeo y la Iniciativa de Empleo Juvenil EDFJID/2021/185 and la ayuda PRE2021-101090, financiado por MCIN/AEI/10.13039/501100011033 y por el FSE+.

EMBEDDED VOICE COMMAND SYSTEM

Radu-Ilie HEREȘANU

Military Technical Academy Ferdinand I, Boulevard George Coșbuc, Bucharest, Romania

Corresponding author email: radu.heresanu@mta.ro

Abstract

In this paper, I use convolutional neural network architectures established in image classification to improve the speech signal classification performance in activation words. The goal is to develop a command system that is vocally actuated by a predefined set of words. To achieve this goal, the voice signal was transformed into MFCC plus Delta feature matrices, which we can consider as images, which were then used to train a model to classify these activation words. By treating the voice signal as an image, it was very advantageous to implement and compare three architectures that are famous for this type of task – VGG16, AlexNet and SqueezeNet which achieved outstanding results in competitions such as ImageNet ILSVRC. From my own analysis, I found that a quantization of the model brings advantages both in terms of performance and prediction speed, the model being reduced in size, the range of values in which the calculations are made being much more suitable for an edge device. Using previous studies, I also tested an augmentation of the characteristics, but the performance was not substantially improved.

Key words*: quantization, augmentation, MFCC, VGG16, AlexNet, SqueezeNet.*

1. INTRODUCTION

Currently, deep learning is successfully applied in various fields, including automatic speech recognition (ASR), where the main research objective is to design the best possible network architectures, for example, DNNs, CNNs, RNNs and end-to-end models. In particular, I adapted three convolutional neural networks used in image classification with the aim of being able to classify certain words spoken by a speaker. Unlike products like Siri, Alexa and Google Assistant, this system uses the device's voice recognition in a different way. Instead of relying solely on connecting to the cloud infrastructure, this system uses technology built into the device to recognize keywords and perform certain simple tasks without the need for an Internet connection. In the context of using an edge device, model size and classification accuracy play a critical role. Therefore, fulfilling these conditions requires the use of techniques such as model quantization, feature augmentation, and the utilization of a representative, balanced, and easily adaptable dataset.

2. CONTENT

The data set used was Google Speech Commands V2. It contains 105,836 wav audio files divided into 36 classes. The pre-processing and feature extraction involved the choice of activation words, the extraction of MFCC and Delta MFCC features, the augmentation of the feature matrices with random masking bands, and finally the division of the data set into train, validation and test. Following the performance measurements, it was found that the total number of activation words (grouped in one or more classes) should be equal to the number of non-activation samples (noise/other words). Modifications were made to the CNNs in order to be able to work with images with the shape (32,98) and to improve their performance. It has been observed that for major changes such as the type of optimization/activation function, the number of convolutional layers, the drop-out percentage, the accuracy and the loss are negatively affected. The main results obtained with these architectures are very good on the data set used. Accuracy is above 90% in almost all cases. Comparing each CNN, I found that for an edge device, a model with fewer parameters, such as SqueezeNet which has 50 times fewer parameters than Alexnet and 100 times fewer than VGG16, lends itself better to embedded processing and an acceptable true match ratio. In order to decrease the prediction latency and the size of the models I applied post-training quantization. This transformation reduced the complexity of the models and the representation of the parameters (weights, activations and other

variables) so that the calculations were simplified. Using the tensorflow library, I have four types of quantization available: dynamic range, float16, integer, integer quantization with int16 activations. Each type of quantization has its role, depending on the device used, but a more accurate classification I found in the official documentation and is presented in a table below. I mainly used dynamic range quantization. For example, to quantize 8-bit values:

$$x\_quant = (x\_float / scale) + zero\_point \quad (1)$$

$$scale = (max\_val - min\_val) / (qmax - qmin) \quad (2)$$

Arhitecture	H5	TFLite	TFLite Quantized	Train		Validation		Test	
				Loss	Acc.	Loss	Acc.	Loss	Acc.
VGG16	118MB	59MB	**14,9MB**	0.545	0.9722	0.7137	**0.9366**	0.4198	**0.957**
AlexNet	77MB	33MB	**9.64MB**	0.018	**0.9941**	0.291	**0.9475**	0.2876	**0.9593**
SqueezeNet	1.1MB	488kB	**156KB**	0.104	0.9687	0.5713	0.8899	0.5746	0.9146

(The dimensions of the models and their performances)

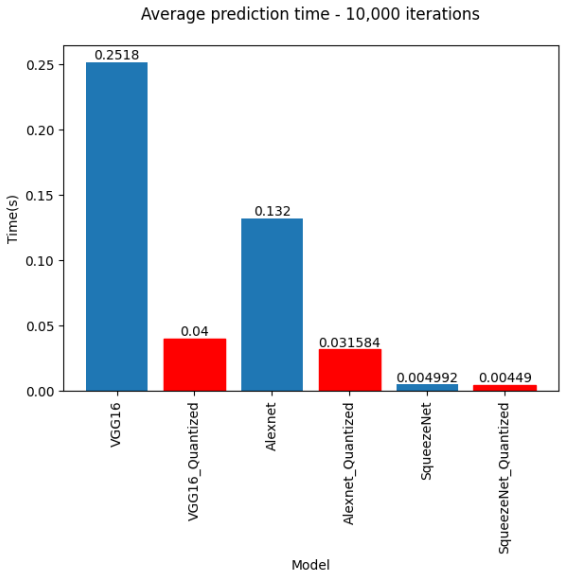

(Average prediction time – 10.000 iterations)

Technique	Benefits	Hardware
Dynamic range quantization	4x smaller, 2x-3x speedup	CPU
Full integer quantization	4x smaller, 3x+ speedup	CPU,EdgeTPU, Microcontrollers
16x8 integer quantization	3-4x smaller, 2x-3x+ speedup	CPU,possibly Edge TPU, Microcontrollers
Float16 quantization	2x smaller, GPU acceleration	CPU, GPU

(The differences between the various quantization techniques)

3. CONCLUSIONS

The results of this study show that current deep learning networks can be successfully modified and designed to perform a wide range of tasks, including ASR applications on low-computing embedded devices.

It has been confirmed that a key aspect to enable speech recognition (as well as other machine learning solutions) on a system on chip and embedded devices is finding the right trade-off between network performance and computational load.

DRUG DETECTION USING K-NEAREST NEIGHBORS ALGORITHM

Iulia-Florentina DARIE[1,2], Ștefan Răzvan ANTON[2,4], Mirela PRAISLER[1]

[1]"Dunărea de Jos" University of Galați, 47 Domnească Street, Galati, Romania
[2]"Paul Dimo" High School, 27 1 Decembrie 1918 Street, Galati, Romania
[3]University Politehnica of Bucharest, 313 Splaiul Independentei, District 6, Bucharest, Romania
[4]Center for Research and Training in Innovative Techniques of Applied Mathematics in Engineering "Traian Lalescu" (CiTi)

Corresponding author email: mirela.praisler@ugal.ro

Abstract

Machine learning algorithms have been successfully applied in the last years for classification problems in various fields. This paper focuses on the the K-Nearest Neighbors (KNN) machine learning algorithm, which was applied in order to detect substances belonging to two classes of drugs that are abused for recreational purpose, i.e., NBOMe, and opioids. To this aim, the ATR-FTIR spectra of a series of compounds belonging to these two classes of illicit drugs were used as input for the Pyhton software. The average accuracy of the model was obtained after 10 runs. The efficiency of this multivariate system was evaluated based on the confusion matrix.

Key words*: machine learning, KNN, NBOMe, opioids, drug detection*

1. INTRODUCTION

Drug abuse represents nowadays a world issue affecting individuals and communities. NBOMe drugs are a class of illicit hallucinogenic compounds known for their high potency. Opioids are a class of drugs known for their medical use, but they are also abused as recreational drugs. In order to detect substances belonging to these two classes of controlled substances, a K-Nearest Neighbors (KNN) algorithm with 5 neighbors was performed. This is an important classification method that has been successfully used in many machine learning and pattern recognition applications.

2. CONTENT

The dataset used consisted of 68 ATR-FTIR spectra selected from the SWGDRUG spectral library. In order to generate the KNN model, the database was split into three different classes: class 1- NBOMe, class 2 – Opioid, and class 3 – Negative. The first class contained 12 NBOMe compounds, the second class included 30 opioids, and the third class was formed by 26 different substances and which do not belong to the modeled classes of controlled substances.
The KNN algorithm was developed using Python software. To this aim, the database was randomly split into two parts, 70% of the spectra forming the training set, and 30% forming the test set. For a better estimation of the accuracy, the training session was repeated 10 times. The obtained average accuracy stands for 79,99% for the training set, and 70,17% for the testing set, illustrating its

substantial potential. The confusion matrix corresponding to the accuracy that has the closest value to the average accuracy is shown in Figure 1.

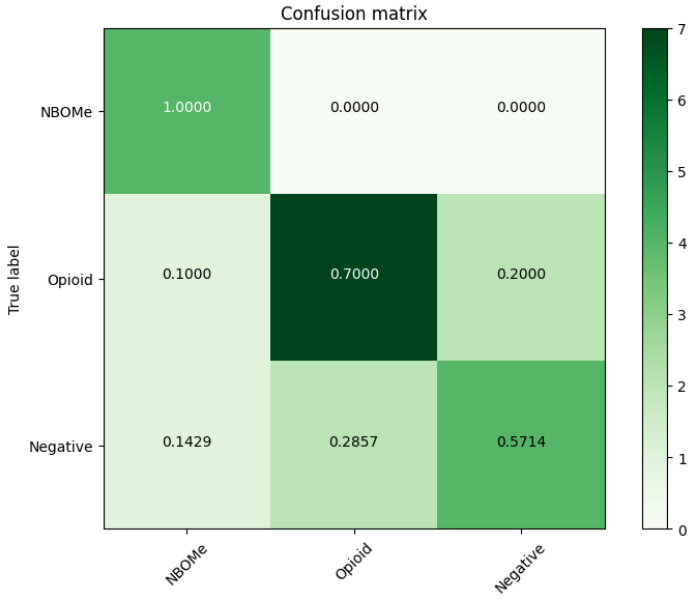

Figure 1. Confusion matrix for the KNN model built to detect NBOMe hallucinogenic amphetamines and opioids.

The confusion matrix indicates that the KNN model classified correctly all (100%) the NBOMes hallucinogenic amphetamines, while only 70% of the opioids were correctly classified. The rest of the opioids were misclassified as NBOMes (10%) or negatives (20%).

3. CONCLUSIONS

The application of machine learning algorithms for drug detection is an emerging field with profound implications for public health and safety. The K-Nearest Neighbors (KNN) algorithm explored in this study demonstrated promising results for the classification and detection of NBOMe and opioid drugs based on ATR-FTIR spectral data. A notable outcome of this research was the model's capacity to accurately identify 100% of NBOMe compounds, which are notorious for their high potency and abuse potential. On the other hand, only 70% of the opioids were correctly classified. The misclassifications primarily occurred between opioids and the negatives class, indicating the need for further refinement of the model to improve the differentiation between these classes. Despite these limitations, this study showcases the potential of machine learning techniques, particularly the KNN algorithm, for building drug detection and classification computer-aided applications. Future research will focus on expanding the spectral database, pre-processing the spectra with various discriminating weighing functions, further refining the model, and exploring its application in a real-world context. This work sets a foundation that may ultimately contribute to the development of rapid, accurate, and non-invasive drug detection methods, crucial for addressing the global issue of drug abuse.

ADVANCED OPTIMIZATION TECHNIQUES FOR UNBALANCED ALLOCATION PROBLEMS USING THE MODIFIED HUNGARIAN ALGORITHM

Ștefan-Cătălin PETRESCU[1], Simona Mihaela BIBIC[2]

[1]University Politehnica of Bucharest, 313 Splaiul Independentei, District 6, Bucharest, Romania

Corresponding author email: stefan.petrescu0208@stud.fils.upb.ro, simona.bibic@upb.ro

Abstract

This paper presents a new perspective by using the application of Modified Hungarian Algorithm (MHA) in different contexts, with special focus on resource allocation. MHA is a powerful computational tool designed to improve unbalanced allocation problems and has been successfully applied in various fields, including healthcare and industrial processes, proving its versatility and effectiveness. The algorithm is implemented in two widely used programming languages, C++ and Python, which further highlights its adaptability. The paper includes a comprehensive comparison of MHA with the classical Hungarian algorithm, which provides insights into their respective efficiencies in solving unbalanced allocation problems. The potential of MHA in future applications and research is also discussed, opening avenues for further exploration and development of this algorithm.

Key words*: Modified Hungarian Algorithm; Unbalanced Assignment Problems; Resource Optimization; C++; Python.*

1. INTRODUCTION

The Modified Hungarian Algorithm (MHA) is a powerful tool for solving unbalanced assignment problems of any type. It builds upon the methods used in the classic Hungarian algorithm and the concept introduced by Q. Rabbani, A. Khan, and A. Quddoos for a modified Hungarian algorithm that solves problems where the number of columns is greater than the number of rows in the table. The algorithm has been implemented and tested in C++ and Python using Visual Studio Code and PyCharm Professional respectively as compilations environements.

2. CONTENT

The MHA brings several improvements over the classic Hungarian algorithm. Unlike the concept introduced by Q. Rabbani, A. Khan, and A. Quddoos, where the matrix is modified until the stop condition is met (i.e., the number of cuts required to cover all zeros is equal to the number of rows in the matrix), the proposed algorithm starts with the initial solution matrix. If this solution is not optimal, the matrix is adjusted, and after each adjustment, it is checked whether an optimal solution can be obtained.

The zero framing procedure used in the proposed algorithm is similar to that used in the Hungarian algorithm, being done on lines, in ascending order of the number of zeros. However, it differs in the choice of the zero on the line. Instead of framing the zero that corresponds to the column with the minimum number of zeros on the column, the zero that corresponds to the minimum value in the initial matrix is framed, ensuring an optimal solution.

The proposed algorithm introduces a new method of adjusting the matrix when the current matrix cannot produce the desired solution. This involves searching for the minimum value element in the

matrix, excluding the zeros, then subtracting it from the non-zero elements in the matrix. This proposed method ensures the achievement of an optimal solution, unlike the adjustment method of the classic Hungarian algorithm, which cannot be used in the case of unbalanced problems, as in some cases the matrix can no longer be adjusted, and the solution is not feasible.

3. CONCLUSIONS

The Modified Hungarian Algorithm (MHA) has proven to be an effective and efficient tool for solving unbalanced assignment problems. Its versatility allows it to be applied in various fields, from healthcare to industrial processes, demonstrating its wide-ranging applicability.

In this paper, we have presented a detailed example of the MHA, comparing it with the Classic Hungarian Algorithm. This comparison has provided valuable insights into the respective efficiencies of these algorithms in solving unbalanced assignment problems. The MHA has been implemented in both C++ and Python, highlighting its adaptability to different programming environments and its potential for wider application.

Furthermore, this work has brought a novel perspective by showcasing the application of MHA in different contexts, particularly in the allocation of resources. The detailed mathematical model and calculation scheme using MHA presented in this paper provide a clear and concise understanding of the algorithm, making it accessible for further research and application.

Looking ahead, the potential of the MHA for future applications is vast. The algorithm's efficiency and versatility open up numerous possibilities for its application in other domains. Future research could explore these potential applications, as well as develop new methods and techniques for optimizing resource allocation.

In conclusion, the Modified Hungarian Algorithm stands as a powerful tool in the field of optimization, offering promising prospects for future research and application.

REFERENCES

[1.] Q. Rabbani, A. Khan, A. Quddoos, *Modified Hungarian method for unbalanced assignment problem with multiple jobs*, Applied Mathematics and Computation 361 (2019), 493-498.

[2.] Van Rossum, G. & Drake Jr, F.L., 1995. *Python reference manual*, Centrum voor Wiskunde en Informatica Amsterdam.

[3.] Mohammad Shyfur Rahman Chowdhury. (2022). *An Improved Hungarian Algorithm for a Special Case of Unbalanced Assignment Problems*. Global Journal of Science Frontier Research, 22(F4), 29–35. https://doi.org/10.34257/GJSFRFVOL22IS4PG29

[4.] S. M. Bibic, S. C. Petrescu, *Advanced Optimization Techniques for Unbalanced Allocation Problems using the Modified Hungarian Algorithm* (*under review*)

A MODEL FOR CELL EVOLUTION IN MALARIA

Karim AMIN[1], Samia MRAD[2]

[1,2] Lebanese International University, Department of Mathematics and Physics, Bekaa, Lebanon

Corresponding author email: karim.amin@liu.edu.lb and samiamrad001@gmail.com

Abstract

We will present a new biological model based on delay differential equations to study the evolution of malaria within host under drug treatment. The analysis of stability for the equilibrium points depends on the theorem of critical case presented in [1] which is an extension of a Lyapunov-Malkin theorem to address the critical scenario of a zero root in the characteristic equation. The equilibrium points are determined and their stability is assessed by utilizing the eigenvalues of the linearized system. In order to ensure the theorem's applicability, translations to zero are performed. Finally, we conclude that the stability depends on the study of the transcendental terms in the characteristic equations.

Key words*: Delay Differential Equation; Malaria Evolution; Characteristic Equation; Stability Analysis; Critical Case.*

1. INTRODUCTION

Malaria is a grave and potentially fatal illness caused by a parasite that commonly infects a specific type of mosquito (Anopheles) that feeds on humans. These symptoms typically manifest 10 to 15 days after being bitten by an infected mosquito, but they can be mild and easily mistaken for other conditions. If left untreated, malaria can rapidly progress to a severe state and result in death within days. Unfortunately, an effective vaccine for malaria is still unavailable due to the parasite's ability to evade the immune system by continuously altering its outer surface. Currently, the primary approach for treating and preventing malaria infection involves the use of antimalarial drugs.

2. MODEL

This section includes the physiological model for Malaria evolution within host under drug treatment. We will use $x_\tau = \mathrm{x(t-\tau)}$ as the notation for the delayed variables. We use delay-differential equations to model the within-host dynamics of a malaria infection, which tracks uninfected red blood cells (x_1), concentration of erythropoietin (x_2), loss during cell cycle (x_3), infected red blood cells (x_4), extracellular malaria parasites (merozoites, x_5) and gametocytes (x_6). The delay differential equations are represented by:

$$\dot{x}_1 = t\left(\frac{1-x_1}{k}\right) - \mu x_1 - \rho x_1 x_5$$
$$\dot{x}_2 = -e_1 x_2 + \left(\frac{a}{1+{x_1}^r}\right)$$
$$\dot{x}_3 = x_3\left(\frac{-e_0}{1+{x_2}^n} + \frac{e_0}{1+(x_{2\tau_1})^n}\right)$$
$$\dot{x}_4 = \rho x_1 x_5 - \mu x_4 - \rho x_{1\tau_2} x_{5\tau_2} S$$
$$\dot{x}_5 = (1-c)B\rho x_{1\tau_2} x_{5\tau_2} S - \rho x_1 x_5 - M x_5$$
$$\dot{x}_6 = c\rho x_{1\tau_2} x_{5\tau_2} S - G x_6$$

3. STABILITY ANALYSIS

The model that takes into consideration the response of the treatment becomes:

$$\dot{x} = f_i(x; x_j), \qquad i = 1;6 \quad j = 1;2$$

After solving the equations $\dot{x} = 0$ we obtain the equilibrium points E_1 and E_2:

$$E_1 = (\overline{x_1}, \overline{x_2}, \overline{x_3}, 0,0,0)$$
$$E_2 = (\widehat{x_1}, \widehat{x_2}, \widehat{x_3}, \widehat{x_4}, \widehat{x_5}, \widehat{x_6})$$

Let A= [a_{ij}] be the matrix in the linear approximation around E_1 corresponding to non-delayed terms, B= [b_{ij}] the matrix corresponding to terms with the delay τ_1, C=[c_{ij}] the matrix that corresponds to the terms with the delay τ_2 .

$$A = \frac{\partial f}{\partial x}, \qquad B = \frac{\partial f}{\partial x_{\tau_1}}, \qquad C = \frac{\partial f}{\partial x_{\tau_2}}$$

The general form of the characteristic equation is:

$$det(\lambda I_n - A - Be^{-\lambda\tau_1} - Ce^{-\lambda\tau_2}) = 0$$

For the equilibrium point E_1 we have:

$$(\lambda - a_{11})(\lambda - a_{22})(\lambda)(\lambda - a_{44})(\lambda - a_{66})\left(\lambda - a_{55} - c_{55}e^{-\lambda\tau_2}\right) = 0$$

The real solutions of the characteristic equation are:

$$\lambda_1 = -(t/k) - \mu < 0, \qquad \lambda_2 = -e_1 < 0, \qquad \lambda_4 = -M < 0, \qquad \lambda_6 = -G < 0$$

We know that if all the roots of the equilibrium points have negative real parts, then the equilibrium point is uniformly asymptotically stable. $\lambda_3 = 0$ is a root, and we are in a critical case for the stability of the nonlinear system. We perform a translation to zero then we conclude that the general theorem on the critical case works for the system and the stability depends on the study of the transcendental term in the characteristic equation:

$$\lambda - a_{55} - c_{55}e^{-\lambda\tau_2}$$

The characteristic equation of E_2 is:

$$(\lambda - a_{44})(\lambda - a_{66})(\lambda)(-a_{15}a_{51} + a_{11}c_{55} - c_{55}\lambda)e^{-\lambda\tau_2}$$
$$+ (\lambda^2 - (a_{11} + a_{55})\lambda + a_{11}a_{55} - a_{15}a_{51})) = 0$$

The real solutions of this characteristic equation are:

$$\lambda_4 = -M < 0, \qquad \lambda_6 = -G < 0$$

$\lambda_3 = 0$ is a root, and again we are in a critical case for the stability of the nonlinear system and the stability depends on the study of the transcendental term:

$$(-a_{15}a_{51} + a_{11}c_{55} - c_{55}\lambda)e^{-\lambda\tau_2} + (\lambda^2 - (a_{11} + a_{55})\lambda + a_{11}a_{55} - a_{15}a_{51}))$$

4. REFERENCE

[1] K. Amin, I. Badralexi, A. Halanay, R. Mghames. *A stability theorem for equilibria of delay differential equations in a critical case with application to a model of cell evolution*. Math. Model. Nat. Phenom. 16 (2021) 36.

A NEW VARIANT OF A MULTIMODAL ROMANIAN VOICE EMOTION DETECTION

Paul-Florinel CĂSĂNDROIU[1], Luciana MOROGAN[2]

Military Technical Academy "Ferdinand I", 39-49 George Coșbuc Avenue, District 5, Romania

Corresponding author email: paulflorinel1234@gmail.com[1], luciana.morogan@mta.ro[2]

Abstract

The evolution of Natural Language Processing technologies transformed them into viable choices for various accessibility features and for facilitating interactions between humans and computers. Multimodal Romanian Voice Emotion Detection (MRVED) [1] was previously introduced in order to enhance Romanian emergency services. Its purpose derived from the idea that the Romanian 112 operator can be supported to evaluate various emergency situations for reducing the response times of emergency services
Starting from the model we mentioned above, we refined it and retrained it on a new and originally created dataset composed of 2 types of voice recordings: (1) recordings made with the help of romanian actors and (2) classified recordings provided by one specific Romanian Communication Service. Our results will be presented within these pages.

Key words*: voice emotion detection, language models, spectrograms*

1. INTRODUCTION

Beyond the purpose of the Multimodal Romanian Voice Emotion Detection (MRVED), captured in [1], fields such as psychology, military, government and many more can benefit from its novelty. As it is known, the emotions that it detects require targeted data related to the field it was meant to address. In [1] MRVED was trained on EmoDB [2] recordings. We refined the system to be suited on a new dataset developed as it will be further described.

2. CONTENT

Dataset. Multimodal Romanian Voice Emotion Detection (MRVED) from [1] was trained to detect seven emotions following the EmoDB dataset restricted to the demands of its purpose. The chosen emotions that it can recognise are anger (A), boredom (B), disgust (D), fear (F), neutral (N) and sadness (S). We complemented the dataset by a new emotion: *irritation* (*I*). Furthermore, the new dataset we worked on is composed of:

- Recordings that were made with the help of romanian actors
- Classified recordings provided by a Romanian communication service.

Our dataset contains 42 recordings (7 recordings were made using romanian actors and 35 classified recordings) from which we extracted a total number of 340832 spectrograms. The usage of the spectrograms will be further described. These spectrograms were used to train, validate and test our system. To split our spectrograms into these 3 categories (training, validation and test spectrograms) we choose to randomly select 10% of the files corresponding to each emotion (10% from the files containing anger, 10% from the files containing boredom, etc). After that we decided to use 20% of the remaining data for validation and the rest of them for training.

System implementation. We used two methods to detect the emotions from voice recordings and we called them *versions*. Both versions determine the emotion from a voice recording, following different methods: for the first version we used 5 models (RandomForestClassifier [3], SVC [4], LogisticRegression [5], DecisionTreeClassifier [6], MLPClassifier [7]) and for the second one we used a neural network called VGG16 [8].

Version 1. The models we already mentioned were trained to recognise emotions from voice recordings such as each of them predict an emotion. These emotions are then feeded to a voting

algorithm that we developped to choose the emotion which was predicted the most (by minimum 3 models). We basically look at each emotion predicted by the model and decide, using the vote concept (consisting in the basic rule "majority wins"), which emotion would be the most appropriate for the recording the system received from the user in order to detect his/her emotion from that recording. In case of a tie of two different emotions, the output of the voting will be of the *EMOTION1/EMOTION2* form. For the preprocessing part of the data, we splitted the audio based on its labels. Each audio file FILENAME.wav has a pair FILENAME.txt which contains the labels for that audio file and each line of the FILENAME.txt file contains the following: START_LABEL END_LABEL [EMOTION] [BACKGROUND] [CHARACTER] TEXT. START_LABEL and END_LABEL contains the strating and ending time of a label based on the time of the recording but in milliseconds; EMOTION contains the emotion of the person who speaks in that time period (the emotions we mentioned earlier will be found here); BACKGROUND contains the background addnotations if there are any; CHARACTER contains the name of the character that is speaking in that audio fragment (not the name itself, but rather what is his/her role in the recording, like caller, operator or voice if the one speaking is neither caller nor operator); TEXT contains the actual words that are spoken. So we used these FILENAME.wav-FILENAME.txt as pairs and we gave them to the models in order to train and test them.

Version 2. We used a slightly modified VGG16 neural network, in which we added a new layer in order to predict the emotions we mentioned earlier (down below you will find 3 figures: figure 1 shows you how many layers a VGG16 model have and how many layers our VGG16 model have, figure 2 shows you the last layer of the original VGG16 model, figure 3 shows you the last 2 layers of our VGG16 model so we can show our last layer and how it looks like after we inserted at the end of the VGG16 model). For the preprocessing part we used the same method as in version 1, but instead of using them directly with our model, we saved each segment in a folder based on its emotion (for example: if a segment had N as emotion, then that segment was saved in the folder called "N"). Then for each segment we created the corresponding spectrograms, having a 1 second window and a 10 milliseconds step. This means that the recording would be split out into frames and the frames that are closer to one another (like $frame_n$ and $frame_{n+1}$) would be 10 ms apart. These spectrograms were used in the VGG16 model for training, validation and testing.

```
Number of layers for VGG16: original model 23, our model 24
```

Fig 1. The number of layers both VGG16 original model and our VGG16 modified model have

```
predictions (Dense)          (None, 1000)              4097000
```

Fig 2. The last layer of the original VGG16 model

```
predictions (Dense)          (None, 1000)              4097000

final_predictions (Dense)    (None, 8)                 8008
```

Fig 3. The last 2 layers of our modified VGG16 model

Hybrid model. The hybrid model means that we combined version 1 and version 2, train each one of them (the 5 models used in version 1 and VGG16 used in version 2) in their unique way, having the same output regarding each version. The output from each version is then redirected into a new kind of voting algorithm (which applies the same rule "majority wins") but this algorithm receives the output of both versions and decides what emotion to show the user (for example if the version 1 has the output A/B and version 2 has the output A, then the voting algorithm splits the output the version 1 had into 2 separate elements A and B, counts the number of times A and B appear in both outputs and then the output it gives is A in this example). In the worst case scenario, the output will

be *EMOTION1/EMOTION2/EMOTION3*, but the other possibilities are *EMOTION1/EMOTION2* and *EMOTION*.

3. CONCLUSIONS

Our dataset has enough data to produce significant results. Overall, version 2 produced better results than version 1, but both managed to have a high accuracy.

4. BIBLIOGRAPHY

[1] https://www.mdpi.com/2076-3417/13/1/639
[2] https://www.kaggle.com/datasets/piyushagni5/berlin-database-of-emotional-speech-emodb
[3] https://scikit-learn.org/stable/modules/generated/sklearn.ensemble.RandomForestClassifier.html
[4] https://scikit-learn.org/stable/modules/generated/sklearn.svm.SVC.html
[5] https://scikit-learn.org/stable/modules/generated/sklearn.linear_model.LogisticRegression.html
[6] https://scikit-learn.org/stable/modules/generated/sklearn.tree.DecisionTreeClassifier.html#sklearn.tree.DecisionTreeClassifier
[7] https://scikit-learn.org/stable/modules/generated/sklearn.neural_network.MLPClassifier.html#sklearn.neural_network.MLPClassifier
[8] https://www.tensorflow.org/api_docs/python/tf/keras/applications/vgg16/VGG16

GROWTH OF SOLUTIONS OF LINEAR DIFFERENTIAL EQUATIONS WITH ENTIRE COEFFICIENTS OF *[P,Q]- Φ* ORDER

Mansouria SAIDANI[1], Benharrat BELAÏDI[2]

[1]Department of mathematics, Laboratory o Pure and Applied Mathematics, University of Mostaganem (UMAB), B. P. 227, Mostaganem, Algeria

[2]Department of mathematics, Laboratory o Pure and Applied Mathematics, University of Mostaganem (UMAB), B. P. 227, Mostaganem, Algeria

Corresponding author email: saidaniman@yahoo.fr

benharrat.belaidi@univ-mosta.dz

Abstract

The aim of this work is to study the growth of solutions of higher order complex linear differential equations with entire coefficients. First, by using the concept of [p,q]-φ order and under some hypotheses on the dominant coefficient, we prove that every non-transcendental solution of the equation

$$A_k(z)f^{(k)}(z) + A_{k-1}(z)f^{(k-1)}(z) + \cdots + A_1(z)f'(z) + A_0(z)f(z) = 0$$

is a polynomial and every transcendental meromorphic solution is of [p+1,q]-φ order which coincides with the [p,q]-φ order of an arbitrary dominant coefficient.

In the second part of this paper, we get some information about the [p,q]-φ order, [p,q]-φ exponents of convergence of zero-sequence and distinct zero-sequence of solutions of the equation

$$A_k(z)f^{(k)}(z) + A_{k-1}(z)f^{(k-1)}(z) + \cdots + A_1(z)f'(z) + A_0(z)f(z) = F(z).$$

Our results improve and extend some previous results due to Agarwal, Datta and Biswas [1]*, Biswas, Datta and Tamang* [3]*, Saidani and Belaïdi* [5].

Keywords*: linear differential equation; entire function; [p,q]-φ order; [p,q]-φ convergence exponent.*

1. INTRODUCTION

Throughout this article, we assume that the reader is familiar with the basic results and standard notation of Nevanlinna's value distribution theory of meromorphic functions (see [4]). In this section we quote the main concepts and definitions used in the realisation of this work.

Definition 1.1 ([6]) Let $\varphi: (0,+\infty) \to (0,+\infty)$ be a non-decreasing unbounded function, and p, q be positive integers that satisfy $p \geq q \geq 1$. Then the $[p,q]$-φ order and $[p,q]$-φ lower order of a meromorphic function f are respectively defined by

$$\rho_{[p,q]}(f,\varphi) = \limsup_{r\to+\infty} \frac{\log_p T(r,f)}{\log_q \varphi(r)}, \qquad \mu_{[p,q]}(f,\varphi) = \liminf_{r\to+\infty} \frac{\log_p T(r,f)}{\log_q \varphi(r)}.$$

Definition 1.2 ([6]) Let f be a meromorphic function. Then, the $[p,q]$-φ exponent of convergence of zero-sequence (distinct zero-sequence) of f is defined by

$$\lambda_{[p,q]}(f,\varphi) = \limsup_{r\to+\infty} \frac{\log_p n(r,\frac{1}{f})}{\log_q \varphi(r)}, \qquad \bar{\lambda}_{[p,q]}(f,\varphi) = \limsup_{r\to+\infty} \frac{\log_p \bar{n}(r,\frac{1}{f})}{\log_q \varphi(r)}.$$

Several authors have studied the complex oscillation properties of linear differential equations

$$A_k(z)f^{(k)}(z) + A_{k-1}(z)f^{(k-1)}(z) + \cdots + A_1(z)f'(z) + A_0(z)f(z) = 0 \qquad (1)$$

and $$A_k(z)f^{(k)}(z) + A_{k-1}(z)f^{(k-1)}(z) + \cdots + A_1(z)f'(z) + A_0(z)f(z) = F(z). \qquad (2)$$

In [3], Biswas, Datta and Tamang have studied the growth of solutions of equations (1) and (2), and obtained that when the coefficients A_j (j=0,1,...,k) are of $[p,q]$-φ order less than the $[p,q]$-φ order of the dominant coefficient A_0, then the $[p+1,q]$-φ order of any transcendental meromorphic solution of equation (1) coincides with the $[p,q]$-φ order of the dominant coefficient A_0 and moreover if $\rho_{[p+1,q]}(F,\varphi) > \rho_{[p,q]}(A_0,\varphi)$, then the $[p+1,q]$-φ order of any transcendental meromorphic solution

of equation (2) coincides with the $[p,q]$-φ order of the function F. Recently, in [1], Agarwal, Datta, Biswas and Tamang have obtained some properties about the $[p,q]$-φ exponent of convergence of zero-sequence (distinct zero-sequence) of solutions of the solutions of equation (2) for $A_k = 1$.

2. MAIN RESULTS

We now present our main results.

Theorem 2.1 Let G be a set of complex numbers satisfying $\overline{\log dens}\{|z|:z\in G\}>0$, p, q be integers such that $p\geq q \geq 1$ and let $A_j(z)$ (j=0,1,..., k) be entire functions such that $A_k(z) \neq 0$. Suppose there exists an integer s, $0\leq s\leq k$ such that $\max\limits_{j=0,1,\ldots,k,j\neq s}\{\rho_{[p,q]}(A_j,\varphi)\} < \mu_{[p,q]}(A_s,\varphi) \leq \rho_{[p,q]}(A_s,\varphi) = \rho < +\infty$, and for some real constant μ satisfying $0\leq\mu<\rho$, we have for any given ε ($0<\varepsilon<\rho-\mu$) sufficiently small,

$$|A_j(z)|\leq \exp_{p+1}\{\mu \log_q(\varphi(r))\},\ j\neq s,\ j=0,1,\ldots,k,$$
$$|A_s(z)|\geq \exp_{p+1}\{(\rho-\varepsilon)\log_q(\varphi(r))\},$$

as $z\to\infty$ for $z\in G$. Then every non-transcendental solution $f(z)\neq 0$ of equation (1) is a polynomial with $deg\ f \leq s$-1 and every transcendental meromorphic solution f of equation (1) with $\lambda_{[p,q]}\left(\frac{1}{f},\varphi\right) < \mu_{[p,q]}(f,\varphi)$ satisfies $\rho_{[p+1,q]}(f,\varphi)=\rho_{[p,q]}(A_s,\varphi)$.

Theorem 2.2 Let G be a set of complex numbers satisfying $\overline{\log dens}\{|z|:z\in G\}>0$, p, q be integers such that $p\geq q \geq 1$ and let $A_j(z)$ (j=0,1,…,k), $F(z)\neq 0$ be entire functions such that $A_k(z)\neq 0$. Suppose there exists an integer s, $0\leq s\leq k$ such that $\max\limits_{j=0,1,\ldots,k,j\neq s}\{\rho_{[p,q]}(A_j,\varphi),\rho_{[p,q]}(F,\varphi)\} < \mu_{[p,q]}(A_s,\varphi) \leq \rho_{[p,q]}(A_s,\varphi) = \rho < +\infty$ and for some real constant μ satisfying $0\leq\mu<\rho$, we have for any given ε ($0<\varepsilon<\rho-\mu$) sufficiently small,

$$|A_j(z)|\leq \exp_{p+1}\{\mu \log_q(\varphi(r))\},\ j\neq s,\ j=0,1,\ldots,k,$$
$$|A_s(z)|\geq \exp_{p+1}\{(\rho-\varepsilon)\log_q(\varphi(r))\},$$

as $z\to\infty$ for $z\in G$. Then every non-transcendental solution $f(z)\neq 0$ of equation (2) is a polynomial with $deg\ f \leq s$-1 and every transcendental meromorphic solution f of equation (2) with $\lambda_{[p,q]}\left(\frac{1}{f},\varphi\right) < \mu_{[p,q]}(f,\varphi)$ satisfies $\overline{\lambda}_{[p+1,q]}(f,\varphi) = \lambda_{[p+1,q]}(f,\varphi) = \rho_{[p+1,q]}(f,\varphi)=\rho_{[p,q]}(A_s,\varphi)$.

3. CONCLUSIONS

In this work, we improve and extend some results of Agarwal, Datta and Biswas [1], Biswas, Datta and Tamang [3], Saidani and Belaïdi [5], Belaïdi [2] by using the concept of $[p,q]$-φ order.

REFERENCES

[1] R. P. Agarwal, S. K. Datta, N. Biswas and S. Tamang, *On the comparative growth analysis of solutions of complex linear differential equations with entire and meromorphic coefficients of* $[p,q]$-φ *order*. Int. J. Nonlinear Anal. Appl. 13 (2022) 2, 2175-2183.

[2] B. Belaïdi, *Iterated order of meromorphic solutions of homogeneous and non- homogeneous linear differential equations*. *ROMAI J.* **11** (2015), no. 1, 33-46.

[3] N. Biswas, S. K. Datta and S. Tamang, *On growth properties of transcendental meromorphic solution of linear differential equations with entire coefficients of higher order*. Commun. Korean Math. Soc. **34** (2019), no. 4, 1245-1259.

[4] A. A. Goldberg, I. V. Ostrovskii, *The distribution of values of meromorphic functions*. Irdat Nauk, Moscow, 1970 (in Russian), Transl. Math. Monogr. 236, Amer. Math. Soc., Providence RI, 2008.

[5] M. Saidani, B. Belaïdi, *Meromorphic solutions to linear differential equations with entire coefficients of* $[p,q]$-*order*. J. Dyn. Syst. Geom. Theor. **16** (2018), no. 1, 33-53.

[6] X. Shen, J. Tu and H. Y. Xu, *Complex oscillation of a second-order linear differential equation with entire cofficients of* $[p,q]$-φ *order*. Adv. Difference Equ. **2014,** 2014:200, 14 pp.

[7] M. L. Zhan, X. M. Zheng, *Solutions to linear differential equations with some coefficient being lacunary series of* $[p,q]$-*order in the complex plane.* Ann. Differential Equations **30** (2014), no. 3, 364-372.

A BEAM OF HOPE: MODELLING APPROACH OF PROTON THERAPY AS CANCER TREATMENT

Ruxandra-Ioana CIPU[1,2], Ștefania Maria MICHNEA [1,2]
Elena Corina CIPU[1,3]

[1]University Politehnica of Bucharest, Centre for Research and Training in Innovative Techniques of Applied Mathematics in Engineering "Traian Lalescu" (CiTi), Bucharest, Romania
[2]Faculty of Medical Engineering, University Politehnica of Bucharest
[3]Department of Applied Mathematics, Faculty of Applied Sciences, University Politehnica of Bucharest

Corresponding author email: ruxandra_ioana.cipu@stud.fim.upb.ro

Abstract

Cancer has been an occurring problem in various patients for decades and this project might be a step towards an improved approach of treatment and pathological prognosis. Proton beam therapy is a type of radiation therapy that uses protons to treat different types of malignancies. It functions by targeting the tumour with doses of high energy protons, reducing the nearby healthy tissue.
Administered radiation dose and the absorbed particles dependency between the administrated radiation dose for several individuals and their medical outcome are computed using different type of approximation functions and graphic representations and comparison are made.
Statistical analysis using Monte Carlo method, a broad class of computational algorithms that rely on repeated sampling to obtain numerical results to estimate survival chances, financial and medical efficiency of proton beam therapy is considered. Data found in research centres that have published patient's outcomes were used. This research paper encompasses the promise and potential of proton beam therapy as a better oncological treatment, evidence being supported by a mathematical point of view.

Keywords*: proton therapy; dosimetry, Monte Carlo simulations.*

EXTENDED ABSTRACT

Proton beam therapy is a type of radiation therapy that uses protons to treat different types of cancer. It functions by targeting the tumor with doses of high energy protons, reducing the damage to nearby healthy tissue. This can be an advantage for older and sicker patients, but the precision of this type of therapy is especially beneficial for patients where the cancer is in an inoperable place such as the spinal cord, the brain, the bones, and soft tissues. This project studies its financial and medical efficiency using statistical methods.

1 How it works?

The protons must be accelerated to gain a high energy to fight the neoplastic cells. This is crucial for what we know as being the Bragg peak, the moment the protons reach cancer tissues, releasing an immense amount of radiation energy to kill the neoplastic cells. These positively charged particles deposit most of their energy at the end of the beam, an ability that allows proton therapy to spare the healthy tissue.

2 Dosimetry calculations

To furthermore demonstrate that PBT has huge promise, we must look at the dosimetry used for such therapies. There is substantial advantage over photon therapy, by utilizing its "Bragg peak". Graphs were made in MATLAB to approximate the dependency between administered radiation dose and the absorbed particles for several individuals. Approximation functions and graphic representations such as exponential curves and sigmoid graphs are used.
For the first graph, we have used the formula for the absorbed dose to calculate the absorbed energy in the lungs when applying proton radiation on lungs.

The second graph is an exponential one that depicts the unaffected individuals influenced by the applied radiation dose that takes different values.

The third MATLAB graph shows a sigmoid function that was constructed with and improved formula containing not only the applied dose, but also the number of targets in the body, represented by the malignant cells hit by radiation.

(Fig. 1)

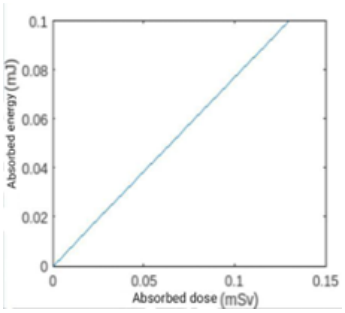

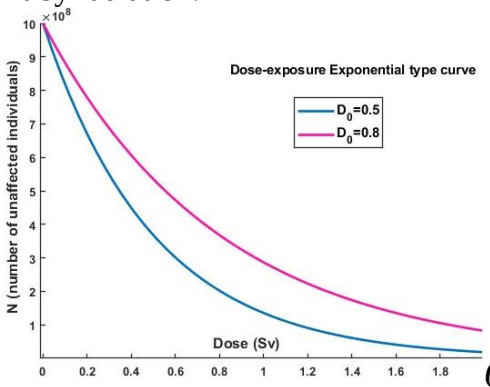

(Fig. 2)

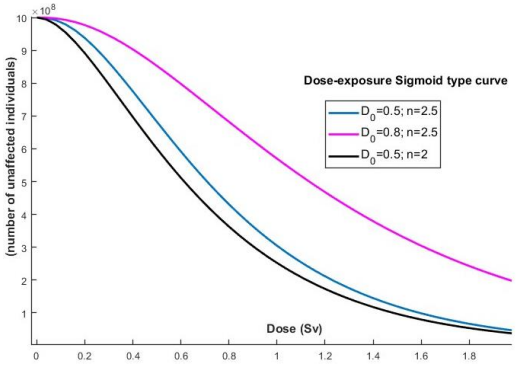

(Fig. 3)

3. Monte Carlo method

The Monte Carlo method is a statistical method which represents a broad class of computational algorithms that rely on repeated random sampling to obtain numerical results. The underlying concept is to use randomness to solve problems that might be deterministic in principle. This method performs risk analysis by choosing the variable that has uncertainty and assigning it a random value. This research includes data simulations of Monte Carlo that have shown us the impact of this treatment type on patients.

CONCLUSIONS

Despite its conceptual and algorithmic simplicity, the computational cost associated with a Monte Carlo simulation can be high. In general, the method requires many samples to get a good approximation, which may incur an arbitrarily large total runtime if the processing time of a single sample is high. The statistical tests made in this paper result in a positive outcome for patients using this kind of therapy. However, the promise and potential of proton beam therapy as an innovation in healthcare remains largely unrealized due to high costs that limit access for patients, as well as a lack of evidence regarding its clinical effectiveness.

REFERENCES:

[1] J.D. Azcona, B. Aguilar, A. Perales, R.Polo, D. Zucca, L. Irazola, A. Viñals, P. Cabello,

[2] J.M. Delgado, D. Pedrero, R. Bermúdez, R. Fayos-Sola, C. Huesa-Berral, J. Burguete *Commissioning of a synchrotron-based proton beam therapy system for use with a Monte Carlo treatment planning system*, Radiation Physics and Chemistry 204 (2023) 110708

[3] Elham Piruzan, Naser Vosoughi, Hojjat Mahani, *Modeling and optimization of respiratory-gated partial breast irradiation with proton beams - A Monte Carlo study*, Computers in Biology and Medicine 147 (2022), 105666 .

[4] Mona Mihăilescu, Nicoleta Eșeanu - "Biofizica si bioinginerie" Politehnica Press, 2015

[5] N. G Burnet, R. I Mackay,2Ed Smith, Amy L Chadwick, Gillian A Whitfield, David J Thomson, Matthew Lowe, Norman F Kirkby, Adrian M Crellin and Karen J Kirkby *Proton Therapy special feature: Review Article. Proton beam therapy: perspectives on the National Health Service England clinical service and research programme*, Doi:10. 1259/bjr. 20190873

https://www.sciencedirect.com/topics/medicine-and-dentistry/monte-carlo-method

THE DEVELOPMENT OF A POPULATION THROUGH TIME USING THE GAME THEORY

Mircea-Răzvan LAZA [1], Simona Mihaela BIBIC [2]

[1, 2]University Politehnica of Bucharest, 313 Splaiul Independentei, District 6, Bucharest, Romania

Corresponding author email: mircea_razvan.laza@stud.fsa.upb.ro, simona.bibic@upb.ro

Abstract

This paper proposes the idea of understanding, solving and demonstrating how the evolution of a species in relation to time can be determined using the game theory. Many species, including us, humans, live a life of multiple interactions per day, but we tend to forget of the primordial implications which determine the strategy to use when it comes to improving our lives in relation to our surroundings and the different factors we are influenced by. Thus, using the game theory, we will understand and will be able to grasp the fundamental aspects of how to choose the best strategy when interacting with our surroundings, how and why, in a species, one party can lose and the other will win (using models such as 2-players based games and dynamical systems) and how to determine where such a population will find an equilibrium in time through Nash's theorem.

Key words*: dynamical systems; evolutionary game theory (EGT); replicator equation; Nash equilibrium; Python*

1. INTRODUCTION

In everyday life, the evolution of a population for any living beings is subject to multiple factors that lead, over time, to a prediction of its density variation. Heuristic spaces dealing with the determination of such predictions use an increased number of factors precisely to achieve a higher success rate. However, the fundamental specificity for these determinations is the primordialism of evolution as a species, which can be represented by the mathematical model of game theory.

2. CONTENT

The way life began its trajectory towards growth and evolution, even at the microscopic level, is represented by the two most important and defining aspects: the struggle for survival and reproduction.

A population *X* that is introduced into a world with limited resources (as humans alike) and has two options to continue its evolution, such as:

- sharing the available food, thus ensuring a considerable proportion of at least sustenance and - in the favorable case - when the food is distributed to each individual in maximum amounts needed, the food will ensure both sustenance and reproduction;
- fighting for the available food, in which case a larger quantity of food (compared to the strategy of sharing with another individual) will ensure 100% sustenance and, in addition, the possibility of reproduction with a 50% chance when meeting a sharing population. The sharing individual will have a 50% chance of survival. But because of fighting and injuries, when an aggressive individual meets another, they end up with no food, thus not surviving.

Thus, population *X* can have active implications in both criteria that are opposite in terms of how they operate, resulting, in fact, in the division into two populations: *X* and *Y*. At that moment, conflicts will arise between the participants in the environment. We can simplify these terms and call this factor in our example a *genetic mutation*. It will act differently depending on the gains or losses of a population, considering the chosen strategy, therefore representing a variable number of populations of individuals.

In the evolution of species, this example is one among many others. Humans, beings capable of reason, have had and will experience an extensive number of factors that drive the species towards balance, extinction or dominance. Stress, economic status, social interactions, our own ability to adapt to new people or environments, interpersonal issues, or even hazardous elements that are beyond our control - represent just a few elements that determine the evolution of our species. However, since we all have the same foundation of instinctive action based on the two operating engines of the brain, the better we understand the described phenomenon, the more we will be able to delve into the possibility of an evolution with more positive influences on a larger scale. That is precisely why this paper aims to address the elements underlying

the fundamental decisions for the previously exposed problem so we can navigate life in a better, more beneficial way when interacting with our surroundings.
The game theory is a framework which uses theoretical and practical information from outside sources and through mathematical models, it studies the interactions among entities capable of rationing. The games it creates can have multiple forms, with the most known being the *2-players based game*, where the players have different options to play with, from which they can choose from.
The Nash equilibrium is a type of game where an outcome of the interaction between the players which, once reached, it means that no player can increase their payoffs during that game by changing their decisions. In this sense, once a decision has been made, they player's future interaction will not be deviated in any manner from the predicted outcome. So, in that regard, the player will suffer any consequences that come with its considered decision. Such cases can also be applied to real life scenarios like our main subject: how a species would evolve in time.
Consider the following differential equations with respect to time, represented by a dynamical system:

$$\begin{cases} \dfrac{dx_1}{dt} = x_1(x_1 + 0.5 \cdot x_2 - \varphi) \\ \dfrac{dx_2}{dt} = x_2(1.5 \cdot x_1 + 0 \cdot x_2 - \varphi) \end{cases}$$

Let x_1 be the sharing mutation and let x_2 be the aggressive mutation. If x_1 meets x_2, it will come out of the interaction with 50% of its food part, therefore having a 50% chance of survival (represented by 0.5 in the first equation). If x_2 meets x_1, it will come out of the interaction with 100% of its food part and 50% of x_1's food part, therefore having a 100% chance of survival and a 50% chance of reproduction (represented by 1.5 in the second equation). By solving the system above, we will be able to determine φ, which, in our case, will play the role of showing how numerical solutions of a dynamical system can lead to a Nash equilibrium of a given game. Through this process, we will be able to solve and demonstrate how a particular mutation will advance in a specific population, by creating a mix between the two (sharing and aggressive) agents. Therefore, both coexisting.
And to replicate this in a more concise manner, the paper proposes using the programming language *Python*. Through its versatile libraries and quick math operations, Python allows us to create a matrix which can be manipulated to generate certain results regarding the time and given rewards/loses for the two players. Based on these calculations, a pictorial representation of the population will be generated through a graph, containing both aggressive and sharing individuals.

3. CONCLUSIONS

Through the game theory and the correlation between the dynamical systems and the Nash equilibrium, we will gather all the information needed. Such mathematical models cand be applied to any being capable of ration. Thus, being a very concise solution of how to determine which strategy to choose in each situation, which is the more beneficial one and why (plus how a strategy can affect both individuals, leading to a coexistence of both parties), we can use such algorithms to predict how the evolution will play out for our given species. Analysing such data will improve our perspective upon how a species came to be in our everyday life and most importantly, how we can use such techniques to improve our lives.

REFERENCES

[1] M. J. Osborne, *An introduction to game theory*, Oxford University Press, 2002
[2] R. Klages, *Introduction to Dynamical Systems – Lecture Notes*, Queen Mary, University of London, 2008
[3] D. Ross, *Game Theory*, The Stanford Encyclopedia of Philosophy, 2021
[4] https://en.wikipedia.org/wiki/Game_theory
[5] https://en.wikipedia.org/wiki/Dynamical_system
[6] https://nashpy.readthedocs.io/en/stable/index.html
[7] S. M. Bibic, M. R. Laza, *The development of a population through time using the game theory* (under review)

Analytical studies for a hybrid mathematical model of COVID-19: The influence of the pandemic on chronically ill people

Bilal BASTI*[1], Maroua Amel BOUBEKEUR[2]

[1] *Laboratory of Pure and Applied Mathematics, Mohamed Boudiaf University of M'sila, Algeria.*

[2] *Laboratory of Pure and Applied Mathematics, University of Mostaganem, Algeria.*

Abstract

This paper discusses and provides some analytical studies for a hybrid mathematical model of COVID-19, which is a SECIRD fractional model that is concerned with the influence of the pandemic on chronically ill people. We compute and derive several stability results based on some parameters that satisfy some conditions that prevent the pandemic from occurring. The paper also investigates the problem of the existence and uniqueness of solutions for the SECIRD model. It does so by applying the properties of Schauder's and Banach's fixed point theorems.

1 Introduction

COVID-19 is caused by the severe acute respiratory syndrome coronavirus 2 (SARS-CoV-2) and can cause respiratory distress, with those suffering from chronic diseases at particular risk. These chronic conditions include heart disease, diabetes, cancer, chronic obstructive pulmonary disease, chronic kidney disease, and obesity. Furthermore, an increase in deaths has been observed among individuals with dementia, circulatory diseases, and diabetes, among other causes (see [36]).

Mathematical modeling is a useful tool for understanding and controlling infectious diseases [15, 27, 32, 35], but traditional approaches are not highly accurate for modeling such diseases. Therefore, fractional differential equations have been introduced to handle these problems, with applications in various fields, including optimization problems, artificial intelligence, and medical diagnoses. Those interested in further reading on the subject can refer to books by (Samko et al. 1993 [33], Podlubny 1999 [29], Kilbas et al. 2006 [23], Diethelm 2010 [16]).

This model requires the division of the total population N into six epidemiological classes namely Susceptible S, Exposed E, Chronic illnesses C, Infected I, Recovered R, and Death class D. Parameters' definition of the SECIRD model for COVID-19 could be presented as follows:

$\circ$ $\psi(\mu, N)$ is a function represents the influx rate that expresses the arrival of people (i.e. birth rate and visitors from other society).

*[1] **Correspondence to:** Bilal Basti, Department of mathematics, Ziane Achour University of Djelfa, 17000, Algeria. Email: bilalbasti@gmail.com; b.basti@univ-djelfa.dz

SCALABLE ACTIVATION FUNCTION EMPLOYMENT IN PHYSICS INFORMED HIGHER ORDER NEURAL NETWORKS FOR INITIAL VALUE PROBLEM APPROXIMATION

Patrik KOVÁŘ[1, 2], Jiří FÜRST[2]

[1]Center of Aviation and Space Research, Faculty of Mechanical Engineering, Czech Technical University in Prague, Jugoslávských partyzánů 1580/30, Prague, Czech Republic.
[2]Department of Technical Mathematics, Faculty of Mechanical Engineering, Czech Technical University in Prague, Karlovo náměstí 13, Prague, Czech Republic

Corresponding author email: Patrik.Kovar@fs.cvut.cz

Abstract

There are many physical phenomena in the engineering applications, which are governed by ordinary differential equations. In the practice these problems are approximated using classical numerical methods. Present contribution deals with an alternative approximation method – higher order neural networks and furthermore, employment of the scalable activation function which can accelerate speed of the convergence is discussed. Basic ideas of the methods are introduced and designed architectures are tested on initial value problem. A comparison of the results quality between three neural network architectures is performed. Improvement in the speed of the convergence has been reached.

***Key words**: machine learning; higher order neural units; ordinary differential equations*

1. INTRODUCTION

When ordinary differential equations (ODEs) desribing natural phenomena are solved, only rarely can analytic formula be found for the solution (LeVeque, 2007). To obtain results, numerical methods are used istead in engineering tasks. An alternative approach is solve ODE by artificial neural network (ANN) (Lagaris, 1998).

In a field of machine learning, there are many means of architectures and learning approaches. One of them is supervised learning which is relatively fast and the implementation is very straightforward. Unfortunately, there is one huge disadvantage - learning data set. It contains inputs and corresponding targets for each sample in the data set. As one can see, cornerstone of the learning is the training data set which is not correct and precise and in this case the problem can occur.

The present paper deals with an alternative method called physics informed neural network (PINN) which is not training data set dependent in that sense we do not have to have labeled targets with its correct value. The only necessary information we need are differential equations which have to be solved. Basic ideas of the method are introduced and ability to solve ODE by well known (Rosenblatt, 1958) multilayer perceptron network (MLP), higher order neural network (HONN) and HONN architecture with scalable activation function (HONNST) is compared in terms of convergence speed, while degrees of freedom (DoFs) of individual approximative solvers are preserved.

2. TEST INITIAL VALUE PROBLEM

The only information we need is differential equation with appropriate initial conditions. Initial value problem presented in (Kovář, 2023) on the interval $\langle 0;\ 2\rangle$ is solved as the test case

$$y' = -2\mathrm{xy},\ \mathrm{y}(0) = 1. \tag{1}$$

One can see that exact solution of this equation can be obtained as

$$\mathrm{y} = \exp(-x^2). \tag{2}$$

2. ARCHITECTURE OF THE NEURAL NETWORKS

N-th order synaptic operation in the neural unit is defined as (Gupta, 2004)

$$s = w_0 x_0 + \sum_{i=1}^{n} w_i x_i + \sum_{i=1}^{n} \sum_{j=i}^{n} w_{ij} x_i x_j + \cdots + \sum_{i_1=1}^{n} \cdots \sum_{i_N=i_{N-1}}^{n} w_{i_1 i_2 \ldots i_n} x_{i_1} x_{i_2} \ldots x_{i_n}, \quad (3)$$

where $x_0 = 1$ denotes threshold and n stands for length of input feature vector.

Designed HONNs are consisted of two neurons in the first layer and single neuron in the output layer and synaptic operation of all neurons is assumed as quadratic polynomial. As the activation function $\sigma(\cdot)$ bipolar sigmoid and scalable hyperbolic tangent (Gnanasambandam, 2022) was used for HONN and HONNST architectures in the first layer, respectively. MLP network was designed as the network with comparable number of DoFs which resulted into five neurons in the first layer. Linear activation in the output layer is assumed in cases of all discussed architectures.
Since desired outputs are known, machine learning is called as supervised learning which is the task of learning a function that maps input to desired output and the error is represented with cost function $\vec{e}$ that has to be minimized. In case of physics informed neural networks, loss function is defined according to equation (1) as

$$\vec{e} = \left|\left|\tilde{y}' + 2x\tilde{y}\right|\right|^2 + K_1\left|\left|\tilde{y}(0) - 1\right|\right|^2, \quad (4)$$

where coefficient $K_1 = 1$ imposes initial conditions, x are inputs for the PINN and $\tilde{y}$ are outputs of the network. Derivatives of the neural outputs $\tilde{y}'$ are obtained through reverse mode of automatic differentiation algorithm described in (Baydin, 2018). Referring to equation (1), the first term on the right-hand side quantifies how much the solution predicted by ANN differs from ODE definition and second term is the initial condition loss and it quantifies how much the predicted solution deviates from satisfying the initial condition. Error propagation through the network is performed using multilayer backpropagation algorithm described in (Bukovský, 2013).

3. RESULTS & CONCLUSIONS

Main results and comparisons are listed in the following table Tab. 1. It turned out that ability to solve test initial value problem by MLP and HONN network was outperformed by designed HONNST. Despite that numbers of learnable parameters (DoFs) were comparable, HONNST's loss function value was almost order of magnitude lower and resulting MSE (related to the analytic solution) was almost by half an order lower.

Tab. 1 Comparison of the mean squared errors performed by individual neural networks.

Neural network	No. parameters	Loss function	MSE
MLP	16	$7.63e-2$	$1.53e-2$
HONN	13	$1.11e-3$	$3.02e-5$
HONNST	15	$3.88e-4$	$7.81e-6$

Introduced architecture HONNST outperformed both remaining network architectures speed of the convergence and solution accuracy, thus the improvement in the learning has been proven.

ACKNOWLEGMENT

This work was supported by the grant agency of the Czech Technical University in Prague, grant No. SGS22/148/OHK2/3T/12.
The authors would also like to thank for the support from the ESIF, EU Operational Programme Research, Development and Education, and from the Center of Advanced Aerospace Technology (CZ.02.1.01/0.0/0.0/16019/0000826), Faculty of Mechanical Engineering, Czech Technical University in Prague.

SECURE WIRELESS POWER TRANSFER

Ana-Alexandra BUNEA[1], Alexandru-Dragoș GEORGESCU[2], Simona Mihaela BIBIC[3]

[1]University Politehnica of Bucharest, 313 Splaiul Independentei, District 6, Bucharest, Romania

Corresponding author email: ana_alexandra.bunea@stud.electro.upb.ro, ageorgescu1604@stud.electro.upb.ro, simona.bibic@upb.ro

Abstract

As our world's future is slowly falling into the hands of technology, it is futile to believe that changes in the use of power would not take place. Consequently, interest in the use of wireless power transfer has increased, due to its high accessibility and versatility. However, we can not introduce this type of transmission without a proper analysis of its safety, albeit its efficiency in solving many of our contemporary issues, such as elimination of fuel consumption or hazardous wired interconnections. Therefore, the aim of this paper is discussing and examining possible issues regarding the security breaches and modeling them through means of the MATLAB platform, in order to provide recommendations to defend against potential attacks.

Key words*: Wireless Power Transfer; Data Security; Attacks; Cyber-security; Malicious nodes.*

1. INTRODUCTION

Popularization of wireless power transfer (WPT) has promoted the multi-disciplinary explorations and integration. Therefore, a series of smart WPT emerges, and these state-of-the-arts will bring a great impact on the modern technology and human society. However, cybersecurity should be considered early on during the design phase in order to incorporate solutions to reduce the risk of nefarious access, safeguard data and information, and enable a safe minimum state of operation during a cyber-event.

2. CONTENT

I. INSIGHT INTO WIRELESS POWER TRANSFER

Wireless power transfer refers to the transmission of electrical energy from a power source to an electrical load without the need for physical conductors such as wires or cables. This technology utilizes various techniques such as electromagnetic radiation, magnetic induction, and resonant coupling to transfer power wirelessly. The energy is typically transferred through the air or other media, and the receiver can convert this energy back into electrical power for use in various devices.

II. SECURITY MODEL AND GOALS

It is expected that ERs (Energy Receivers) and ETs (Energy Transmitters) have transceivers to execute communication over wireless channels that are distinct from and basically less secure than those used for power transfer. Malicious nodes are ERs and ETs that don't behave in a reliable manner. By adding malicious nodes one at a time or by wirelessly modifying existing ones, the attacker seeks to reduce the efficiency of power transfer and disrupt the operation of the WPTN (Wireless Power Transfer Networks). In like manner, malicious nodes can eavesdrop radio packets, copy or modify the contents

of the packets, create new ones to introduce into the network, and give false information—such as the inaccurate battery or RF (Radio Frequency) exposure levels—in response to requests.

III. SAFETY ISSUES

In practice, environmental dynamics bring about additional difficulties to ensure EMR safety.

- Wireless power density is hard to estimate and control.

Example: the radio exposure can be over the limit due to reflection and refraction of the signals originated from other wireless devices.

- Ensuring safety where end-users are allowed to deploy new ETs and modify the locations of existing ETs/ERs at run-time is challenging.

Example: Several ETs can be active simultaneously, aimed at charging ERs collaboratively to satisfy energy demands of the receivers as fast as possible meanwhile optimizing the transferred energy. On the other hand, as more ETs are deployed, end users might be exposed to more radiation.

- For scenarios where ERs are wearable, body movements might lead to unpredictable exposure influence on different parts of the body.

IV. SECURITY ATTACKS

WPT systems have specific additional vulnerabilities due to the system control, overall architecture, and safety mitigation strategy. WPT vulnerabilities and their potential impacts vary greatly across a wide range of stakeholders. The following is an overview of a few possible vulnerabilities and associated impacts: charging attacks, interference attacks, spoofing attacks, application attacks and monitoring attacks.

V. STUDY CASE- DETECTING JAMMING ATTACKS

Jamming is the main reason for many problems in the real-world applications. For example, in border security, an intruder has the ability to prevent the communication and cross the border without being detected. Consequently, in an unwanted environment, it is very important to detect the place where the channel is jammed or deliver the messages out of the jammed area.

3. CONCLUSIONS

In the final analysis, it is only fitting to say that wireless power transfer is a promising technology that has the capability to transform the way we power our devices. However, in terms of cybersecurity, continued research is still needed to understand the potential vulnerabilities especially for high power WPT as well as the corresponding methodologies for response and recovery when a cyber-event occurs. Consequently, recommended solutions to mitigate vulnerabilities and reduce risks on public safety may include encryption utilization, a controls system monitor, use of multiple data inputs.

RESULT OF GLOBAL EXISTENCE AND FINITE TIME BLO-UP IN A NEW CLASS OF NON-LINEAR VISCOELASTIC WAVE EQUATION

Zakia TEBBA[1]
[1]University of Laarbi Tebessi Tebessa –Algeria-
tebbazakia93@gmail.com

Abstract

A new class of nonlinear viscoelastic wave equation is studied. Under appropriate conditions imposed on h, the global existence of solutions with any initial data is proved when m ≥ p, and a finite time blow-up with negative initial energy is obtained when p > m.
©***Key words**: Global existence, Blow-up, Source term, Wave equation, Viscosity*

1. INTRODUCTION

We are in the process of studying the following non-linear viscoelastic wave equation

$$\begin{cases} u_{tt} - \Delta u - \Delta u_{tt} + \int_0^t h(t-s)\Delta u(s)\,ds + cu_t |ut|^{m-2} = du|u|^{p-2}, x \in \Omega, t > 0, \\ u(x,t) = 0, x \in \partial\Omega, t \geq 0, \\ u(x,0) = u_0(x), u_t(x,0) = u_1(x), x \in \Omega, \end{cases} \quad (1)$$

here Ω be an open bounded Lipschitz domain in $\mathbb{R}^n$ (n ≥ 1), with a Lipschitz-countinuous boundary ∂Ω, p > 2, m ≥ 1, and c, d are strictly positive constants. First, it can easily be noticed that when the viscoelastic and the dispersion terms are null (h = 0, Δu_{tt} = 0), the problem has been handled and its existence and non-existence has been proven. In the case m > 2, d = 0, the nonlinear damping term $cu_t|u_t|^{m-2}$ assures decay and global existence of the solutions for arbitrary initial data

2. SOME PRELIMINARIES

(G1) Suppose m ≥ 1, p > 2, and

$$\max\{m, p\} \leq \frac{2(n-1)}{n-2}, n \geq 3,$$

(G2) Assume that h is a C^1 function satisfying

$$1 - \int_0^\infty h(s)ds = l > 0$$

We define the energy functional as follows:

$$E(t) = \frac{1}{2}\|u_t\|_2^2 + \frac{1}{2}\|\nabla u_t\|_2^2 + \frac{1}{2}\left(1 - \int_0^t h(s)\,ds\right)\|\nabla u\|_2^2 + \frac{1}{2}(h \circ \nabla u)(t) - \frac{d}{p}\|u\|_p^p (2).$$

Where: $(h \circ v)(t) = \int_0^t h(t-s)\|v(t) - v(s)\|_2^2\, ds$, and h satisfying the following assumptions

$$h(s) \geq 0, h'(s) \leq 0, \int_0^\infty h(s)ds < \frac{(p/2)-1}{(p/2)-1+(1/2p)}. (3)$$

Theorem1. Assume that $(u_0, u_1) \in H^1(\Omega)\times L^2(\Omega)$ and suppose that the assumptions (G1) and (G2) hold. Then, for some $T_m > 0$ the problem (1) admit a unique local solution

$$u \in C\left([0,T_m), H_0^1(\Omega)\right), u_t \in C\left([0,T_m), H_0^1(\Omega)\right) \cap L^{m+1}\left(\Omega \times [0,T_m)\right).$$

3. GLOBAL EXISTENCE RESULT

Theorem2. Let $E_0 < 0$, $2 \le p \le m$ and let the condition

$$m \le \frac{2(n-1)}{(n-2)}, n \ge 3,$$

hold. Then problem (1) admit a unique solution

$$u \in C\left([0,\infty), H_0^1(\Omega)\right), u_t \in C\left([0,\infty), H_0^1(\Omega)\right) \cap L^{m+1}\left((\Omega)\times(0,\infty)\right).$$

for any $u_0 \in H_0^1(\Omega), u_1 \in L^2(\Omega)$.

4. FINIT TIME BLOW UP

To state and demonstrate our result, we refer to:

Lemma. Assume the condition (G1) hold. Then there exists a positive constant $C > 1$ which depends only on Ω, such that

$$\|u\|_p^s \le C\left(\|\nabla u\|_2^2 + \|u\|_p^p\right), (4)$$

for any $u_0 \in H_0^1(\Omega)$ and $2 \le s \le p$.

We let

$$H(t) := -E(t).$$

Corollary. Suppose that the conditions (2) and (4) satisfying, then

$$\|u\|_p^s \le C\left(-H(t) - \|u_t\|_2^2 - \|\nabla u_t\|_2^2 - (h \circ \nabla \upsilon)(t) + \|u\|_p^p\right), \; forall t \in [0,T)$$

for any $u \in H_0^1(\Omega)$ and $2 \le s \le p$.

Theorem 5. Let $m > 1$, $p > \max\{2,m\}$ satisfying (G1). Let (3) be fulfilled and assume that

$$E_0 = \frac{1}{2}\|u_1\|_2^2 + \frac{1}{2}\|\nabla u_0\|_2^2 + \frac{1}{2}\|\nabla u_1\|_2^2 - \frac{d}{p}\|u_0\|_p^p < 0$$

Then there exist a finit time T^* such that

$$T^* \le \frac{1-\alpha}{\Gamma\alpha\left[L(0)\right]^{\alpha/(1-\alpha)}}.$$

where Γ, α ($\alpha < 1$) are positive constant and L is given by (19) below.

5. CONCLUSIONS

We studied in this work a class of nonlinear hyperbolic viscoelastic problem with constant exponents nonlinearities, and we obtained a different result of global existence and blow-up of this problem, of course under suitable assumptions on the exponents of nonlinearity and the initial data.

SOLVING OPTIMIZATION PROBLEMS THROUGH DUALITY

Maria CONSTANTINESCU[1], Simona Mihaela BIBIC[1]

[1]University Politehnica of Bucharest, 313 Splaiul Independentei, District 6, Bucharest, Romania

Corresponding author email: cmaria@stud.fsa.upb.ro, simona.bibic@upb.ro

Abstract

The duality principle in linear programming (LP) represents an optimal method of solving the primal linear problems. Thus, to find the optimal solution of the initial problem it can be achieved using the duality option both for LP problem and Simplex Algorithm. Therefore, implementation of this method has the consequence of utilizing a smaller number of variables, respectively iterations. In this paper, we will compare and analyze two different simulated algorithms in C++ programming environment to provide the solution to an LP problem, and its characteristics and information about it.

Keywords: *Linear Programming Problem; Simplex Algorithm; duality principle; optimization; C++.*

1. LINEAR PROGRAMMING AND APPLICATIONS (AN OVERVIEW)

In today's competitive business landscape, the effective use of time and resources is important for maintaining a competitive edge. Businesses strive to optimize their problem to achieve maximum productivity and profitability. Optimization techniques offer a systematic approach to decision-making, resource allocation, and optimization in complex real-world scenarios. By leveraging these techniques, organizations can take calculated risks that can lead to great achievements.
One easy optimization technique is Linear programming (LP). Linear programming (LP) is a method to achieve the best outcome (such as maximum profit or lowest cost) in a mathematical model. It involves formulating a mathematical model with linear constraints and an object function, which allow the identification of an optimal solution within the space of feasible solutions.

2. MATHEMATICAL MODEL

The mathematical problem often involves determining the points at which a given linear function, known as the objective function, achieves its maximum or minimum value. When subject to linear constraints, the associated mathematical model is referred to as a linear optimization problem.

3. DOMAINS OF APPLICABILITY

- MARKETING: it is used to find the optimal combination of media for effective advertising.
- ARCHITECTURE: the construction field frequently uses linear equations when measuring and cutting all types of materials for job sites.
- ENERGY INDUSTRY: it is used to optimize the electric load, generators, transmission and distribution lines.
- FINANCE: LP is used by accountants, auditors, budget analysts, and insurance underwriters in analysing the best outcome.

4. DUALITY PRINCIPLE

One of the fundamental concepts in LP is the duality principle, which provides an optimal method for solving primal linear problems. Any feasible solution to the primal problem is at least as large as any feasible solution to the dual problem. The solution to the primal is an upper bound to the solution of the dual, and the solution of the dual is a lower bound to the solution of the primal.

5. THE DUAL PROBLEM ASSOCIATED

The objective is to maximize or minimize a function subject to certain constraints, just like in the primal problem. The variables and constraints in the dual problem are derived from the variables and constraints of the primal problem. The duality theorem has an economic interpretation, where the primal linear programming (LP) problem can be seen as a "resource allocation" problem, while the dual LP problem can be interpreted as a *resource valuation* problem. It also allows for the formulation of alternative optimization approaches, such as the dual simplex method.

6. ADVANTAGES OF DUAL LINEAR PROBLEM

Offers valuable information about the sensitivity of the objective function coefficients and constraint bounds. Sometimes finding an initial feasible solution to the dual is much easier than finding one for the primal. Effective for solving problems with a large number of constraints.

7. DISADVANTAGES OF DUAL LINEAR PROBLEM

- Does not provide a direct interpretation of the optimal solution like the primal problem.
- Implementing the dual problem requires additional computational effort.
- Not suitable for solving small-scale linear programming problems.

8. CONCLUSIONS

In summary, the Dual Simplex algorithm and the Dual Problem provide powerful tools for solving optimization problems. They offer a reliable approach for tackling optimization problems across diverse domains such as operations research, economics, logistics, and finance.

RFERENCES

[1.] https://en.wikipedia.org/wiki/Dual_linear_program
[2.] https://math.stackexchange.com/questions/243706/what-are-the-advantages-of-studying-the-dual-problem-in-linear-programming
[3.] https://web.mit.edu/15.053/www/AMP-Chapter-04.pdf
[4.] International Journal of Advance Research, Ideas and Innovations in Tehnology: Linear programming problem applications in engineering curriculum.
[5.] The Use of the Duality Principle to Solve Optimization Problems -Dr. Rowland Jerry Ekeocha, Uzor Chukwunedum, Anetor Clement Covenant University, Ota, Nigeria.
[6.] Global Journal of Researches in Engineering: G Volume 15 Issue 1 Version 1.0 Year 2015.

MULTIFRACTAL ANALYSES OF MUSIC PIECES

Andra MARIA-FULAȘU [1, 2], Vlad CHIRA [1, 2], Mihai REBENCIUC[1, 2], Antonela TOMA [1, 2], Cătălin CREȚU [3]

[1]University Politehnica of Bucharest, 313 Splaiul Independentei, District 6, Bucharest, Romania
[2]Center for Research and Training in Innovative Techniques of Applied Mathematics in Engineering "Traian Lalescu"
[3] The Electroacoustic Music and Multimedia Center of the National University of Music, Bucharest, Romania

Corresponding author email:
andra.maria@stud.upb.fsa.ro, vlad_andrei.chira@stud.acs.pub.ro, m.rebenciuc08@gmail.com, antonela.toma@upb.ro

Abstract

Throughout history, humans have sought to understand the underlying principles and structures that govern musical compositions, driven by an innate curiosity to unravel the complexities of soundscapes. In recent years, researchers from diverse disciplines, including mathematics, physics, and musicology, have turned their attention to the emerging field of multifractal analyses, exploring its potential in deciphering the intricate patterns and multifaceted nature of musical compositions. This study sets out to analyze the applications of multifractal analysis to a musical piece, "Bolero" by Ravel, using two different methods. One makes use of generalized dimensions and multifractal spectrum in a classical manner, while the other proposes a new way of analyzing the melodic and rhythmic structures.

Key words*: metric digitalization, multifractal analyses, sequential multifractal, matrix metric, encodings.*

1. INTRODUCTION

No one can deny that music is an important part of our lives. Apart from the general understanding that people have, we wanted to investigate if music can have other representations and figure if music can have a fractal or multifractal character. This study is divided into two distinct methods, one called classical – being based on another paper – and a new way of analysing musical pieces – metric digitalization. The case study follows a classical musical piece – Bolero by Ravel,

2. CONTENT

2.1. The Classical Method

The first part of this study bases itself on the paper (see [(1)]), where multifractals are understood in the thermodynamical way. It is important to note that this method divides musical pieces into melody and rhythm, studying them independently and is not able to get a whole perspective of the songs analysed. It has been criticized by the musical world, as it seems incomplete. Important formulas used include:

The Holder exponent:

$$\alpha = \lim_{r \to 0} \frac{\log p_i(r)}{log\ r}$$

Formulations used to determine the multifractal spectrum:

$$\alpha(q) = \lim_{r \to 0} \frac{\sum_i \mu_i(r,q)\ \log p_i(r)}{\log r} \qquad f(q) = \lim_{r \to 0} \frac{\sum_i \mu_i(r,q)\ \log \mu_i(r,q)}{\log r}$$

Multifractal spectrum of "Bolero" by Ravel:

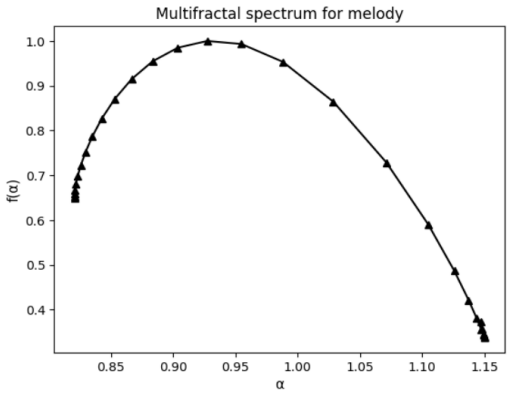

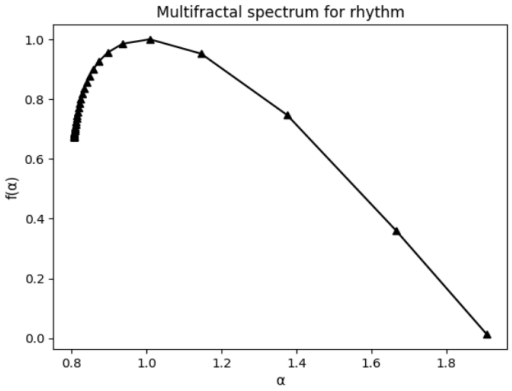

2.2. Metric

Digitalization

The second part of our analyses focuses on transposing a musical piece into matrices, introducing new matrix metrics to find the contractions needed for a fractal or multifractal. This method also introduces sequential fractals and multifractals, both formed by applying the contraction to the latest result, starting from applying the contraction to the initial matrix.

We first encoded the musical notes as follows: Do→0; Do# →1; Re → 2; Re# → 3; Mi →4; Fa→5; Fa# → 6; Sol→ 7; Sol# →8; La→9; La# →10; Si→11; Do→12 (next octave); Musical/Lexical space→ -1; The rhythm is encoded in accordance to the lowest duration in the musical piece analysed: $\frac{1}{16} \rightarrow 1$; $\frac{1}{4} \rightarrow 4$; $\frac{3}{4} \rightarrow 12\ etc.$ $\frac{1}{32} \rightarrow 1$; $\frac{1}{16} \rightarrow 2$; $\frac{1}{4} \rightarrow 8\ etc.$ Using these encodings, Bolero by Ravel was (..) into two matrices who can create a new matrix, the melody matrix, using the matrix metrics formula (1).

$$Let\ N = M + (z_i, z_j) = M + P - (|x_i - x_j|)$$

The next step in our research is finding the contractions that can be applied to the music matrix, in order to find out if music can have a fractal or a multifractal aspect.

3. CONCLUSIONS

Our research sets out to find out the fractal or multifractal aspect of musical pieces. Using two different methods, each having advantages and disadvantages, we were able to transpose a music sheet into representations and matrices. The classical method has its certain limitations, as we can only work on components – melody and rhythm – and it is not suitable for all musical pieces – the lyrical aspect of songs cannot be represented. (It has also been criticised by musicians, as you cannot tell if a song is more melodious or rhythmic by just analysing the graphs that resulted from their formalism). Although metric digitalization is still in development, it has the potential to cater to all musical pieces and - provides insights regarding the musical piece, including rhythm, melody and lyrics.

References:

- Z. Su, T. Wu. "Multifractal analyses of music sequences" *Physica D: Nonlinear Phenomena*, vol. 221, issue 2, pp. 188-194, 2006.
- M. Rebenciuc, A. Toma, C. Cretu, A. Maria-Fulasu, Fractals in some metric spaces from the perspective of fractional calculus and metric digitalization

MULTIFRACTAL COMPARISON OF A POEM IN TWO LANGUAGES

Andra MARIA-FULAȘU [1, 2], Vlad CHIRA [1, 2], Mihai REBENCIUC[1, 2], Antonela TOMA [1, 2]

[1]University Politehnica of Bucharest, 313 Splaiul Independentei, District 6, Bucharest, Romania
[2]Center for Research and Training in Innovative Techniques of Applied Mathematics in Engineering "Traian Lalescu"

Corresponding author email:
andra.maria@stud.upb.fsa.ro, vlad_andrei.chira@stud.acs.pub.ro, m.rebenciuc08@gmail.com, antonela.toma@upb.ro

Abstract

Poetry, with its inherent artistic nuances and cultural elements, poses unique challenges when examining its linguistic and structural characteristics. This paper aims to bridge the gap between quantitative analysis techniques and the subjective realm of poetry by introducing multifractal analysis as a means to measure and compare the multifaceted nature of poems. This study focuses on finding the differences between a poem written in two distinct languages: english and romanian, whilst using encodings and metrical digitalization. The aim of the study is to identify any differences in the underlying structure of the poem between the original language and the translated version.

***Key words**: metric digitalization, encodings, sequential multifractal, matriceal metrics, lyrics.*

1. INTRODUCTION

Most musical pieces manage to send their message through the lyrics they attribute to a certain musical score. Knowing how lyrics can impact a song's meaning, we wanted to see how lyrics in different languages are able to modify the multifractal aspect of a musical piece. The case study is based on Mihai Eminescu's poem "Pe langa plopii fara sot" and the problems that arise in its translations. In order to introduce the values used into our programming sequence, we made use of 4 dimensional matrices, in order to be able to access the lyrics down to the letters, that were integrated in syllables.

2. CONTENT

We first introduce the encodings used. We will make use of 3 matrices: melody, rhythm and lyrics

For the pitches, we use the following encodings:

Do→0; Do# →1; Re → 2; Re# → 3; Mi →4; Fa→5; Fa# → 6; Sol→ 7; Sol# →8; La→9; La# →10; Si→11; Do→12 (next octave);

For the rhythm, we chose the lowest duration as our base point, and it got the encoding 1. For the other durations, we multiplied the basic encoding as needed. For example: $\frac{1}{16} \rightarrow 1$; $\frac{1}{4} \rightarrow 4$; $\frac{3}{4} \rightarrow 12$ $etc.$

We encode both the English and the Romanian alphabets, as well as the punctuation marks, taking into account diminishing the importance of punctuation marks, as they only serve as a means of separating or showing the intonation used for a sentence. The encodings used for the lyrics are as follows:

For the English alphabet:

a=0 b=3 c=4 d=5 e=6 f=7 g=8 h=9 i=10 j=12 k=13 l=14 m=15 n=16 o=17 p=18 q=19 r=20 s=21 s=22 t=23 u=25 v=26 w=27 x=28 y=29 z=30. For uppercase, we add 0.5 to all the values mentioned above.

For the Romanian alphabet:

a=0; ă=1 â=2 b=3 c=4 d=5 e=6 f=7 g=8 h=9 i=10 î=11 j=12 k=13 l=14 m=15 n=16 o=17 p=18 q=19 r=20 s=21 s=22 t=23 ț=24 u=25 v=26 w=27 x=28 y=29 z=30. For uppercase, we add 0.5 to all the values mentioned above.

Punctuation marks:

The space (musical and lyrical) → -1

- →-2; , →-3; .→-4; ;→-5; !→ -6; ?→-7; & → -8

Numbers: 0→31; 1→32 … 9→40

Musical/lyrical space → -1

After having the whole music piece encoded, we constructed the matrices (melody, rhythm and lyrics) and using specific matriceal metrics we were able to combine them. The programming sequence had to use generalised 4-dimensional matrices, in order to be as flexible as possible. This method ensured that this formalism can be applied to any song. Working with the data in this way, every character can be accessed, being grouped into a syllable with a variable length.

Needing to work with the distances between each syllable, we introduced the generalised Hausdorff distance, measuring how far apart two sets are:

$$d_H(I, J) = \max\{d_h(I, J), d_h(J, I)\} = \max\{d_h(I, J), d_h{}'(I, J)\}$$

In order to combine our matrices, we use specific matriceal metrics:

$$let\ N = M + (z_i, z_j) = M + P - (|x_i - x_j|)$$

The multifractal aspect is going to be highlighted using sequential multifractals:

Let F be a (p-) sequential multifractal if:

$$F = \bigcup_{i=1}^{p} F_1 \cup F_{1,2} \cup .. \cup F_{i,ni},$$

$F_i = \varphi_{i,1}(F_i)$, $F_{i,2} = \varphi_{i,2}(F_i)$,..., $F_{i,ni} = \varphi_{i,ni}(F_{i,\,n_i-1})$, *where* $\varphi_{i,1}, \varphi_{i,2}, .., \varphi_{i,ni}$ *are contractions with the coefficients* $1 > c_{i,1} > c_{i,2} > .. > c_{i,ni}$

3. CONCLUSIONS

The study explores the multifractal properties of a poem in two different languages using mathematical analysis. The aim of the study is to identify any differences in the underlying structure of the poem between the original language and the translated version. The approach allows for an examination of the relationship between language and the structure of poetic texts, shedding light on the ways in which translation can affect the complexity and richness of literary works. The results of the study contribute to a deeper understanding of the role of language in shaping the aesthetic and cultural significance of literary texts.

Since this method is versatile, it can also be expanded to fit any alphabet. It would be of high interest to study the poem translated in other languages and see how the translation affects our results.

References:

1. M. Rebenciuc, A. Toma, C. Cretu, A. Maria-Fulasu, Fractals in some metric spaces from the perspective of fractional calculus and metric digitalization

VECTORS, MULTIVECTORS AND RECTANGULAR MATRICES VERSUS SQUARE MATRICES (WITH PYTHON IMPLEMENTATIONS)

Mihai REBENCIUC [1,2], Vlad-Andrei CHIRA [1,2]

[1]University Politehnica of Bucharest, 313 Splaiul Independentei, District 6, Bucharest, Romania
[2]Center for Research and Training in Innovative Techniques of Applied Mathematics in Engineering "Traian Lalescu"

Corresponding author email: m.rebenciuc08@gmail.com, vlad_andrei.chira@stud.acs.pub.ro

Abstract

In this paper we propose an extension of the notions of the determinant and of the inverse of a square matrix to rectangular matrices. The determinant of rectangular matrix is compatible with the expression involving permutations from the definition– but it is modified, as well as with the algorithms for row or column expansion (traditionally known as Laplace expansion). The inverse of a (m,n) - rectangular matrix is of the same type – but relative to a new multiplicative operation which becomes the usual product operation when applied to square matrices. The multiplicative operation between (m,n) - rectangular matrices is obtained based on a multiplicative operation between vectors from R^n - the finite dimensional case of a (pre)-Hilbert real space. Some of these results have implementations in Python and are applied on examples of vector and linear algebra.

Key words*: multivectors, determinant rectangular matrices, inverse rectangular matrices, generalised matrices.*

1. INTRODUCTION

This research introduces the multivector as a vector space and, in particular, the notion of a vector scalar of coordinate λ. It also focuses on s-vectors, a multiplicative operation that determines a uncommutative multiplicative structure. Rectangular determinants are also introduced, generalising a notion that is of utmost importance when it comes to matrices.

2. CONTENT

2.1 Multivectors

Relative to the product pre-Hilbert space $(H^X, <\bullet, \bullet>^X)$, we name $u = (u_1, u_2, \dots, u_n) \in H^X$ generically ***multivector.*** A special case of the multivector is named scalar-multivector, shortened to ***s-multivector*** if there is at least one position in the multivector with a scalar $(\lambda, u) \in H^X, \lambda \in \mathbb{R}, u \in H$.

We introduce a multiplicative operation between s-vectors $\odot_i$: sH^2 -> sH where i ∈ {-1, 1, 0} as follows:

$(\lambda, u) \odot_{-1} (\mu, v) = (\lambda\mu - < u, v >, \lambda v + \mu u)$

$(\lambda, u) \odot_{1} (\mu, v) = (\lambda\mu + < u, v >, \lambda v + \mu u)$

$(\lambda, u) \odot_{0} (\mu, v) = (\lambda\mu, \lambda v + \mu u)$

In particular, we define $\boxdot$: sH^2 -> sH such that $(\lambda, u) \boxdot (\mu, v) = (\lambda\mu, \lambda v + u) = \lambda(u, v) + (0, u)$
Based on the definition we observe that $(\lambda, u) \odot (1, v) = (\lambda, u) \boxdot (1, v)$

The $\boxdot$ operation has the following properties:

- Non-commutativity with respect to addition
- Non-distributivity with respect to addition
- (sH, $\boxdot$) forms a noncommutative multiplicative monoid with the set of invertible elements $I_v = R^* \times H$
- $\boxdot$ is associative (by definition)

2.2. Rectangular matrices

The set of rectangular matrices $\mathcal{M}_{m,n}(\mathbb{R})$ has the following basic properties:

1. $(\mathcal{M}_{m,n}(\mathbb{R}), +, \cdot)$ does not form a ring in general because the set is not closed under multiplication, but it does form a ring in particular cases in which there exists left and right identity matrices.
2. The unique pseudo-inverse of a matrix can be defined as follows: $A^+ \in \mathcal{M}_{m,n}(\mathbb{R})$ such that $AA^+A = A$ and $A^+AA^+ = A^+$
3. The notion of the determinant is not defined for rectangular matrices

We propose a new notion of the determinant for rectangular matrices up to 4D-Minkowski. The definition is obtained through modified permutations [1]. The basis for this new notion is the Laplace expansion of the determinant. This new notion of the determinant is also invariant to the transpose operation. The determinant of a row vector:

$$a = (a_1, a_2, \dots, a_n), det\ (a) = |a| = (a_1, \dots, (-1)^{i-1}a_i, \dots, (-1)^{n-1}a_n)$$

In particular if a is a scalar, its determinant is the scalar itself.

Example - the determinant of a 2x3 matrix:

$A = (a_{ij}) \in \mathcal{M}_{m,n}(\mathbb{R})$, det (A) = |A| $= (\Delta_1^*, {}^*\Delta_2)$ where $\Delta_1^* = \begin{vmatrix} a_{11} & a_{12} - a_{13} \\ a_{21} & a_{22} \end{vmatrix}$ ${}^*\Delta_2 = \begin{vmatrix} -a_{11} + a_{12} & a_{13} \\ a_{22} & a_{23} \end{vmatrix}$

These formulas will be generalized and will even have a variation for m>n.

We define the operation $\boxdot: \mathcal{M}_{m,n}(\mathbb{R})^2 \to \mathcal{M}_{m,n}(\mathbb{R})$, C = A⊡B, C= ($C_1$ C_2), $C_1 = A_1 * B_1$, $C_2 = A_1 * B_2 + A_2$

Properties of the ⊡ operation for matrices:

1. Non-commutativity and non-distributivity with respect to addition
2. $(\mathcal{M}_{m,n}(\mathbb{R}), \boxdot)$ forms a multiplicative monoid.
3. The ⊡ operation is associative: (A⊡B) ⊡C = A⊡(B⊡C)

The ⊡ operation collapses into the usual matrix multiplication for square matrices and therefore the same thing happens with the inverse.

3. CONCLUSIONS

In conclusion, the introduction of the two new operations which are used to generalize the determinant to non-square matrices has opened up a new realm of possibilities and, as further research is conducted, we plan to extend these notions to other fields of mathematics and applied mathematics.

4. REFERENCES

- Rebenciuc Mihai, Fulasu Andra, Chira Vlad; (2023) Operations, relations norms with multivectors and rectangular matrices versus square matrices, manuscript.
- Ben-Israel, Adi, and Thomas N. E. Greville. "Generalized Inverses: Theory and Applications." Springer, 2003.
- Horn, R., & Johnson, C. (2012). Matrix Analysis. Cambridge: Cambridge University Press. doi:10.1017/CBO9780511810817
- Brown, William C. Matrices and Vector Spaces. Dekker, 1991.
- Liu, Shuangzhe & TRENKLER, OTZ. (2008). Hadamard, Khatri-Rao, Kronecker and other matrix products. International Journal of Information & Systems Sciences. 4(1): Pages 160-177
- Shuangzhe Liu, Víctor Leiva, Dan Zhuang, Tiefeng Ma, Jorge I. Figueroa-Zúñiga, Matrix differential calculus with applications in the multivariate linear model and its diagnostics, Journal of Multivariate Analysis, Volume 188, 2022, 104849
- Jerzy K. Baksalary, Oskar Maria Baksalary, Particular formulae for the Moore–Penrose inverse of a columnwise partitioned matrix, Linear Algebra and its Applications, Volume 421, Issue 1, 2007, Pages 16-23

ON THE GEOMETRY OF METALLIC RIEMANNIAN MANIFOLDS

Cristina - Elena HREŢCANU[1]

[1]Ştefan cel Mare University of Suceava, str. Universitatii, no. 13, Suceava, Romania

Corresponding author criselenab@yahoo.com

Abstract

Metallic means family contains some generalizations of the Golden mean, such as the silver mean, the bronze mean and many others. In this paper we focus on some properties of metallic Riemannian manifolds and we study the geometry of submanifolds endowed with structures induced by metallic Riemannian structures, due to an analogy with the theory of submanifolds in almost product manifolds. We give some characterizations of semi-slant and hemi-slant submanifolds in metallic Riemannian manifolds and we obtain integrability conditions for the distributions involved. Some examples of structures induced on submanifolds by some metallic Riemannian structures defined on Euclidean space are given.

Key words*: metallic means family; metallic Riemannian manifold; invariant submanifold; semi-slant submanifold; hemi-slant submanifold.*

1. INTRODUCTION

Metallic means family share important mathematical properties that constitute a bridge between mathematics and design, e.g., silver mean has been used in describing fractal geometry. Metallic means family was introduced by Vera W. de Spinadel in (Spinadel, 2002). Some members of the metallic means family (golden mean and silver mean) appeared already in the sacred art of Egypt, Turkish, India, China and other ancient civilizations.

The name of metallic number is given to the positive solution of the equation $x^2 = px + q$, where p and q are positive integers. Some properties studied in this paper are related with the *generalized secondary Fibonacci sequence*, given by: $G(n+1)=pG(n)+qG(n-1)$, where $G(0)=a$ and $G(1)=b$ are real numbers.

The ratio $G(n+1)/G(n)$ of two consecutive generalized secondary Fibonacci numbers converges to: the golden mean $\phi = \frac{1+\sqrt{5}}{2}$, for $p=q=1$, determined by the ratio of two consecutive classical Fibonacci numbers; the silver mean $\sigma_{2,1} = 1 + \sqrt{2}$, for $p=2$ and $q=1$, determined by the ratio of two consecutive Pell numbers (Falcon, 2008); the bronze mean $\sigma_{3,1} = \frac{3+\sqrt{13}}{2}$, for $p=3$ and $q=1$, which plays an important role in studying topics such as dynamical systems and quasicrystals; the subtle mean $\sigma_{4,1} = 2 + \sqrt{5}$, for $p=4$ and $q=1$, which plays a significant role in the theory of Cantorian fractal-like micro-space-time and is involved in a fundamental way in noncommutative geometry and four manifold theory (Naschie,1999); the copper mean $\sigma_{1,2} = 2$, for $p=1$ and $q=2$; the nickel mean $\sigma_{1,3} = \frac{1+\sqrt{13}}{2}$, for $p=1$ and $q=3$ and so on.

2. METALLIC RIEMANNIAN MANIFOLDS AND ITS SUBMANIFOLDS

Using a polynomial structure, which was generally defined in (Goldberg, 1970), we consider in (Hretcanu, 2013) a polynomial structure on a Riemannian manifold $(M; g)$, called *metallic structure*, determined by an *(1;1)-tensor field J*, which satisfies the equation: $J^2 = pJ + qI$, where I is the identity operator on the Lie algebra of vector fields on M and p, q are positive integers.

Metallic Riemannian manifolds can be seen as a generalization of the Golden Riemannian manifolds, defined and studied in (Hretcanu, 2007), (Crasmareanu, 2008) and (Hretcanu, 2009).

A Riemannian metric g is *J-compatible* if *g(JX, Y)=g(X, JY)*, for every $X, Y \in \chi(M)$, which means that *J* is a self-adjoint operator with respect to g. This condition is equivalent in our framework by *g(JX, JY)=p g(X, JY)+q g(X, Y).*

A Riemannian manifold *(M, g)* endowed with a metallic structure *J* such that the Riemannian metric g is *J-compatible* is named a *metallic Riemannian manifold* and (g, J) is called a *metallic Riemannian structure* on *M*.

The metallic structure J is an isomorphism on the tangent space T_xM, for every $x \in M$. It follows that *J* is invertible and its inverse is not a metallic structure but is still polynomial, more precisely a quadratic one. The eigenvalues of *J* are the metallic numbers $\sigma_{p,q} = \frac{p+\sqrt{p^2+4q}}{2}$ and $p - \sigma_{p,q}$.

Every almost product structure *F* induces two metallic structures on *M* given by $J_{\pm} = \frac{p}{2} I \pm \frac{2\sigma_{p,q}-p}{2} F$.

Conversely, every metallic structure *J* on *M* induces two almost product structures on this manifold.

Let us consider that *N* is a submanifold, isometrically immersed in a metallic Riemannian manifold *(M, g, J).* Then, N is an invariant submanifold with respect to ***J*** if and only if the induced structure *(P, g)* on *N* is a metallic Riemannian structure, whenever *P* is non-trivial (Hretcanu, 2013).

In (Hretcanu, 2018) we have found some integrability conditions for the distributions which are involved in slant and semi-slant submanifolds in metallic Riemannian manifolds and we have also given some examples of semi-slant submanifolds in metallic Riemannian manifolds.

In (Hretcanu, 2019) we study the properties of hemi-slant submanifolds in metallic Riemannian manifolds and we give some integrability conditions for the distributions involved. Examples of hemi-slant submanifolds in metallic and Golden Riemannian manifolds are given in this paper.

In (Hretcanu, 2020) and (Hretcanu, 2021) we study warped product submanifolds in metallic Riemannian manifolds and warped product submanifolds in locally Golden Riemannian manifolds with a slant factor.

3. REFERENCES

1. Crasmareanu M., Hretcanu C.E, *Golden differential geometry*, Chaos Solitons \& Fractals 38(5) (2009), 1229-1238;
2. Falcon S., Plaza A., *On 3-dimensional k-Fibonacci spirals*, Chaos, Solitons \& Fractals 38(4) (2008), 993-1003;
3. Goldberg S.I., Yano K., *Polynomial structures on manifolds*, Kodai Math. Sem. Rep. 22 (1970) 199-218;
4. Hretcanu C.E., Crasmareanu M., *On some invariant submanifolds in a Riemannian manifold with golden structure*, An. Stiint. Univ. Al. I. Cuza Iasi Mat. (N.S.) 53 (Suppl.) (2007) 199-211;
5. Hretcanu C.E., Crasmareanu M.C., *Applications of the Golden Ratio on Riemannian Manifolds*, Turkish J. Math. 33(2) (2009) 179—19.
6. Hretcanu C. E., Crasmareanu M. C., *Metallic structures on Riemannian manifolds*, Rev. Un. Mat. Argentina, 54(2) (2013), 15—27.
7. Hretcanu, C.E., Blaga, A.M., *Slant and semi-slant submanifolds in metallic Riemannian manifolds*, J. Funct. Spaces (2018), 2864263
8. Hretcanu, C.E., Blaga, A.M., *Hemi-slant submanifolds in metallic Riemannian manifolds*, Carpathian J. Math. (2019), 35, 59–68.
9. Hretcanu, C.E., Blaga, A.M., *Warped product submanifolds in metallic Riemannian manifolds*, Tamkang J. Math. (2020)
10. Hretcanu, C.E., Blaga, A.M., *Warped product submanifolds in locally Golden Riemannian manifolds with a slant factor*, Mathematics (2021), 1, 0.
11. Hretcanu, C.E.; Blaga, A.M. Types of Submanifolds in Metallic Riemannian Manifolds: A Short Survey. Mathematics (2021), 1, 0.
12. M.S. El Naschie, *The golden mean in quantum geometry, knot theory and related topics*, Chaos, Solitons \& Fractals 10(8) (1999), 1303—1307.
13. V.W. de Spinadel, *The metallic means family and forbidden symmetries*, Int. Math. J., 2 no. 3 (2002), 279—288.

A NEW EPIDEMIOLOGICAL COMPARTMENTAL MODEL INCLUDING SEASONALITY AND IMMUNITY

Carlos ANDREU-VILARROIG[1]

[1]Universitat Politècnica de València, Camí de Vera, s/n, 46020, Valencia, Spain.

Corresponding author email: caranvi1@upv.es

Abstract

Mathematical modelling is one of the most important tools for studying and predicting the dynamics of infectious diseases, such as influenza. In this paper, we present a new compartmental model, the IRn. Our model explains the dynamics of seasonal infectious diseases, taking into account a key factor: the immunity of individuals in the population. Once the differential equations of the model have been derived, we have performed a series of numerical simulations based on a real-world problem, the seasonal influenza, to study the effect of the model parameters on the solutions. The results of our study show that our model is consistent with the epidemiological reality of seasonal infectious diseases.

Key words*: infectious diseases; immunity; seasonality; compartmental models; non-linear differential equations.*

1. INTRODUCTION

Mathematical modelling is one of the most important tools for studying and predicting the dynamics of infectious diseases, such as influenza. Within this, compartmental models (such as SIR, SIRS, SEIR, etc.) based on differential equations are the most widespread [1]. However, there are two problematic aspects that are not easily modelled for many diseases: seasonality (i.e., periodic recurrence of epidemic waves) and natural immunity (i.e., the protection of individuals who have passed the disease against reinfection). Usually, the compartmental models proposed so far try to resolve the two aspects separately, which tends to generate forced solutions that are inconsistent with reality. In this paper, we present a new model, the IRn model, which describes the dynamics of a seasonal infectious disease, considering simultaneously the natural immunity of individuals who have passed the disease. As an example of real-world application, some simulations of the seasonal influenza epidemic in a population have been performed, taking as parameter values those found in the literature.

2. CONTENT

In the IRn model, we assume that the entire population at time t is divided in $n+1$ subpopulations: the infected and infectious $I(t)$ and the n recovered $R_1(t), \dots, R_n(t)$, where $n \in \mathbb{N}$. The total population $N(t) = I(t) + \sum_{i=1}^{n} R_i(t)$ can be considered constant or variable over time due to birhts and deaths.

The differential equations system that governs the variations of the subpopulations is given by:

$$\begin{cases} I'(t) = \sum_{i=1}^{n} \beta_i \frac{I(t)R_i(t)}{N(t)} - \gamma I(t) + \delta(t)\mathbf{1}_{\{I(t)<1\}} \\ R_1'(t) = \gamma I(t) - r_1 R_1(t) - \beta_1 \frac{I(t)R_1(t)}{N(t)} - + \delta(t)\mathbf{1}_{\{I(t)<1, R_1 = \max_k\{R_k\}\}} \\ \dots \\ R_i'(t) = r_{i-1}R_{i-1}(t) - r_i R_i(t) - \beta_i \frac{I(t)R_i(t)}{N(t)} - + \delta(t)\mathbf{1}_{\{I(t)<1, R_i = \max_k\{R_k\}\}} \\ \dots \\ R_i'(t) = r_{n-1}R_{n-1}(t) - \beta_n \frac{I(t)R_n(t)}{N(t)} - + \delta(t)\mathbf{1}_{\{I(t)<1, R_n = \max_k\{R_k\}\}} \end{cases}$$

with $I(0), R_1(0), \dots, R_n(0)$ as initial conditions where $\gamma \in \mathbb{R}_+$ is the recovery rate, $\beta_i \in \mathbb{R}_+, \forall i = 1,2, \dots, n$ is the infection rate for the R_i recovered subpopulation, and $r_i \in \mathbb{R}_+, \forall i = 1,2, \dots, n-1$ is

the transition rate between the R_i and R_{i+1} recovered subpopulations. The number of recovery stages can be established by defining a partition $\{t_1, \dots, t_n\}$of a sufficiently large time interval $[0, M]$ in which an individual loses practically all immunity. Then, we define the transition rates as $r_i = \frac{1}{t_{i+1}-t_i}, \forall i = 1,2, \dots, n-1$, and the infection rates $\beta_i = \beta_i(t) = s(t_i)\beta(t), \forall i = 1,2, \dots, n$, where $s(t) \in [0,1]$ is the susceptibility (monotonically increasing) function, and $\beta(t) = \frac{\beta_0}{2}\left(1 + \cos\left(\frac{2\pi}{T}t + \phi\right)\right)$ is the common infection rate function. Thus, at time instant t, each type of recovered subpopulation R_i will have different susceptibility degree, and consequently a different infection rate $\beta_i(t)$, more specifically, $\beta_i(t) < \beta_{i+1}(t)$, so that the further the recovery individuals progress, the higher infection rate, i.e., the more probability to be infected again.

As a real-world case, the IRn model have been applied to the seasonal influenza in Spain. For numerical simulations, we have taken the week as time step, and we have simulated the model during a period of 1040 weeks (around 20 years). As model parameters, based on the influenza information in the literature, we have chosen $\gamma = 1$ (weeks^{-1}) [2], $M = 520$ (weeks, around 10 years), $n = 520$, $s(t) = 1 - e^{-kt}$, with $k = 0.005$, [3], $T = 52$ (weeks, around 1 year), $\phi = 0$, $\beta_0 = 1.8$ (weeks^{-1}) and $N = 10^6$ (constant) and $I(0) = 1, R_n(0) = N - 1$ and $R_i(0) = 0, \forall i = 1,2, \dots, n-1$ as initial conditions. Numerical simulations (Figure 2) have been carried out in MATLAB R2022b, by using the *ode45* solver.

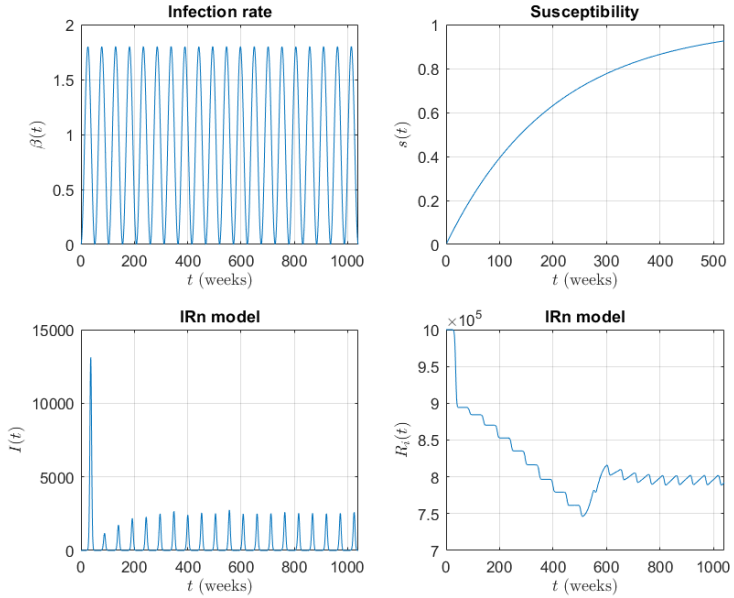

Figure 1: Results of the IRn model numerical simulations.

3. CONCLUSIONS

The results clearly show that the IRn model is periodic (seasonal) due its variable infection rates $\beta_i(t)$. Additionally, the $n-1$ compartments with different degree of susceptibility/immunity provoke that, after a first wave with a large number of infected (there is no natural immunity initially), the waves stabilize until reaching an oscillatory equilibrium. Thus, we demonstrate in this first analysis that the IRn model realistically explains the transmission of seasonal infectious diseases including the natural immunity of individuals.

REFERENCES

[1] Brauer, Fred. "Compartmental models in epidemiology." Mathematical epidemiology (2008): 19-79.
[2] Seasonal Flu. Center for Disease Control and Prevention. https://www.cdc.gov/flu/index.htm [Accessed: 15/06/2023]
[3] Ranjeva, Sylvia, et al. "Age-specific differences in the dynamics of protective immunity to influenza." Nature Communications 10.1 (2019): 1660.

ON TEMPERED EXPONENTIAL DICHOTOMY FOR RANDOM SEMI-DYNAMICAL SYSTEMS

Ioan-Lucian POPA[1,2], Traian CEAUȘU[3] , Larisa Elena BIRIȘ[4]

[1] Department of Computing, Mathematics and Electronics,
"1Decembrie 1918" University of Alba Iulia, Alba Iulia, 510009, Romania
[2]Faculty ofMathematics and Computer Science, Transilvania University of Bra ̧sov,
Iuliu Maniu Street, 50, 500091, Brașov, Romania
[3]West University of Timisoara, Department of Mathematics, Timisoara, Romania
[4]West University of Timisoara, Department of Mathematics, Timisoara, Romania

Corresponding author email: lucian.popa@uab.ro

Abstract:

We consider the metric semi-dynamical system $(\Omega, \mathcal{F}, P, \theta)$ which is a probability space, with $\theta: \Omega \to \Omega$,$ measurable. A linear random one-sided discrete-time system on a Banach space X over a measurable semi-dynamical system θ, is a measurable application $\phi: Z_+ \times \Omega \in \mathcal{B}(X)$. For a more detailed presentation regarding these notions we can point out the references [1] and [6]. In the following, we shall review only the properties which will be of interest in this paper:

(a) $\phi(0,\omega) = I_X, forall\ \omega \in \Omega$;

(b) $\phi(0,\omega) = I_X, forall\ \omega \in \Omega$ for all $n, m \in Z_+$ and $\omega \in \Omega$.

Throughout this work the notation (θ, ϕ) will be used for a linear random one-sided discrete-time system (RDTS).

This paper considers nonuniform exponential dichotomy concept for a linear random one-sided discrete-time system (θ, ϕ). These concepts are generalizations from the deterministic case. Using this, characterizations in terms of Lyapunov functions respectively Lyapunov norms are presented. Also, an approach in terms of considered concepts for the inverse and adjoint random discrete time systems is derived. This paper is a companion of our earlier works [2] and [8] where results in terms of nonuniform exponential stability and tempered exponential splitting have been presented.

***Key words**:* nonuniform exponential dichotomy, one-sided discrete-time random dynamical system, Lyapunov functions

MSC: 37H30, 37C10, 37H10

References:

[1] L. Arnold, Random dynamical systems. Springer Monographs in Mathematics. Springer-Verlag, Berlin, (1998).

[2] L. E. Biris, T. Ceausu, I.-L. Popa, N. M. Seimeanu, Lyapunov Conditions for One-Sided Discrete-Time Random Dynamical Systems, CARPATHIAN J. MATH. Volume **38** (2023), No. 3, Pages 777-788

[3] S.-N. Chow, H. Leiva, Two definitions of exponential dichotomy for skew-product semiflows in Banach spaces, Proc. Amer. Math. Sc. 124(1996), 1071–1081.

[4] N. D. Cong, Topological dynamics of random dynamical systems, Clarendon, Oxford, 1997.

[5] D. C. Nguyen, Topological dynamics of random dynamical systems. Oxford Mathematical Monographs. The Clarendon Press, Oxford University Press, New York, (1997).

[6] T. S. Doan, Lyapunov exponents for random dynamical systems, PhD Technischen Universitat Dresden, (2009).

[7] Popa, I.-L.; Ceaus ̧u, T.; Megan, M. Nonuniform power instability and Lyapunov sequences, Appl. Math. Comput. **247** (2014), 969–975.

[8] Popa, I.-L. Lyapunov functions for random semi-dynamical systems in terms of tempered exponential splitting, Math. Methods Appl. Sci. **44** (2021), no. 15. 11923–11932.

ON SOME NEW INERTIAL VISCOSITY FIXED POINT ALGORITHMS WITH APPLICATIONS TO CONVEX MINIMIZATION, IMAGE RESTORATION, AND POLYNOMIOGRAPHY

Chonjaroen CHAIRATSIRIPONG[1], Anantachai PADCHAROEN[2], Ovidiu BAGDASAR[3] and Tanakit THIANWAN[1,*]

[1]Department of Mathematics, School of Science, University of Phayao, Phayao 56000, Thailand
[2]Department of Mathematics, Faculty of Science and Technology, Rambhai Barni Rajabhat University, Chanthaburi 22000, Thailand
[3]School of Computing and Mathematics, University of Derby, Kedleston Road, Derby DE22 1GB, United Kingdom

Corresponding author email: tanakit.th@up.ac.th

Abstract

In this paper, we propose a novel inertial viscosity iterative algorithm that approximates a common fixed point of an infinite family of nonexpansive mappings in a Hilbert space. We first prove that under suitable conditions the proposed method has strong convergence, and then we apply the results to solve convex minimization problems, to the problem of image restoration, and to the recent field of polynomiography. For complex polynomial equations, we show the use of the proposed iteration with both real and complex parameters, and the resultant polynomiographs give intriguing patterns. The real parts of the parameters change the symmetry of polynomiographs, whereas the imaginary ones produce asymmetric twisting. We also achieve the viscosity approximation method with inertial effect in a novel accelerated image restoration form. To illustrate the efficacy of our method, we provide some numerical simulations. We emphasize that the results accounted for in the manuscript extend and complement various results in this field of study.

Key words*: inertial; viscosity; weak/strong convergence; convex minimization; image restoration; polynomiography*

1. INTRODUCTION

The linear framework for the image restoration problem is based on the equation

$$Ax = b + y, \tag{1}$$

where the operator $A \in \mathbb{R}^{m\times n}$ describes the degradation, $x \in \mathbb{R}^{n\times 1}$ is the input into the system, $b \in \mathbb{R}^{m\times 1}$ is the observed noisy and blurred image, while y is the noise added to the output image. In image restoration, one aims to solve an inverse problem, namely to recover x given $A, b,$ and y. Numerous algorithm for solving problem (1) are known, with numerous practical applications. For example the LASSO model (Tibshirani, 1999) stated as

$$min_x\{\| Ax - b \|_2^2 + \psi \| x \|_1\}, \tag{2}$$

where ψ is a regularization parameter, that $\psi > 0, \| x \|_1 = \sum_{i=1}^{n} |x_i|$, and $\| x \|_2 = \sqrt{\sum_{i=1}^{n} |x_i|^2}$.

In the current paper we build on the recent work (Padcharoen & Kitkuan 2021) to build a new inertial viscosity iterative fixed-point algorithm for solving a common fixed point of a family of nonexpansive mappings in real Hilbert spaces. We also proved strong convergence theorems of the proposed method under some suitable control conditions. We then applied our results to solve convex minimization problems, image restoration problems, and polynomiography.

The following formula can be created by extending problem (2).

$$min_x\{h(x) + g(x)\}, \tag{3}$$

where $h: \mathbb{R}^n \to \mathbb{R}$ is a convex smoothless function and differentiable with ℓ-Lipschitz continuous gradient, where $\ell > 0$, i.e.,

$$\| \nabla h(x) - \nabla h(y) \| \leq \ell \| x - y \|, \forall x, y \in \mathbb{R}^n$$

and $g: \mathbb{R}^n \to \mathbb{R} \cup \{+\infty\}$ is a proper convex and lower semi-continuous function.

2. CONTENT

Let H be a real Hilbert space, $\{T_n: H \to H\}$ a family of nonexpansive mappings, f a k-contraction mapping on H with $k \in (0,1), \{\eta_n\} \subset (0,\infty)$ and $\{\alpha_n\}, \{\tau_n\}, \{\delta_n\}, \{\lambda_n\}, \{\beta_n\}, \{\gamma_n\} \subset (0,1)$.

Algorithm 1

Initialization: Take $x_0, x_1 \in H$. Choose $\theta \geq 0$.

For $n \geq 1$, set

$$\theta_n = \begin{cases} \min\left\{\theta, \frac{\eta_n \alpha_n}{\|x_n - x_{n-1}\|}\right\} & if \quad x_n \neq x_{n-1}; \\ \theta & otherwise. \end{cases}$$

Compute

$$w_n = x_n + \theta_n(x_n - x_{n-1}),$$
$$z_n = (1 - \tau_n)x_n + \tau_n\big((1-\gamma_n)w_n + \gamma_n T_n w_n\big),$$
$$x_{n+1} = \alpha_n f(x_n) + \beta_n x_n + \delta_n\big((1-\lambda_n)T_n w_n + \lambda_n T_n z_n\big).$$

We then prove a strong convergence theorem for a family of nonexpansive operators by assuming *NST*-condition (*I*) (Nakajo et al., 2007) as follows.

Theorem1. Let $\{T_n\}$ be a family of nonexpansive mappings and $T: H \to H$ a nonexpansive mapping such that $\emptyset \neq F(T) \subset \bigcap_{n=1}^{\infty} F(T_n)$. Suppose that $\{T_n\}$ satisfies *NST*-condition (*I*) with T. Let $\{x_n\}$ be the sequence generated by Algorithm 1 such that the following additional conditions hold:

(1). $\alpha_n + \beta_n + \delta_n = 1$; (2). $0 < a \leq \tau_n \leq a' < 1$; (3). $0 < b \leq \gamma_n \leq b' < 1$;

(4). $0 < c \leq \lambda_n \leq c' < 1$; (5). $0 < d \leq \delta_n \leq d' < 1$; (6). $\lim_{n\to\infty} \eta_n = 0$;

7. $\lim_{n\to\infty} \alpha_n = 0 \quad and \quad \sum_{n=1}^{\infty} \alpha_n = \infty$

for some positive real numbers $a, b, c, d, a', b', c', d'$. Then the sequence $\{x_n\}$ converges strongly to $w \in F(T)$, where $w \in P_{F(T)} f(w)$.

Two applications are considered. We use the blurring functions from MATLAB: a Gaussian blur (Matlab function is,"fspecial ('gaussian',5,5)") and random noise to create the blurred and noisy image (observed image). Then, we show some examples of the polynomiographs obtained by using Algorithm 3 with real and complex-valued parameters using different color maps.

3. CONCLUSIONS

This paper presented a new accelerated fixed point algorithm using the ideas of viscosity and inertial techniques for solving a common fixed point problem of a family of nonexpansive operators. The strong convergence theorem of our proposed method, Theorem 1, is established and proved under some suitable conditions and applied to our results to solve a minimization problem in the form of the sum of two proper lower semicontinuous and convex functions. As applications, we applied Algorithm 1 to solve image restoration problems. Furthermore, we did some numerical experiments to illustrate the performance of the studied algorithms and show that the ISNR of our algorithm is higher than those of the method, NAGA, or FISTA. In addition, we present polynomiographs for complex polynomials. We show the use of our algorithm with both real and complex parameters, and the resultant polynomiographs display quite intriguing patterns. Real parts of the parameters affect symmetry, but imaginary parts create asymmetric twisting of polynomiographs, according to our findings. We get some nice-looking polynomiographs that are also artistically fascinating.

MATHEMATICAL APPROACHES FOR BIOSIGNALS AND APPLICATIONS

Mihaela-Cristina STRÎMTOREANU[1], Mirela-Violeta MANEA[1], Simona BIBIC[2], Mariana-Mirela STĂNESCU[2]

[1]Faculty of Materials Science and Engineering
University Politehnica of Bucharest, 313 Splaiul Independentei, District 6, Bucharest, Romania
[2]Faculty of Applied Sciences
University Politehnica of Bucharest, 313 Splaiul Independentei, District 6, Bucharest, Romania

Corresponding author email: mstrimtoreanu@stud.sim.upb.ro

Abstract

In this paper we are going to study the potential of the Van der Pol and Duffing equations for biosignal analysis with specific applications, which models represent valuable resources for comprehending the complex nature of biosignals. From another point of view, these equations offer deep understanding into dynamic and chaotic behavior of biological systems and are capable to describe their most important features. Thus, the mathematical approach highlights concealed characteristics within physiological processes and increase their applications to a variety of domains, including the study of electrocardiography (ECG) and electroencephalography (EEG). The accuracy and flexibility of these models are further improved by introducing new algorithm combining wavelet-based and fractional calculus methods to analyse the biosignals and offer up new research directions.

Key words*: fractional calculus; wavelet analysis and applications; evolutionary algorithms and applications; data analysis and information security.*

1. INTRODUCTION

In this presentation, we are going to explore the importance of the Van der Pol and Duffing equations in the wider field of biosignal analysis. We will discuss how these equations have been enhanced by novel forms that rely on wavelet-based and fractional calculus techniques, making them even more effective in this sector.

2. CONTENT

2.1 Biosignals

Biosignals such as electroencephalograms (EEGs) and electrocardiograms (ECGs) play a significant role in understanding the electrical activity of the human body.
These signals provide valuable information about brain and heart functions, aiding in diagnosing various neurological and cardiovascular conditions.
There is a variety of other biosignals, including: electromyogram (EMG), electrooculogram (EOG), blood pressure (BP), pulse oximetry (SpO2), heart rate variability (HRV).

2.2 EEG and ECG

The primary emphasis of the study is on: electroencephalogram or EEG (measures brain electrical activity, used in neurology, Fourier and Wavelet transforms can help model and analyze the dynamics of brain activity) and electrocardiogram or ECG (records heart electrical activity, diagnosing cardiac conditions and heart health monitoring, an important tool for this biosignal is Van der Pol equation).

2.3 Duffing - Van der Pol equation

These equations provide a mathematical framework for analyzing the intricate dynamics of ECG data, which can be simulated using MATLAB.

2.4 Wavelet analysis

An approach for analyzing the temporal and frequency aspects of biosignals is wavelet analysis. It offers a multiscale technique to capture transient events and non-stationary properties that Fourier-based techniques potentially miss. This method relies on comprehending the complex dynamics of biosignals and gathering relevant information for biomedical applications.

2.5 Fractional wavelet transform

An adaptation of the standard wavelet transform that includes a fractional order parameter is the fractional wavelet transform (FWT). As opposed to discrete scales, it offers a continuous variety of scales, allowing for a more flexible examination of data.

2.6 Applications and MATLAB

This final chapter consists of multiple parts, including: the Haar wavelet and its simulation in MATLAB, coupled cardiac oscillators, which depicts the cooperation and interactions of several cardiac nodes and processes, the mathematical model of the heart and the construction of the cardiac system, and a comparison of a normal and abnormal ECG.

3. CONCLUSIONS

The future holds promising possibilities for further advancements in EEC and ECG analysis. All things considered, we can envision a future where the diagnosis, treatment, and management of arrhythmias are more accurate, personalized, and successful, ultimately resulting in better patient outcomes and cardiovascular health, with a thorough understanding of the coupled cardiac oscillators and ongoing advancements in ECG analysis.

REFERENCES

[1] Fisch BJ. Fisch and Spehlmann's EEG Primer. Basic Principles of Digital and Analog EEG, Elsevier; 1999

[2] Quiroz-Juárez, M.A.; Rosales-Juárez, J.A.; Jiménez-Ramírez, O.; Vázquez-Medina, R.; Aragón, J.L. ECG Patient Simulator Based on Mathematical Models. *Sensors* 2022, *22*, 5714. https://doi.org/10.3390/s22155714

[3] karthik raviprakash (2023). ECG simulation using MATLAB (https://www.mathworks.com/matlabcentral/fileexchange/10858-ecg-simulation-using-matlab), MATLAB Central File Exchange.

[4] Martha L. Abell, James P. Braselton, Differential Equations with Mathematica (Fifth Edition), 2023

[5] Cardarilli, G.C.; Di Nunzio, L.; Fazzolari, R.; Re, M.; Silvestri, F. Improvement of the Cardiac Oscillator Based Model for the Simulation of Bundle Branch Blocks. *Appl. Sci.* 2019, *9*, 3653. https://doi.org/10.3390/app9183653

[6] MathWorks-Wavelet toolbox

[7] Barbosa RS, Machado JAT, Vinagre BM, Calderón AJ. Analysis of the Van der Pol Oscillator Containing Derivatives of Fractional Order. Journal of Vibration and Control. 2007;13(9-10):1291-1301. doi:10.1177/1077546307077463

EKELAND'S VARIATIONAL PRINCIPLE ON NON-TRIANGULAR METRIC SPACES

Natthaya Boonyam[1], Poom Kumam [1,2], and Parin Chaipunya[1,2]*

[1] *Department of Mathematics, Faculty of Science, King Mongkut's University of Technology Thonburi, 126 Pracha Uthit Rd. Bang Mod, Thung Khru, Bangkok, 10140, Thailand*

[2] *Center of Excellence in Theoretical and Computational Science (TaCS-CoE), King Mongkut's University of Technology Thonburi, 126 Pracha Uthit Rd. Bang Mod, Thung Khru, Bangkok, 10140, Thailand*

*Corresponding address (E-mail: parin.cha@kmutt.ac.th)

In this paper, we introduce Ekeland's variational principle on non-triangular metric space. We applied the proposed variational principles to obtain existence theorems for a class of equilibrium problems. Finally, we deduce the existence of equilibrium reformulation.

Keywords: Ekeland's Variational Principle, Equilibrium Problem, Existence of an equilibrium, Non-triangular metric space, Lower semi-continuous functions.